

This dissertation has been  
microfilmed exactly as received

69-2502

YANG, (Tony) Tien-sheng, 1928-  
EFFECTS OF GEOMETRIC PARAMETERS ON THE  
ULTIMATE STRENGTH BEHAVIOR OF MODEL  
REINFORCED CONCRETE FOLDED PLATE  
STRUCTURES.

The University of Oklahoma, Ph.D., 1968  
Engineering, civil

University Microfilms, Inc., Ann Arbor, Michigan

THE UNIVERSITY OF OKLAHOMA  
GRADUATE COLLEGE

EFFECTS OF GEOMETRIC PARAMETERS ON THE ULTIMATE  
STRENGTH BEHAVIOR OF MODEL REINFORCED  
CONCRETE FOLDED PLATE STRUCTURES

A DISSERTATION  
SUBMITTED TO THE GRADUATE FACULTY  
in partial fulfillment of the requirements for the  
degree of  
DOCTOR OF PHILOSOPHY

BY  
(TONY) TIEN-SHENG YANG

Norman, Oklahoma

1968

EFFECTS OF GEOMETRIC PARAMETERS ON THE ULTIMATE  
STRENGTH BEHAVIOR OF MODEL REINFORCED  
CONCRETE FOLDED PLATE STRUCTURES

APPROVED BY

Weldon W. Aldredy

L. A. Combs

William H. Huff

Gerry R. ...

Fulton K. Fears

DISSERTATION COMMITTEE

## ACKNOWLEDGEMENTS

This study was conducted in the School of Civil Engineering at the University of Oklahoma under the supervision of Dr. W. W. Aldridge and was supported by a National Science Foundation Grant. Electronic computer services were supplied by the University Computer Center.

The author wishes to express his sincere thanks and profound gratitude to Dr. Aldridge for his guidance and assistance which have made this study possible from the beginning. Also, expressions of gratitude are extended to Professor G. W. Reid for his assistance.

Many thanks go to Messrs. Jagdish Ghodi and Pankaj Shah for their assistance with the physical research program and to the assistants who contributed to the project.

PLEASE NOTE: Appendix pages  
are not original copy. Print  
is indistinct on many pages.  
Filmed in the best possible  
way.

UNIVERSITY MICROFILMS.

## ABSTRACT

Several commonly used geometric arrangements of reinforced concrete folded plate structures were investigated by means of computer solutions. A representative prototype simple span structure selected from the computer study was analyzed and designed by various methods in accordance with the currently recommended analysis and design procedure <sup>(1,2,3)</sup>. The results were compared and evaluated to choose the method which is feasible for actual model and prototype construction. One 1/8 scale direct model structure was built by the recognized methods of similitude and was monotonically load tested to failure. The general behaviors, the load-deflection relation, the load-strain relation, and cracking pattern of the structure were compared with various theoretical predictions.

The conclusions justified by the test results combined with that of the computer solution study are: 1) the influence of the geometric parameters, the span-to-rise ratio, plate height-to-thickness ratio, the angle between adjoining plate and the angle between plate and the horizontal, and

---

<sup>1</sup>Superscript numerals in parentheses refer to references listed in Bibliography.

disturbances of the edge plates are significant, 2) the warping of the cross section is inevitable and must not be ignored in the inelastic load range, 3) the service load can be predicted quite closely by the linear elastic theory considering effects of the relative joint displacements, 4) nonlinear beam theory failed to predict service load but predicted yield load, 5) overall load-deflection responses cannot be predicted accurately by either method but the load-deflection response at the service load can be predicted by the elastic method, 6) internal stresses underwent a redistribution with loadings to ultimate, 7) accurate prediction of the load-deflection response can be achieved only by developing the nonlinear folded plate theory considering the warping of the cross section, 8) the actual responses of load-deflection and load-strain are three different stages nonlinear and can be expressed by a general equation  $P = \frac{x}{a + bx}$ ; where  $P$  = load in psf,  $x$  = strain ( $\mu$  in./in.) or deflection (in.), and  $a, b$  = constants.

Folded plate structures are classified into two categories and two different methods of analysis are recommended for analysis depending on the span-to-rise ratio.

## TABLE OF CONTENTS

ACKNOWLEDGEMENTS .....	iii
ABSTRACT .....	iv
LIST OF TABLES .....	x
LIST OF ILLUSTRATIONS .....	xii
CHAPTER I. INTRODUCTION	
1.1 Introduction .....	1
1.1.1 General .....	1
1.1.2 Prismatic Reinforced Concrete Folded Plate Structures .....	3
1.2 Scope of Study .....	5
1.3 Objectives of Study .....	5
1.4 Literature Review .....	6
1.4.1 Analysis .....	6
1.4.1.1 Linear Elastic Analysis Methods .....	6
1.4.1.2 Inelastic, Nonlinear Analysis Methods ..	11
1.4.2 Previous Tests .....	12
CHAPTER II METHOD OF ANALYSIS FOR SIMPLY SUPPORTED FOLDED PLATE STRUCTURES	
2.1 Linear Elastic Analysis Method .....	22
2.1.1 Basic Analysis .....	23
2.1.2 Correction Analysis .....	26

TABLE OF CONTENTS - continued:

CHAPTER II - continued:

2.1.3	Superposition .....	27
2.2	Nonlinear, Inelastic Analysis Method .....	27
2.3	Derivation of Equations .....	30
2.3.1	Plate Loads Resolved from the Vertical Joint Loads .....	30
2.3.2	Free Edge Stresses Distribution .....	31
2.3.3	Plate Deflections Expressed in Terms of Equalized Edge Stresses .....	33
2.3.4	Relative Joint Displacements - Williot Diagrams .....	35

CHAPTER III COMPUTER STUDY OF VARIOUS GEOMETRIC  
ARRANGEMENTS OF FOLDED PLATE STRUCTURES

3.1	Analysis Parameters .....	36
3.2	Range of Applicability for the Various Analysis Methods .....	38
3.3	Computer Study of Various Geometric Arrange- ments of Prototype Folded Plate Structures ...	42
3.4	Conclusion .....	56

CHAPTER IV ANALYSIS AND DESIGN OF THE TEST SPECIMENS

4.1	General .....	59
4.2	Prototype Structure Design and Analysis by Linear Elastic Methods .....	60
4.2.1	Analysis .....	60
4.2.2	Design .....	66
4.2.3	Comparison of the Results of Two Different Linear Elastic Methods .....	68

TABLE OF CONTENTS - continued:

CHAPTER IV - continued:

4.3	Overall Behaviors of the Selected Prototype Structure - by "Nonlinear Inelastic Beam Theory" .....	69
4.4	Model .....	70
4.4.1	General .....	70
4.4.2	Direct Inelastic Model Analysis .....	73
4.4.3	The Selected Prototype Versus Model Correlations .....	74
4.4.4	Microconcrete .....	75
4.4.5	Model Reinforcement .....	80
4.5	Summary .....	81

CHAPTER V CONSTRUCTION AND TESTING OF MODEL STRUCTURE

5.1	General .....	93
5.2	Construction of Model Structure .....	94
5.2.1	Supporting Frames .....	94
5.2.2	Model Structure .....	98
5.3	Load Testing System .....	102
5.3.1	General .....	102
5.3.2	"Whiffle-tree" Loading System .....	105
5.3.3	Design and Verification of "Whiffle-tree" Loading System .....	107
5.3.4	Performance of Loading System .....	108
5.4	Instrumentation .....	108
5.4.1	General .....	108

TABLE OF CONTENTS - continued:

5.4.2	Deflection System .....	108
5.4.3	Strain System .....	110
5.5	Description of the Model Test .....	112
5.6	Analysis and Discussion of the Test Results ....	114
5.6.1	Cracking and Load versus Strain Responses ..	114
5.6.2	Load versus Deflection Response .....	125
5.6.3	Collapse .....	139
CHAPTER VI CONCLUSIONS AND RECOMMENDATIONS		
6.1	General .....	144
6.2	Conclusion .....	146
6.3	Recommended Practice .....	148
6.3.1	General .....	148
6.3.2	Recommended Practice for the Second Range Structure .....	149
6.4	Suggestions for Future Research .....	149
SYMBOLS AND NOTATIONS .....		151
BIBLIOGRAPHY .....		155
APPENDIX A .....		162
APPENDIX B .....		170
BIOGRAPHY .....		184

## LIST OF TABLES

Table 1.1	Dimensions, Shape and Support Conditions of Enami's Models.....	13
Table 3.1	Solution Methods Recommended by Whitney, et.al., for Different Values of the L/R Ratio.....	39
Table 3.4	Solution Methods Recommended by Linear Elastic Methods.....	57
Table 4.1	Reinforcement Quantity Comparison Between Analyses Neglecting and Considering Relative Joint Displacements.....	69
Table 4.2	Correlations Between Model and Prototype Structures.....	75
Table 4.3	Summary of Cylinder Tests.....	82
Table 4.4	Summary of Mechanical Properties of Model Reinforcement.....	83
Table 5.1	Summary of Model Quality Control Cylinder Tests.....	101
Table 5.2	As-Built Dimensions.....	103
Table 5.3	Summary of Model Plate Thickness.....	106
Table 5.4	Summary of Dimensions and Test Results of the Beams for Verification of "Whiffle-tree" Loading System.....	109
Table 5.5	Summary of Mechanical Properties of Model Reinforcement with Brazed Connections.....	113
Table 5.6	Comparison of the Plate Load Variations Along the Ridge Lines Between the Test Results and That of the Design Calculated With the Plate Theory Considering Relative Joint Displacement.....	133

LIST OF TABLES - CONTINUED:

Table 5.7	Comparison of the Load Obtained From the Load-Strain Response With That of the Design and That of Load Obtained with Non-linear Beam Theory.....	133
Table 5.8	Summary of Vertical Deflections at $l/4L$ and $l/2L$ Along the Same Edge Line at Service Load.....	135
Table 5.9	Final Stresses on the Top Surfaces of the Plates at Failure of the Model.....	141
Table 5.10	Comparison of the Maximum Capacity Load of the Model With the Calculated Maximum Capacity Load Based on the Nonlinear Beam Theory and With the Required Ultimate Capacity of the ACI Code.....	141

## LIST OF ILLUSTRATIONS

Figure 1	Simple Span Folded Plate Roof Structure.....	4
Figure 2.1	Illustration of Principle of Superposition.....	25
Figure 2.6	Modified Hognestad Stress-strain Curve.....	29
Figure 2.2	Plate Loads Resolved From The Vertical Joint Loads.....	30
Figure 2.2a	Joint n as F.B.....	30
Figure 2.2b	Plate n as F.B.....	30
Figure 2.3	Free Edge Stress Distribution.....	31
Figure 2.4	Deflection versus Edge Stresses.....	33
Figure 2.5	Relative Joint Displacements - Williot Diagrams.....	35
Figure 3.1	Dimensional Parameters and Collapse Mode.(7).....	41
Figure 3.2.1	6-Plates Sawtooth Unit.....	44
Figure 3.2.2	6-Plates Hat Unit.....	45
Figure 3.2.3	6-Plates Hat Unit.....	46
Figure 3.2.4	8-Plates Unit.....	47
Figure 3.3.1	$M/WR^2$ versus $L/R$ , Strs. 1a1, 1a3, 1d1 and 1d3.....	48
Figure 3.3.2	$M/WR^2$ versus $L/R$ , Strs. 2a1, 2a3, 2b1, 2b3, 2c1, and 2c3.....	49

LIST OF ILLUSTRATIONS - CONTINUED:

Figure 3.3.3	$M/WR^2$ versus $L/R$ , Strs. 3a1, 3a3, 3b1, 3b3, 3c1 and 3c3 .....	50
Figure 3.3.4	$M/WR^2$ versus $L/R$ , Strs. 4a1, 4a2, and 4a3 .....	51
Figure 3.3.5	$f/(WL^2/tR)$ versus $L/R$ , Strs. 1a1, 1a3, 1d1 and 1d3 .....	52
Figure 3.3.6	$f/(WL^2/tR)$ versus $L/R$ , Strs. 2a1, 2a3, 2b1, 2b3, 2c1, and 2c3 .....	53
Figure 3.3.7	$f/(WL^2/tR)$ versus $L/R$ , Strs. 3a1, 3a3, 3b1, 3b3, 3c1 and 3c3 .....	54
Figure 3.3.8	$f/(WL^2/tR)$ versus $L/R$ , Strs. 4a1, 4a2 and 4a3 .....	55
Figure 4.1	Prototype Structure .....	61
Figure 4.2	Summary of Aggregate Gradations .....	77
Figure 4.3a	Aggregates and Cylinder Molds .....	78
Figure 4.3b	Strain Instruments for Concrete .....	78
Figure 4.3c	Typical Cylinder Failures .....	78
Figure 4.3d	Typical Wire Tensile Test Specimens.....	78
Figure 4.4	Stress-strain Curves for Prototype and Microconcrete .....	79
Figure 4.5	Load-deflection Curve of Model by "Program LDDFN" .....	71
Figure 4.6	Stress-strain Curves for Model Reinforcements .....	84
Figure 4.7a	Model Structure .....	85
Figure 4.7b	Half Cross-section of Model .....	86
Figure 4.7c	Top Reinforcement Layout .....	87
Figure 4.7d	Bott. Reinforcement Layout .....	88
Figure 4.7e	Longitudinal and Stirrup Reinforcements Layout for Plates #1 and #2..	89

LIST OF ILLUSTRATIONS - CONTINUED:

Figure 4.7f	Longitudinal and Stirrup Reinforcements Layout for Plate #3 .....	90
Figure 4.7g	Top and Bottom Reinforcement Details ...	91
Figure 4.7h	Details of End Diaphragm .....	92
Figure 5.1a	Verification of Loading System .....	95
Figure 5.1b	Hydraulic Ram, Load Cell, Pump, Chair, Chucks, etc. ....	95
Figure 5.1c	Model, Supporting Frames, "Whiffle-tree" and Strain Gage Monitoring Equipment .....	95
Figure 5.1d	Deflection of the Model .....	95
Figure 5.2a	End Diaphragm Steels and Dowels .....	96
Figure 5.2b	Model Steel Cages for Plates .....	96
Figure 5.2c	Layout of Strain Gages on Micro-concrete Surfaces .....	96
Figure 5.2d	Instruments for Measuring Deflections ..	96
Figure 5.3a	Top View of the Model After Testing ....	100
Figure 5.3b	Typical Cracking Due to Longitudinal Action and Concrete Crushing at Bottom Ridge of the Model .....	100
Figure 5.3c	Cracking of Plates Along the Inside Face of the End Diaphragm .....	100
Figure 5.3d	Rotation of Plates at Support of the Model .....	100
Figure 5.3e	Typical Cracking Along the Ridge Line 2' at End of Plates Due to Slab Action..	100
Figure 5.3f	Typical Cracking Due to Combination of Longitudinal Transverse and Diagonal Stresses .....	100
Figure 5.4	Code Schema for As-Built Dimensions ....	104

LIST OF ILLUSTRATIONS - CONTINUED:

Figure 5.5	Layout For Strain and Deflection Dial Gages .....	111
Figure 5.6a	Longitudinal Strain on the Steel-Reinforcement .....	115
Figure 5.6b	Longitudinal Strain on Steel-Reinforcement .....	116
Figure 5.6c	Transverse Strain on the Top Surface of the Model .....	117
Figure 5.6d	Deflections at Mid-Span .....	118
Figure 5.6e	Longitudinal Deflections at End Diaphragms .....	119
Figure 5.6f	Vertical Deflections at Quarter Span ...	119
Figure 5.6g	Cracking Response .....	120
Figure 5.6h	Cracking Response .....	121
Figure 5.7a	Longitudinal Strain on the Steel-Reinforcement of Ridge Lines 0' and 1'.....	126
Figure 5.7b	Longitudinal Strain on the Steel Reinforcement of Ridge Lines 2' and 3 .....	127
Figure 5.7c	Transverse Strain on the Top Surface of the Model .....	128
Figure 5.7d	Deflections of Ridge Lines 0 and 0' ....	129
Figure 5.7e	Deflections of Ridge Lines 1 and 1' ....	130
Figure 5.7f	Deflections of Ridge Lines 2 and 2' ....	131
Figure 5.7g	Deflections of Ridge Line 3 .....	132
Figure 5.8	Comparison of Deflection at Mid-span of Ridge Line 0', $(\Delta_v)_{0'M}$ , Predicted by Different Methods .....	140

## CHAPTER I

### INTRODUCTION

#### 1.1 Introduction

##### 1.1.1 General

In the past forty years a great deal of work has been done in the development of theoretical analysis methods and the reliability of the methods for structures based on the classical concepts of linear elastic behavior of the materials. However, these works have demonstrated some serious limitations of these methods of analysis. These research studies have in turn led to the development and acceptance of new concepts - plastic design concepts for structural steel, ultimate strength design concepts for reinforced concrete, and non-linear mechanics concepts.

Throughout the entire range of loading, the actual response of a structural system to applied loads is little understood due to the complexity of the real material properties and the methods of analysis. Other areas that have only begun to develop are technology of construction and testing of either full-scale or model structures. With reference to the complexity of the methods of analysis,

electronic high speed digital computers provide the capability for handling large complex problems. However, convenience does not necessarily imply understanding, and sophisticated manipulation does not guarantee that the rational analysis will accurately predict the behavior of the physical structure. Clearly, the ultimate test of any abstraction proposed for use in a mathematical model of a structural system is its reliability in making accurate predictions of the responses of the real system.

The failure of the classical linear models to yield accurate predictions for stresses beyond the elastic range has forced the engineer to seek observations of responses of actual structural members. Most of the early tests, done primarily by Hennebique, Mensch, Emperger, Maillart, and Danrusso, dating back to the late 1800's <sup>(4)</sup> as well as those undertaken more recently, have been tests on the components of structural systems (beams, columns, etc.) rather than tests on systems of the components (space frames, etc.). Without question, the testing of the large numbers of prototype structural (full-scale) systems required for probabilistic studies would be impractical as well as expensive. Also, even in those cases where tests of prototypes are feasible, a direct model study can be made to yield much more information for a given expenditure of labor and money. As a consequence, direct modeling technology has received a large measure of attention in recent years.

### 1.1.2 Prismatic Reinforced Concrete Folded Plate Structures

Only in the last decade have engineers turned their attentions to tests of prismatic folded plate structures (or as they are sometimes called, prismatic or hipped plates) constructed from their more natural building material - reinforced concrete. Thus the response of reinforced concrete folded plate structures to applied loads is of fundamental importance and needs to be better understood.

This study deals solely with the simple span, symmetrical in geometry and loaded about two axes, folded plate structures which are composed of rectangular plates connected monolithically along the edges supported on two end supporting members - end diaphragms or gable frames (Fig. I). The structure shown in Fig. I is a typical folded plate structure; however, the possible cross section arrangements are almost unlimited. (1, 5, 6) Although it is principally used for roof structures, it has also been adapted to bins, floors and even foundations. It offers an economical, simpler, and pleasing construction. Because of its inherent stiffness it has proven exceptionally economical for longer span structures in contrast with conventional structures such as slabs and beams.

The ASCE Task Committee on shell structures, in December, 1963<sup>(1)</sup> has classified the various analysis methods into four categories (Sec. 1.4.1.1.) and recommended the use of the ordinary (linear elastic) theory with corrections for relative

joint displacements. The results of the tests of model reinforced concrete folded plate roof structures, by Aldridge<sup>(7)</sup> and Scordelis and Gerasimenko<sup>(8,9)</sup> have indicated that the above recommended method will fail by at least one order of magnitude to predict the ultimate load deflection responses in some of these thin slab-type structures. Some of these errors are apparently due to the non-linear and inelastic behavior of the cracked concrete. However, Aldridge<sup>(7)</sup> and Calvo<sup>(10)</sup> have indicated that the influence of variations in geometric parameters may be extremely significant.

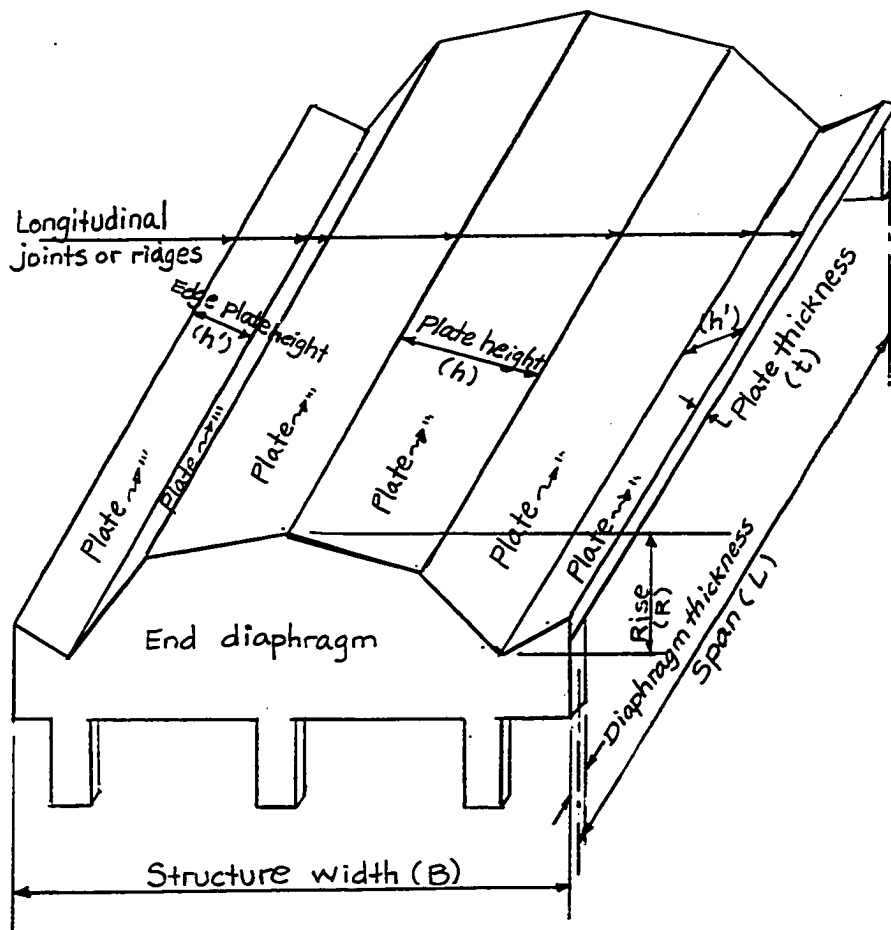


Fig. 1. Simple span folded plate roof structure

## 1.2 Scope of Study

The principal purpose of this study is to critically evaluate the currently recommended analyses and design procedures in a particular case where study has not been done previously. Three major problems in this study are:

1. The influence of variations in geometric parameters,
2. Load-deflection response, and
3. Load-strain relations.

As in the general engineering practice this study was made possible only by introduced abstractions and idealization - assumptions - which in turn impose serious limitations on the subject. The assumptions will be discussed in detail in the following chapters. Effects of creep and shrinkage were not considered. In fact these effects can be minimized by running test in short period and by adding shrinkage control curing compound as plastiment, to provide some retardation of concrete.

## 1.3 Objective of Study

The objective of this study are:

1. To evaluate the currently recommended analysis and design procedures, (1,2,3)
2. To contribute to the knowledge concerning the responses of reinforced concrete structural systems in these areas: (a) folded plate structures, (b) ultimate strength technology, (c) strain measuring technology, and (d) modeling technology, and

3. To assist in the development of relevant, comprehensive, and reliable non-linear mathematical models for use in the design of folded plate structures.

#### 1.4 Literature Review

##### 1.4.1 Analysis

###### 1.4.1.1 Linear elastic ordinary analysis method.

In 1930, Ehlers<sup>(36)</sup> published the first folded plate theory, as distinguished from the ordinary beam theory, based on a linear variation of longitudinal stress in each plate with hinged but unyielding joints. Later in the same year - 1930 - Craemer<sup>(37,38)</sup> and Gruber<sup>(39)</sup> developed the method considering the transverse moments due to continuity of the joints. The method was introduced to this country in 1947 by Winter and Pei.<sup>(11)</sup> The theory dealing with relative displacement of joints was first proposed by Gruber<sup>(39)</sup> and Gruening in 1932.<sup>(40)</sup> Further developments of the theory were made by Vlassow,<sup>(13)</sup> the Portland Cement Association,<sup>(14)</sup> Gaafar,<sup>(15)</sup> Yitzhaki,<sup>(16,17)</sup> Brielmaier,<sup>(18)</sup> Werfel,<sup>(21)</sup> Rudiger,<sup>(13)</sup> Goldberg and Leve,<sup>(20)</sup> and Mast.<sup>(22)</sup> The Task Committee on Folded Plate Construction in December, 1963 classified the various linear elastic analysis methods into four principal categories as (a) beam method, (b) folded plate theory neglecting relative joint displacements, (c) folded plate theory considering relative joint displacements,

and (d) elasticity method. There are limitations of applicability for these linear elastic methods and the assumptions must be underlined clearly. In addition to the fundamental assumptions each of the methods contains its own characteristic assumptions.

The fundamental assumptions for all the methods are:

1. The material is homogeneous and linearly elastic.
2. The actual deflections are minor related to the over all configuration of the structure.
3. The principle of superposition holds.
4. Longitudinal joints are fully monolithic with the slab acting continuously through the joints.
5. Each supporting end diaphragm is infinitely stiff parallel to its own plane but is perfectly flexible normal to its plane.

Beam Method - This is a conventional beam analysis method which assumes a planar variation of longitudinal stress across the entire structure. In other words, the structure is assumed to deflect in such a manner that all points on the same cross sections deflect the same amount so that the cross section maintains its original shape through the deflection. Thus the familiar expression  $f = \frac{Mc}{I}$  applies. Several authors (5,8,18,24,25,26,27,30,4) have studied the applicability of this theory to the aggregate cross section of the folded plate structure.

Folded Plate Theory Neglecting Relative Joint Displacements -

The theory considers one-way slabs in the transverse direction and ordinary beams in the longitudinal direction. However, the changes in transverse bending moments and in longitudinal stresses due to relative joint displacement are considered negligible in comparison with those set up by the loading (primary analysis). An equivalent statement is that transversely the structural action is to be considered as a continuous one-way slab supported at the intersection of the elastic but relatively rigid longitudinal plates. Consequently, the general assumptions implied by the beam action are:

1. Longitudinal plate stresses vary linearly across the width of each plate but the transverse rate of variations of stress may be different in the various plates.
2. Membrane shearing stresses in each plate have negligible effect on the deflection of the structure.
3. In each plate the normal stresses in the transverse direction are considered in the equilibrium conditions but may be neglected in deflection considerations, and those of the continuous one-way slab action are.
4. Slab bending is predominantly a one-way slab action in the transverse direction, and the longitudinal slab bending may be neglected.
5. The torsional resistance of the plates is negligible

and, therefore, the stresses and deflections due to the torsional stresses may be ignored.

6. Radial shearing stresses normal to the slab have an insignificant effect on the deflections of the structure.

Winter and Pei<sup>(11)</sup> proposed a relatively simple and practical technique - a relaxation technique, analogous to moment distribution - for computing the stress variation across the plate section.

Folded Plate Theory Considering Relative Joint Displacement -

The theory is identical with the preceding method - Folded Plate Theory Neglecting Relative Joint Displacements - except that this method takes into account the effect of relative displacement of the joints on the transverse moments and membrane stresses. Several practical methods which fall into this theoretical category are: (a) Vlassow's Method, (12,13) (b) Portland Cement Association Bulletin,<sup>(14)</sup> (c) Gaafar's Method,<sup>(15)</sup> (d) Yitzhaki's Method,<sup>(16,17)</sup> and (e) Iteration Method.<sup>(18)</sup>

The methods presented by Vlassow and the PCA Bulletin recommend an analysis of folded plates structures by the solution of a set of simultaneous linear algebraic equations (in general,  $2N-2$  equations where  $N$  is the number of plates) on the basis of a Fourier series. Therefore, the accuracies of the results will depend on the number of terms employed in the Fourier series.

Gaafar and Yitzhaki used the principle of superposition coupled with the principle of virtual displacement and that of virtual force respectively to analyze folded plate structures by solving  $N-2$  simultaneous equations.

Iteration Method - This method takes into account the effect of relative joint displacements by successive iterative calculations. In many cases the solution diverges.

Elasticity Method - Rudiger,<sup>(19)</sup> and Goldberg and Leve<sup>(20)</sup> analyze the folded plate structures by solving  $4N$  simultaneous algebraic equations - a combination of the equations of the classical plate theory for loads normal to the plane and that of the elasticity theory for loads in the plane of the plates. The method used by Werfel<sup>(21)</sup> is based on  $4(n-1)$  sets of  $(n-1)$  simultaneous equations and one set of  $2(n-1)$  simultaneous equations. All these methods solve the equations in terms of a Fourier series and the accuracy depends on the higher order terms considered. Mast<sup>(22)</sup> uses  $2(n-1)$  sets of  $(n-1)$  simultaneous equations for the first terms of the Fourier series, and usually only three sets of  $(n-1)$  simultaneous equations for higher order terms. These methods apply where the plates are relative short compared to the width, and where there is no translation of individual joints. It requires extensive computations and thus is practical only when the computer is available.

The Task Committee on Folded Plate Construction<sup>(1)</sup> recommended the use of the Ordinary Theory Considering

Relative Joint Displacement in 1963. However, the ACI Committee 334 recommended<sup>(2)</sup> the use of any structural analysis "based on elastic behavior and involving assumptions which are suitable to approximations of three-dimensional elastic behavior."

An extensive bibliography is listed in the ASCE Phase I Report on Folded Plate Construction.<sup>(1)</sup>

#### 1.4.1.2 Inelastic, nonlinear analysis method.

Aldridge and Breen<sup>(23)</sup> classified the various ultimate strength methods into three separate categories: (1) Beam Method, (2) Nonlinear Folded Plate Theory, and (3) Modified Yield Line Theory.

Beam Method - This method<sup>(24,25,26,27,28)</sup> applies the reinforced concrete ultimate strength procedures to the entire cross section of the folded plate structure as an ordinary beam.

Nonlinear Folded Plate Theory - Farmer<sup>(29)</sup> used the iterative solution by considering nonlinear moment curvature relationships for both the transverse slab strips and the longitudinal plate beams for the folded plate system.

Modified Yield Line Theory - Enami<sup>(30)</sup> and Dykes<sup>(31)</sup> have used Johansen's Yield Line Theory<sup>(32,33,34,35)</sup> for slabs to describe the behavior of reinforced concrete models.

An extensive bibliography is listed in "The Literature Review<sup>of</sup> Reported Results in the Field of Ultimate Strength of

Reinforced Concrete Folded Plate Structures" which was presented by Aldridge and Breen to the ASCE Task Committee on Folded Plate Construction.<sup>(23)</sup>

In summary, the development of inelastic methods of solution is still in its infancy; however, the limited test data (see 1.4.2) have shown promising correlation with various inelastic methods at ultimate.

#### 1.4.2 Previous Tests<sup>(7,23)</sup>

Only the principal investigations of reinforced concrete folded plate structures - model and/or prototype - test data are listed below.

(a) Enami. In 1957 at the University of Tokyo Enami<sup>(30,44,45)</sup> tested twelve mortar models (Table 1.1), four simple V-shaped unit, five hat ()-shaped unit and three inscribed polygon-shaped (four plates inscribed in a cylinder ) unit, to collapse by inverting them in the opening of a box filled with water. Load was applied normal to the plates by hydraulic head, and deflections were measured. Eleven of twelve models failed quite closely according to normal yield line patterns but one with simple span support failed like a beam. Enami's principal conclusion was that the behavior of the structures could be predicted with a modified limit analysis which refers to the changing moment pattern and closely resembles the yield line theory. Undoubtedly the test results showed pronounced nonlinear effects over a wide load range.

Enami also pointed out that the ultimate load of the one, which did not follow the yield line pattern, was somewhat higher than predicted by simple beam theory. This appears reasonable since the test method restrains rotation of the end diaphragms.

No. of Plates	Longitudinal span (m)	Transverse span (m)	Plate thick. (cm)	Plate width (cm)	End diaphragms.	Support conds.	Edge beams
2(  )	2	1	1	53.86	yes	Simple	yes
2(  )	2	1	1	53.86	yes	Fixed	yes
2(  )	2	1	1	53.86	yes	Simple	no
3(  )	2	1	1	36.39	yes	Simple	yes
3(  )	2	1	1	36.39	yes	Simple	yes
3(  )	2	1	1	36.39	yes	Simple	yes
3(  )	2	1	1	36.39	yes	Fixed	yes
4(  )	2	1	1	27.42	yes	Simple	yes
4(  )	2	1	1	27.42	yes	Fixed	yes
2(  )	0.5	1	0.5	26.93	yes	Simple	yes
3(  )	0.5	1	0.5	18.20	yes	Simple	yes
4(  )	0.5	1	5	13.70	yes	Simple	yes

Table 1.1 Dimensions, shape and support conditions of Enami's models

(b) Benito. In 1957 Benito tested one 1/15 scale model<sup>(46)</sup> of a prestressed folded plate roof section of interlocking triangular-shaped plates twelve centimeters thick at the

Central Laboratory of the College of Civil Engineering in Madrid; however, no test data are available on the model test.

(c) Senler. In 1958 Senler<sup>(47)</sup> tested one simple support reinforced mortar model of an irregular section (  ) loaded with the sand bags as reported by Posey.<sup>(48)</sup> Failure appeared near end diaphragms due to shearing stresses.

However, the first noticed cracking was flexural. A factor of safety against collapse of 2.8 was noted.

(d) Syracuse. Professor Wasil directed the reporting of results of a single test of a simply supported five plate hat-shaped (  ) model which was conducted under the direction of Moorman<sup>(28)</sup> at Syracuse University in 1959. The model with the following dimensions in feet: Span 26, width 13.67, rise 4, and plate thickness 0.125 was reinforced in accordance with the folded plate theory considering relative joint displacements and was tested by means of sand bag loading. Good correlation for measured deflections and steel strains were noted for symmetrical loads beyond about twenty-five percent of the ultimate strength computed by using the cracked section theory ignoring the reinforced steel in the inclined plates. The underestimated failure by twenty percent might be caused by the ignored steel in the sloping plate. Further, it is possible that the sand bag piles may produce non-uniformly distributed load.

(e) Dykes. In 1960, Dykes<sup>(31)</sup> performed the tests of six

simple two V-shaped reinforced mortar models. These models represented a move from simple slab towards stressed skin construction rather than true shell type with the basic dimensions in inches: Span 295.0, width 20.5, rise 6.80 and plate thickness 0.5. All models were reinforced at the middepth plane of the plates with steel wire mesh (1.3 percent constant steel percentage). All models were supported vertically and laterally along (a) two edges, (b) one edge and both ends, or (c) two edges and both ends and were loaded to collapse by a lever system which distributed discrete point loads. This loading simulated a uniform load (loading points located on four inch centers longitudinally and transversely). The author's principal conclusion was that the collapse load for all cases could be predicted within 10.7 percent, by using Yield Line Theory.

(f) Edwards. In 1961 Edwards<sup>(25)</sup> reported the test of a single prototype pretensioned reinforced concrete folded plate structure of a two plate V-shaped unit which was designed for thirty pounds per square foot using the simple beam theory. The unit was precast as single plates and later joined by welding #3 dowel bars on sixteen inch centers and then grouting the joint. The unit was uniformly loaded to 158 psf where the test was discontinued. No attempt was made to describe the behavior of the structure but the ratio of the moment capacity provided to the required moment capacity, calculated with the Whitney stress block ignoring 10 of 22 strands, was 1.37.

(g) Chacos and Scalzi. In 1961, Chacos and Scalzi<sup>(24)</sup> carried out a test of simple supported reinforced mortar model of a three plate hat-shaped unit () to collapse by a loading of bricks applied to the top plate only. The ratio of test moment to calculated moment by using the Whitney stress block and simple beam theory was 0.982.

(h) Schwaighofer and Seethaler. Schwaighofer and Seethaler<sup>(27)</sup> conducted the test of a single post-tensioned prototype reinforced concrete folded plate structure of Y-shape. The design of the prototype was preceded by a study of a plastic model which indicated that transverse ties across the top of the section (both at the supports as well as interior to the span) would adequately control the transverse bending. Consequently, the prototype was designed as a simple beam. The unit was simply supported and was uniformly loaded with concrete blocks to 230 psf where the test was discontinued. No comments were made regarding the ultimate strength of the section.

(i) Glanville. In 1963 Glanville<sup>(26)</sup> tested three simple supported pretensioned prototype folded plate roof sections of V-shape to collapse loaded with a four point compression whiffle tree made of I-beams. The first unit was prestressed with straight tendons and was made of normal weight concrete, while the remaining two units were made of lightweight concrete and prestressed with draped tendons. All the units were stiffened with tie bars in lieu of end diaphragms.

Using the simple beam theory coupled with the Whitney stress block and the actual steel stress obtained from a stress-strain diagram, Glanville was able to predict the ultimate capacities of all the units within 5 percent.

(j) Bikhovsky, et. al. Bikhovsky, Hemmerling, Korenev, Rzhantsin, and Rouchimsky<sup>(42)</sup> made the tests of scaled shell models of the inscribed polygon shape made up with pre-cast units at the Central Research Institute for Building Structures (Russia). The results of the tests have apparently not been reported, unless in Russia.

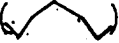
(k) Phanasomburana. In 1963 Phanasomburana<sup>(50)</sup> tested a single 1/5 scale model reinforced concrete folded plate unit of five plates () with basic dimensions in centimeters: plate thickness 5; plate width 72.1, span 400; cantilever overhangs 50 over each end and rise 40. The unit was simply supported on end diaphragms and columns and was uniformly loaded with sand bags and pig iron bars. However, the test was discontinued prior to failure. The cracking of the structure was predominantly longitudinal flexural, but was accompanied by minor diagonal tension cracking at load levels near the maximum applied load which had a load factor of 4.04 against collapse. No transverse cracking was noted.

(l) Vishwanath, et. al. In 1965 Vishwanath, Mhatre, and Seetharamulu<sup>(43)</sup> tested a single supported ferro-cemento pre-cast prototype folded plate of an inverted trapezoidal

unit () loaded by a discrete point loading which simulated a uniform line load at two edges of the bottom plate. The basic dimensions of the structure were: plate thickness 1 inch, plate width 10.24 ft., span 17.5 ft., rise 2.12 ft. The ferro-cemento panels were cast as a single plate which had two layers of galvanized steel mesh ( $3/4$  " x  $3/4$  " x 16 guage) reinforcement separated by mild steel bars designed for longitudinal plate bending. Later panels were joined by welding #3 dowel bars at joints and then grouting the joints. The structure failed in longitudinal shear at the edges. It was also noted that the free edge disturbances on the deflections and strains of the top edge lines were quite significant.

(m) Scordelis and Gerasimenko. In February, 1966 Scordelis and Gerasimenko<sup>(8)</sup> tested two simple supported reinforced concrete models of six plate hat-shape () to collapse. Both units had the dimensions in inches: plate width = 30, span = 70, thickness = 1.5, rise = 5. Model "a" was designed by a folded plate analysis based on the elasticity method while Model "b" was designed by elementary beam theory. The models were loaded at each interior joint by equal concentrated loads to approximate distributed line loads through a "whiffle-tree" system of simple beams interconnected by wires and threaded rods to the load points on the models. General behavior, cracking, deflections, and strains for each model were observed. Both models indicated

significant relative joint displacements under the service load. Thus the models responded in a manner predicted by the folded plate theory and not by the beam theory. The first visible cracks, transverse cracks normal to the longitudinal axis caused by longitudinal stresses, diagonal tension cracks near the supports, and cracks in the diaphragms occurred at 2.25 times, and 1.34 times the service load for models a and b respectively. These cracking patterns were almost identical except that crackings in Model b were more pronounced and wider. Ultimate failure occurred at 4.5 times the service load in both models caused by diagonal tension cracking in the shell near the supports, and cracking in the supporting diaphragms that was produced by warping of the diaphragms induced by longitudinal strain in the plate elements. Both models sustained large mid-span deflections (1.6 in. for Model a and 3 in. for Model b before ultimate failure. It was concluded that ordinary folded plate theory could be used to predict the behavior in the working load range. while either folded plate theory or elementary beam theory will yield a satisfactory design in terms of deflections at working load, ultimate strength, and over-all behavior.

(n) Aldridge. In 1966, four reinforced microconcrete models simple span folded plate structures (1/8 scale) of six plates hat shape  were loaded to collapse, three of the four conducted by Aldridge,<sup>(7)</sup> one by Calvo<sup>(10)</sup> by

using "whiffle-tree" loading system through 512 discrete points to approximate a uniform loading at the University of Texas. All the units had the dimensions, width 4'-3/4", span 8'-0", plate thickness 4", rise (R) 11.5", span/rise = 8.35 except the fourth unit had 4'-0" span length. Models 1 and 2 were reinforced concrete model designed with folded plate theory, neglecting relative joint displacements and considering relative joint displacements for 1 and 2 respectively. The third unit was pretensioned reinforced concrete model designed with the folded plate theory considering relative joint displacements. The fourth unit was designed with folded plate theory considering joint displacements. The general behavior, cracking, deflections, and ultimate strength were observed. The overall cracking behavior of models 1, 2, and 3 were predominantly longitudinal action (transverse crack normal to the longitudinal axis) and only minor cracking in the direction of the ridge lines was noted. On the other hand the cracking in the direction of the ridge lines of the short model, Model 4, was more nearly balanced with flexural and diagonal tension cracking. The load-deflection response predictions by the linear elastic theory were too small in respect to the observed deflections. The ultimate strengths were predicted closely by ordinary reinforced concrete ultimate strength methods for simple beams (Nonlinear Beam Theory). The principal conclusions were: (1) the ultimate load

carrying capacities of the test structures were predicted closely by the Nonlinear Beam Theory, (2) The load-deflection responses predicted by the Nonlinear Beam Theory were in slightly better agreement than by that of the linear elastic theories, (3) The currently recognized linear elastic theories will provide a safe but uneconomically designed structure.

There is a good reason to believe that the end diaphragms supported on lubricated roller cages used in that test may provide the ideal simply supported boundary condition; however, it may also cause additional rotation of the end diaphragms which in turn produce additional deflection on the structure (deflection = rotation x distance).

## CHAPTER II

### METHOD OF ANALYSIS FOR SIMPLY SUPPORTED FOLDED PLATE STRUCTURES

#### 2.1 Linear Elastic Analysis Methods

Only two methods of the four categories listed in the introduction (1.4.1.1), Folded Plate Theory Neglecting Relative Displacements and Folded Plate Theory Considering Relative Joint Displacements are considered herein. For the other two methods the interested reader is referred to the bibliography of the papers (5,8,18,24,25,26,27,30,41,20, 22,51) listed at the end of this dissertation. Actually the method of "Folded Plate Theory Considering Relative Joint Displacements" covers the methods of "Folded Plate Theory Neglecting Relative Joint Displacements." With the fundamental and general assumptions listed in Sec. 1.4.1.1, the principle of superposition is applied with either the principle of virtual displacement (similar to the Influence Deflection Method for ordinary frame analysis) as suggested by Gaafar (15) or the principle of virtual force as suggested by Yitzhaki (16,17) in this analysis. Consequently, this analysis is divided into three parts, 1) Basic analysis, consists of two steps: (a) transverse slab analysis and (b) longitudinal plate analysis, 2) Correction Analysis

and 3) Superposition (see Fig. 2.1). In this study the principle of virtual force and the principle of superposition are employed. The analysis will be described in detail in Fig. 2.1 (Illustration of the principle of superposition, p.25).

### 2.1.1 Basic Analysis

The Basic Analysis is actually a "Folded Plate Theory Neglecting Relative Joint Displacements" as first presented in this country by Winter and Pei <sup>(11)</sup>.

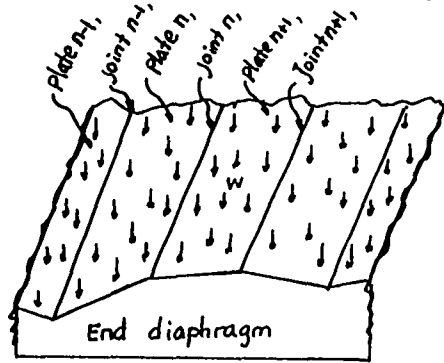
(a) Transverse slab analysis - All surface loads are considered as carried transversely by the plate acting as a series of continuous one-way slabs unyielding supported at the joints. (see Fig. 2.1b). Either the three-moment equation, slope-deflection, or moment distribution method can be used to compute the slab moments, the shears, and the reactions at each joint. Moment distribution is used in this study in hand calculations.

(b) Longitudinal plate analysis - The joint reactions obtained in transverse slab analysis are resolved into plate loads in the planes of the plates,  $P_{n,n-1} = r_n \frac{\cos \phi_n}{\sin \alpha_n}$ ,  $P_{n,n+1} = r_n \frac{\cos \phi_{n+1}}{\sin \alpha_n}$ ,  $P_n = P_{n,n-1} - P_{n-1,n}$  (see sec. 2.3.1), and from these loads computing the longitudinal stresses, and the free edge stresses in the plates by the elastic equations on the assumption that each plate carries its load independently of each other, considering each plate to be hinged along the longitudinal

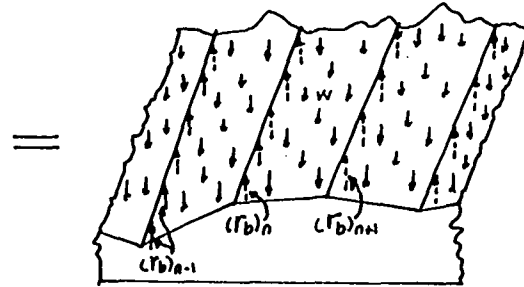
direction and reacted by shears along the plate plane at end diaphragms. Usually unequal free edge stresses result on the two sides of a common joint of two adjacent plates. This incompatibility should not exist, and longitudinal shears will develop at the joints to equalize the edge stresses. The equalized edge stresses can be achieved either by solving simultaneous first-degree equations of compatible longitudinal stresses <sup>(18)</sup> or free edge stress distribution <sup>(11)</sup>, a relaxation technique analagous to moment distribution. The free edge stress distribution method which is a relatively quick and simple method was used in this study for hand solutions. The longitudinal shearing forces,  $N_1, N_2, \dots, N_n, \dots$ , that occur at each joint to equalize the edge stresses need not be directly computed. On the contrary, the equalized edge stresses can be directly computed by distributing the unbalanced free edge stresses in proportion to the relative reciprocals of the plate areas, and carrying over to the other end by factor of -0.5 (see sec. 2.3.2 for stress distribution factors).

From the equalized edge stresses, the plate deflections at mid-span (maximum deflections) can be computed,  $(\delta_n)$  at mid-span =  $\frac{L^2}{2.6EH} (f_{n-1,n} - f_{n,n-1})$  (see sec. 2.3.3), and relative joint displacements are obtained geometrically either by analytical or graphical (a Williot diagram) methods. The analytical method is used in this study and the equations

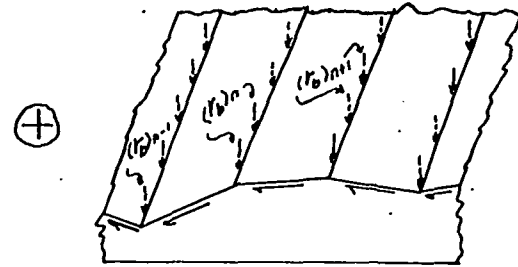
Figure 2.1 Illustration of the principle of superposition.



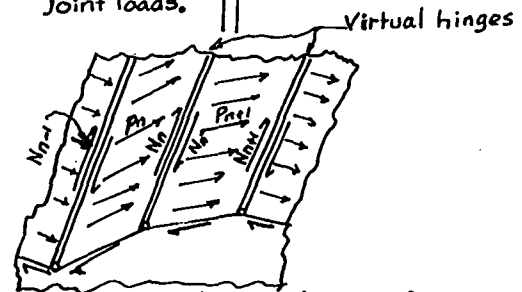
(a) Actual structure.



(b) Structure with virtual unyielding supports for continuous one-way slab analysis.



(c) Structure with virtual joint loads.

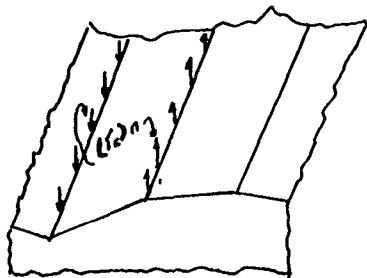


(c.1) Structure with virtual hinges for longitudinal plate analysis.

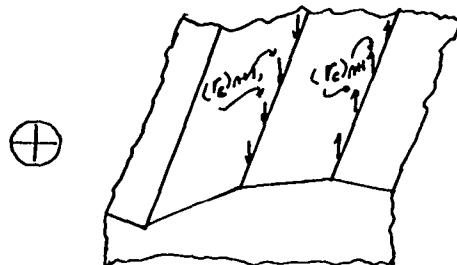


(c.2) Structure with virtual hinges for correction analysis.

⊙  $m_{n,n}$  and  $m_{n,n+1}$  are transverse moments.



(c.2.1) Structure with virtual forces (a couple) in plate n.



(c.2.2) Structure with virtual forces (a couple) in plate n+1.

used are:

$$\Delta_{n,n-1} = \delta_n \cot \alpha_n - \frac{\delta_{n+1}}{\sin \alpha_n} \quad (2.28)$$

$$\Delta_{n,n+1} = -\delta_{n+1} \cot \alpha_{n+1} + \frac{\delta_n}{\sin \alpha_n} \quad (2.29)$$

$$\Delta_n = -\frac{\delta_{n+1}}{\sin \alpha_n} + \delta_n (\cot \alpha_n + \cot \alpha_{n-1}) - \frac{\delta_{n-1}}{\sin \alpha_{n-1}} \quad (2.31)$$

(See sec. 2.3.4 for equations (2.28), (2.29) and (2.31).)

Generally speaking, where the span-to-rise (L/R) ratio and thickness-to-plate height (slab span) ratio are small, the "elastic supports" (plate joints) are relatively rigid and the relative joint displacements computed will be comparatively small. In other words the relative joint displacements are negligible. Consequently, the correction analysis can be ignored, and the preceding analysis will be referred to as a method of "folded plate theory neglecting joint displacements."

### 2.1.2 Correction Analysis

If the relative displacements ( $\Delta_{n-1}, \Delta_n$  etc.) are significant; in other words all joints deflect unequally, the correction analysis is required for both of the transverse one-way slab analysis and the longitudinal plate analysis in the basic analysis which satisfies only the statics condition. From the relative displacements the fixed-end moments can be found, for a hinged end  $M^f = 3EI \frac{\Delta_n}{h^2}$ , for the ends fixed  $M^f = 6EI \frac{\Delta_n}{h^2}$ , and the end moments, the shears and the reactions at each

joint can be obtained by following the same procedure of the transverse slab analysis in the basic analysis. The joint reactions obtained in the analysis due to the relative joint displacement created in the basic analysis should not exist, and will be corrected to null by applying an arbitrary couple successively to each plate. Practically a virtual unit couple (1 ft. #) is used and N-2 unknowns, which nullify the joint reactions, are determined by solving the N-2 simultaneous equations. The procedure in this correction analysis is the same as in the basic analysis except sine curve distributions are assumed for both the loading and the deflections instead of uniform load and parabolic deflection curves (see sec. 2.3).

### 2.1.3 Superposition

The results of the basic analysis are combined with those of correction analysis to give the final forces, shears, moments, stresses, and displacements.

## 2.2 Nonlinear, Inelastic Analysis Methods

In this study only one method, Nonlinear Beam Method, will be considered. This method has been well documented<sup>(52)</sup>, and has been widely accepted as a research tool. Nonlinear Beam Method uses the simple theory coupled with the Whitney stress block or Hognestad stress block<sup>(52)</sup> and the actual steel stress obtained from a stress-strain diagram as done by Glanville<sup>(26)</sup> and Aldridge<sup>(7)</sup>. In this study a Fortran

computer program LDDFN, which has been developed by Aldridge<sup>(7)</sup>, was used and is listed in Appendix A. The program computes the load-deflection and the load-moment responses of simple span reinforced concrete beams of generalized cross section loaded with uniformly distributed load or one or two concentrated loads. The program consists of a main program and three subroutines, AXLD, CMOM, SHAPE. Subroutine AXLD consists of two parts; the first part calculates the force in the concrete in the beam by using a modified Hognestad stress block and the assumption that strain distribution is linear (Bernoulli's hyperthesis), (see Fig. 2.6). The latter part calculates the forces in the steels in the beam by using actual stress obtained from a stress-strain curve which are read in the main program. With the forces and their locations on the cross section known, the resisting moment is calculated. Subroutine CMOM calculates the moment diagram, the values at each increment along the beam, for a single concentrated load, or two equal concentrated loads at any point on the beam, or a uniform load on the beam. Subroutine SHAPE uses the conjugate beam method and numerical integration (developed by Newmark and programmed by Breen<sup>(53)</sup>) to find load-deflection and load-moment responses.

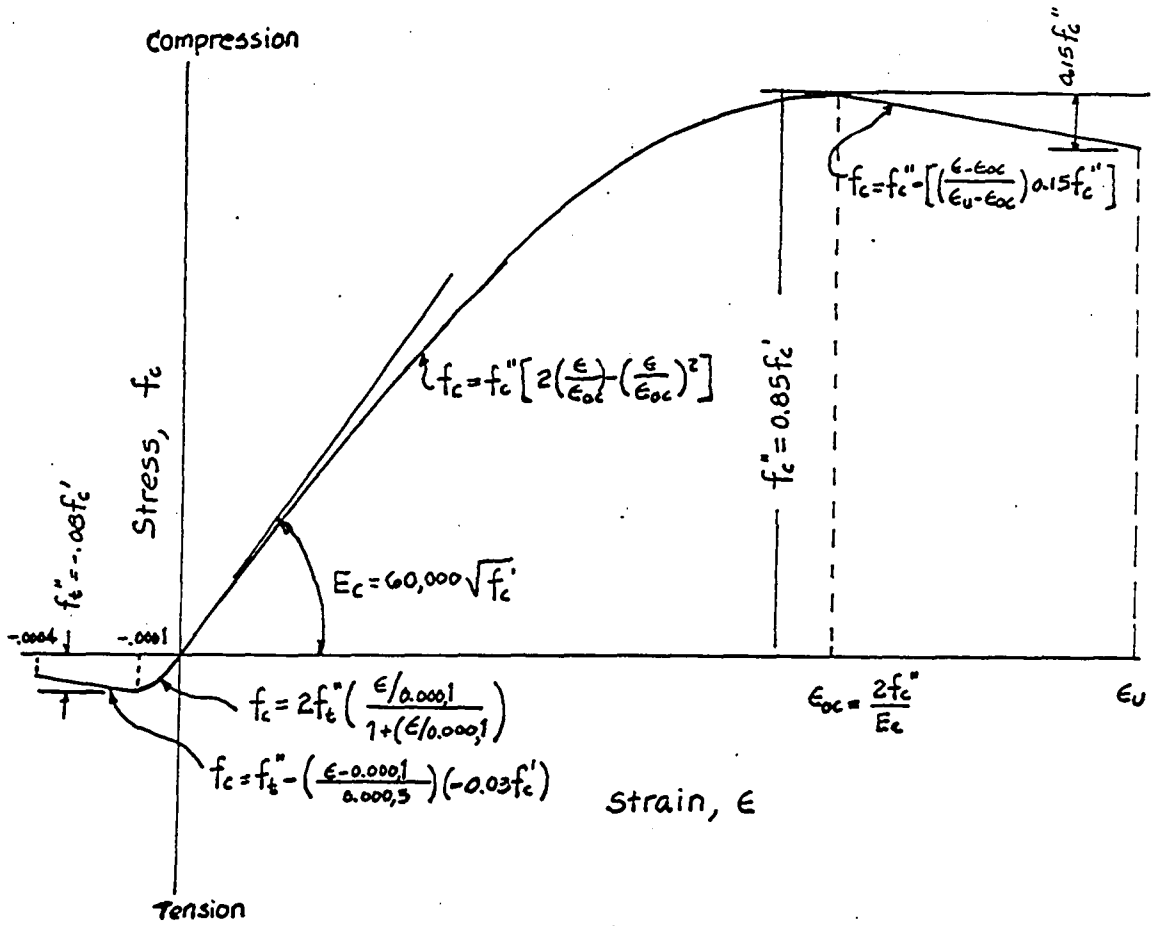


Figure 2.6 Modified Hognestad stress-strain curve.

<u>Variable in Figure 2.6</u>	<u>Variable used in computer</u>
$f_c$	FPC
$f_c''$	FPPC
$f_t''$	EPPT
$\epsilon$	EPS
$\epsilon_{oc}$	EPSIO
$\epsilon_u$	EPSMAX

2.3 Derivation of Equations

2.3.1 Plate Loads Resolved From The Vertical Joint Loads

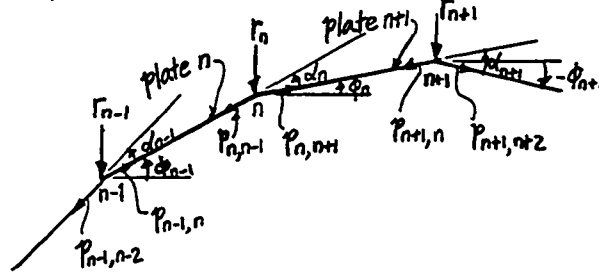
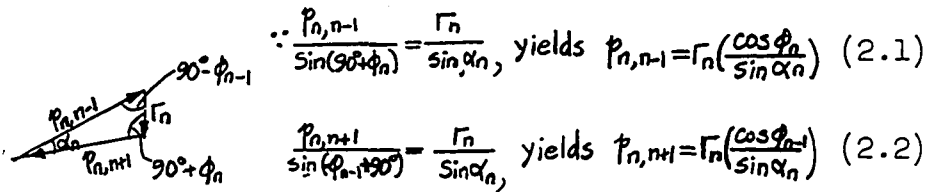


Fig. 2.2 Plate loads resolved from the vertical joint loads



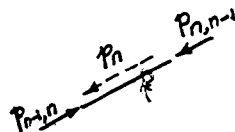
$$\therefore \frac{p_{n,n-1}}{\sin(90^\circ + \phi_n)} = \frac{\Gamma_n}{\sin \alpha_n}, \text{ yields } p_{n,n-1} = \Gamma_n \left( \frac{\cos \phi_n}{\sin \alpha_n} \right) \quad (2.1)$$

$$\frac{p_{n,n+1}}{\sin(\phi_n + 90^\circ)} = \frac{\Gamma_n}{\sin \alpha_n}, \text{ yields } p_{n,n+1} = \Gamma_n \left( \frac{\cos \phi_n}{\sin \alpha_n} \right) \quad (2.2)$$

Fig. 2.2a Joint n as F.B. Similarly,

$$p_{n-1,n-2} = \Gamma_{n-1} \left( \frac{\cos \phi_{n-1}}{\sin \alpha_{n-1}} \right) \quad (2.3)$$

$$p_{n-1,n} = \Gamma_{n-1} \left( \frac{\cos \phi_{n-2}}{\sin \alpha_{n-1}} \right) \quad (2.4)$$



$$p_n = p_{n,n-1} - p_{n-1,n} \quad (2.5)$$

Fig. 2.2b Plate n as F.B.

2.3.1a Maximum plate stresses at mid-span.

For uniform load,  $f_{n-1,n} = -f_{n,n-1} = \frac{M_n}{S_n} = \frac{p_n L^2}{8S_n} \quad (2.6)$

For sine curve load,  $f_{n-1,n} = -f_{n,n-1} = \frac{M_n}{S_n} = \frac{p_n L^2}{\pi^2 S_n} \quad (2.7)$

(here  $M_n = \frac{p_n L^2}{\pi^2}$  See Eq. (2.24))

### 2.3.2 Free Edge Stresses Distribution

The free edge stresses are mathematically analogous to fixed end moments; the relative reciprocals of the plate areas are analogous to the relative stiffness factors; and the carry-over factor of  $-1/2$  is analogous to  $1/2$  in the moment distribution.

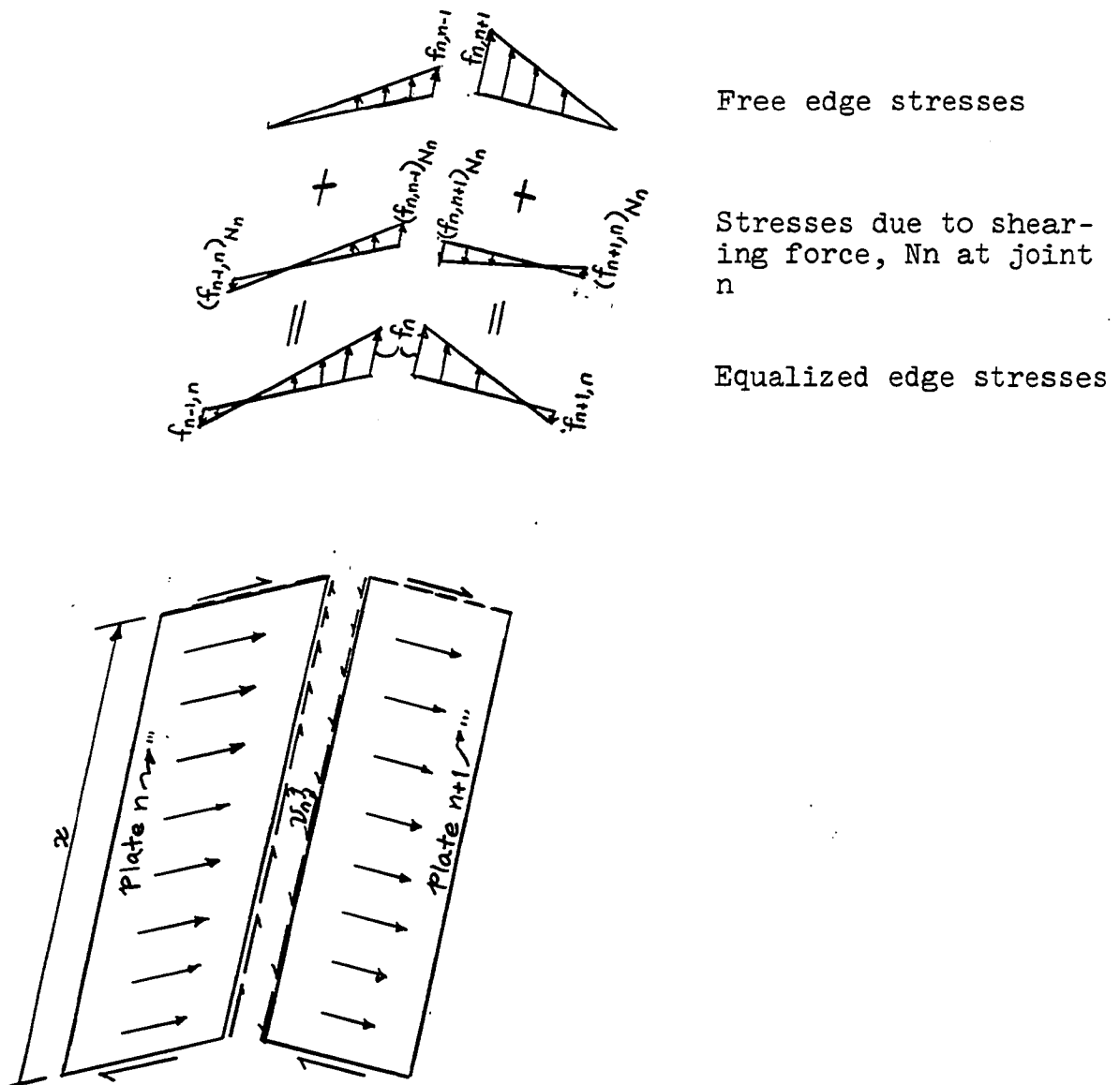


Fig. 2.3 Free edge stress distribution

The longitudinal shearing force which represents the sum of all the shearing stresses ( $N = \int vt \, dx$ ) along the plate edge causes direct and flexural stresses at the cross section:

$$\text{In plate } n, (f_{n-1,n})_{\text{due to } N_n} = \frac{N_n}{A_n} - \frac{M_n}{S_n} = \frac{N_n}{A_n} - \frac{N_n(\frac{h}{2})}{\frac{A_n h}{6}} = -2\left(\frac{N_n}{A_n}\right) \quad (2.8)$$

$$(f_{n,n-1})_{\text{due to } N_n} = \frac{N_n}{A_n} + \frac{M_n}{S_n} = \frac{N_n}{A_n} + \frac{N_n(\frac{h}{2})}{\frac{A_n h}{6}} = 4\left(\frac{N_n}{A_n}\right) \quad (2.9)$$

Carry over factor from joint  $n$  to joint  $n-1$ ,  $C_{n, n-1} = \frac{(f_{n-1,n})_{\text{due to } N_n}}{(f_{n,n-1})_{\text{due to } N_n}} = -1/2$

Similarly:

$$\text{In plate } n+1, (f_{n, n+1})_{\text{due to } N_n} = -4\left(\frac{N_n}{A_{n+1}}\right) \quad (2.10)$$

$$(f_{n+1, n})_{\text{due to } N_n} = 2\left(\frac{N_n}{A_{n+1}}\right) \quad (2.11)$$

Carry over factor from joint  $n$  to joint  $n+1$ ,  $C_{n, n+1} = -1/2$

$$\text{Equalized edge stresses, } f_n = f_{n-1} + \frac{4N_n}{A_n} = f_{n,n+1} - \frac{4N_n}{A_{n+1}}$$

$$\text{Solving for } N_n, \text{ gives } N_n = 1/4 \left( \frac{A_n A_{n+1}}{A_n + A_{n+1}} \right) (f_{n,n+1} - f_{n,n-1}) \quad (2.12)$$

Substituting into eqs. (2.9) and 2.10)

$$(f_{n, n-1})_{\text{due to } N_n} = \frac{A_{n+1}}{A_n + A_{n+1}} (f_{n,n+1} - f_{n,n-1}) \quad (2.13)$$

$$(f_{n, n+1})_{\text{due to } N_n} = -\frac{A_n}{A_n + A_{n+1}} (f_{n,n+1} - f_{n,n-1}) \quad (2.14)$$

Therefore,

Stress distribution factor of plate  $n$  at joint  $n$ ,

$$D_{n,n} = \frac{A_{n+1}}{A_n + A_{n+1}} \quad (2.15)$$

Stress distribution factor of plate  $n+1$  at

joint  $n$ ,

$$D_{n,n+1} = \frac{-A_n}{A_n + A_{n+1}} \quad (2.16)$$

### 2.3.3 Plate Deflections Expressed in Terms of Equalized Edge Stresses

Based on the general assumptions (1.4.1.1), the plate deflection,  $\delta$  can be expressed by the familiar second order ordinary differential equation,  $\frac{d^2\delta}{dx^2} = \frac{M}{EI} = \frac{1}{\rho}$  in terms of the moment and material properties, E and I. Further, the moment, M can be expressed in terms of equalized edge stresses. Consequently, the plate deflection can be expressed in terms of equalized edge stresses, material properties and plate dimensions as follows:

$$\text{From Fig. 2.4, } d\theta = \frac{dz}{\rho} = \frac{e_b dx}{c_b} = -\frac{e_t dx}{c_t} = \frac{e_b - e_t}{c_b + c_t} dx = \frac{e_b - e_t}{h} dx = \frac{f_b - f_t}{Eh} dx \quad (2.17)$$

$$\text{From the elementary theory of strength of material, } \frac{1}{\rho} = \frac{d\theta}{dx} = \frac{M}{EI} \quad (2.18)$$

Solving for M from (2.17) and (2.18), yields,

$$M = \frac{I}{h} (f_b - f_t) \quad (2.19)$$

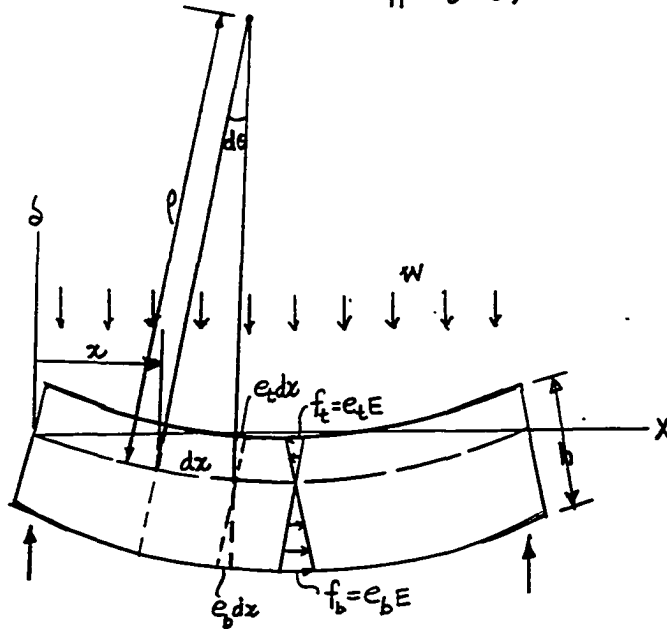


Fig. 2.4 Deflection versus edge stresses

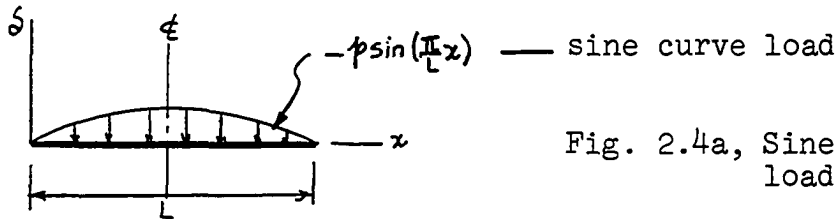
(a) For uniform load, the center span deflection (maximum deflection) which is very familiar to engineers, is:

$$\delta_{max.} = -\frac{5}{48} \frac{ML^2}{EI} \quad (2.20)$$

By substituting eq. (2.19) into eq. (2.20), yields:

$$\delta_{max.} = -\frac{5}{48} \frac{L^2}{Eh} (f_b - f_t) = -\frac{1}{9.6} \frac{L^2}{Eh} (f_b - f_t) \quad (2.21)$$

(b) For sine curve load, the center span deflection (maximum deflection) can be obtained by integrating twice of the second order differential equation of the deflection curve of beam,  $\frac{d^2\delta}{dx^2} = \frac{M}{EI}$ , then expressing in terms of the equalized edge stresses by using eq. (2.19).



From elementary theory of Strength of Materials,

$$V(\text{shear}) = (\text{sine curve load})dx = -\int p \sin\left(\frac{\pi}{L}x\right)dx = \frac{L}{\pi} p \cos\left(\frac{\pi}{L}x\right) + C_1 \quad (2.22)$$

$$\text{B.C. @ } x = \frac{L}{2}, V = 0, \text{ yields } C_1 = 0$$

$$M = \int V dx = \frac{L^2}{\pi^2} p \sin\left(\frac{\pi}{L}x\right) + C_2 \quad (2.23)$$

$$\text{B.C. @ } x = 0, M = 0, \text{ yields } C_2 = 0$$

$$\text{Max. } M \text{ occurs at center span and } M_{max} @ \frac{L}{2} = \frac{L^2}{\pi^2} p \quad (2.24)$$

$$\text{Slope } \theta = \frac{d\delta}{dx} = \int \frac{M}{EI} dx = \frac{L^2}{\pi^2} \frac{p}{EI} \int \sin\left(\frac{\pi}{L}x\right) dx = -\frac{L^3}{\pi^3} \frac{p}{EI} \cos\left(\frac{\pi}{L}x\right) + C_3 \quad (2.25)$$

$$\text{B.C. @ } x = \frac{L}{2}, \theta = 0, \text{ gives } C_3 = 0$$

$$\text{Plate deflection } \delta = \int \theta dx = -\frac{L^3}{\pi^3} \frac{p}{EI} \int \cos\left(\frac{\pi}{L}x\right) dx = -\frac{L^4}{\pi^4} \frac{p}{EI} \sin\left(\frac{\pi}{L}x\right) + C_4 \quad (2.26)$$

$$= -\frac{L^2}{\pi^2} \frac{M}{EI} + C_4$$

B.C@x=0 (or x=L),  $\delta=0$ , gives  $C_4=0$

By substituting eq.(2.19) into eq.(2.26), gives  $\delta = -\frac{L^2 l}{\pi^2 E h} (f_b - f_t)$  (2.27)

### 2.3.4 Relative Joint Displacements - Williot Diagrams

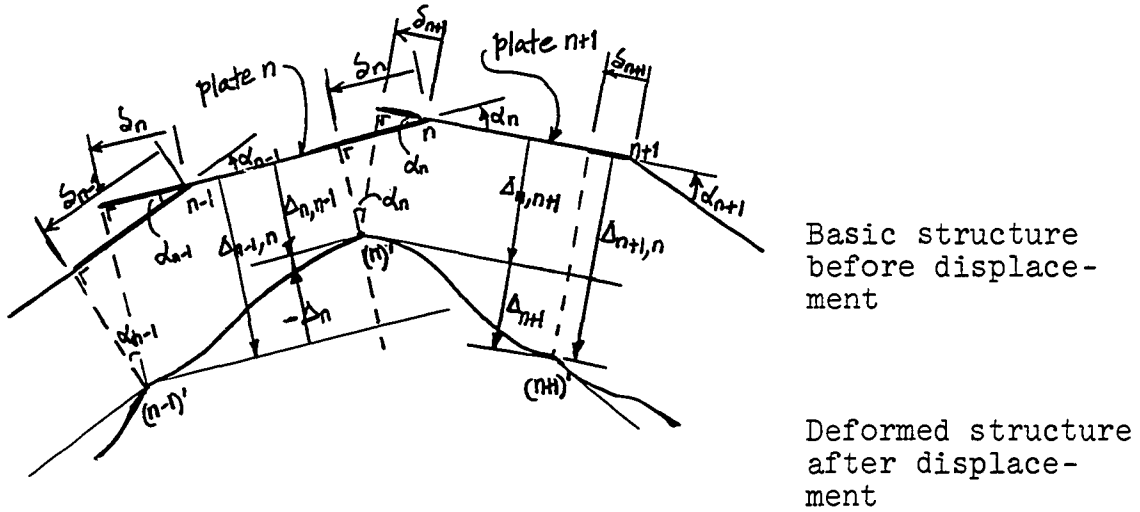


Fig. 2.5 Relative joint displacements - Williot diagrams

$$\therefore \frac{\Delta_{n,n-1}}{\delta_n - \frac{\delta_{n+1}}{\cos \alpha_n}} = \frac{\delta_{n+1}}{\delta_{n+1} \tan \alpha_n} = \cot \alpha_n, \text{ yields } \Delta_{n,n-1} = \delta_n \cot \alpha_n - \frac{\delta_{n+1}}{\sin \alpha_n} \quad (2.28)$$

$$\Delta_{n,n+1} = \frac{\Delta_{n,n-1}}{\cos \alpha_n} + \delta_{n+1} \tan \alpha_n = \frac{\delta_n}{\sin \alpha_n} - \frac{\delta_{n+1}}{\cos \alpha_n \sin \alpha_n} + \delta_{n+1} \tan \alpha_n$$

$$= (\delta_n / \sin \alpha_n) - \delta_{n+1} \cot \alpha_n \quad (2.29)$$

$$\text{Similarly, } \Delta_{n-1,n} = \frac{\delta_{n-1}}{\sin \alpha_{n-1}} - \delta_n \cot \alpha_{n-1} \quad (2.30)$$

From eqs. (2.28) and 2.30), yields

$$\Delta_n = \Delta_{n,n-1} - \Delta_{n-1,n} = -\frac{\delta_{n+1}}{\sin \alpha_n} + \delta_n (\cot \alpha_n + \cot \alpha_{n-1}) - \frac{\delta_{n-1}}{\sin \alpha_{n-1}} \quad (2.31)$$

## CHAPTER III

### COMPUTER STUDY OF VARIOUS GEOMETRIC ARRANGEMENTS OF FOLDED PLATE STRUCTURES

#### 3.1 Analysis Parameters

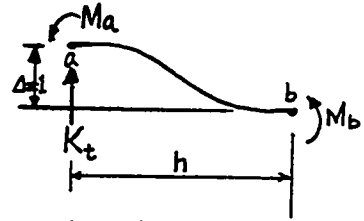
The forces (axial, shear, and moment) in folded plate structures are functions of  $L$ (span),  $h$ (plate height),  $t$ (plate thickness),  $\phi$ (the angle between plate and the horizontal) and  $\alpha$ (the angle between adjacent plates,  $\alpha$  maintained not less than  $15^\circ$  and not more than  $165^\circ$ ), and this can be expressed mathematically as  $F(f, v, m) = f(L, h, t, \phi, \alpha)$ . Since  $R$ (rise) is a function of  $h, \alpha$  and  $\phi$ , the force function can be rewritten as  $F(f, v, m) = f(L, R, t)$ . These parameters influence the range of applicability for a specific folded plate method listed in Sec. 1.4.1.1, and has been used to define practical limits of pure "beam" or pure "shell" behavior by several authors.<sup>(5,7,41)</sup> The stiffness, usually used in measuring the rigidity of a beam, is defined as that force (reaction, moment, etc.) which, when applied to a beam, will cause a unit deflection (a unit displacement, a unit rotation, etc.). Consequently, stiffness, transverse and longitudinal, is a

function of parameters mentioned above, and can be used to relate the interaction between beam and slab in the folded plate structure. Transverse and longitudinal stiffnesses can be derived from the equations in Sec. 2.3 as follows:

(a) Transverse Stiffness,  $K_t$  for Forces

$$M_a \text{ and } M_b \propto E \frac{I(\Delta)}{h(h)} \propto \frac{Et^3}{h^2} \Delta \quad (3.1)$$

$$R \text{ (or } V) \propto \frac{M_a + M_b}{h} \quad (3.2)$$



Substituting into eq. (3.2) with eq. (3.1) and dropping constants, yields  $R(\text{or } V) \propto \left(\frac{t}{h}\right)^3 \Delta$  (3.3)

$$K_t \propto \left(\frac{t}{h}\right)^3 \quad \text{with } \Delta=1, \quad (3.4)$$

(b) Longitudinal Stiffness,  $K_l$  for Forces

$$M_n = \frac{f_n L^2}{8} \propto \frac{r_n L^2}{\alpha_n \phi_n} \quad (\text{from eqs. 2.1 \& 2.5}) \quad (3.5)$$

$$f_n \propto \frac{M_n}{S_n} \propto \frac{r_n L^2}{t h^2 \alpha_n \phi_n} \propto \frac{r_n L^2}{t R^2} \quad (\text{from eq. 2.6}) \quad (3.6)$$

$$\delta_n \propto \frac{L^2}{h} (f_{n-1, n} - f_{n, n-1}) \propto \frac{r_n L^4}{t R^2 h} \quad (\text{from eq. 2.21}) \quad (3.7)$$

$$\Delta_n \propto \frac{\delta_n}{\alpha_n} \propto \frac{r_n L^4}{t R^2 h \alpha_n} \propto \frac{r_n L^4}{t R^3} \quad (\text{from eq. 2.31}) \quad (3.8)$$

$$\therefore r_n = \frac{t R^3 \Delta_n}{L^4} \quad (3.9)$$

$$K_l \propto \left(\frac{R}{L}\right)^3 \left(\frac{t}{L}\right) \quad \text{with } \Delta_n=1. \quad (3.10)$$

Thus the transverse and longitudinal rigidity can be measured by  $K_t \propto \left(\frac{t}{h}\right)^3$  and  $K_l \propto \left(\frac{R}{L}\right)^3 \left(\frac{t}{L}\right)$  respectively, and a relative rigidity coefficient  $C$ . between longitudinal and transverse action can be expressed as,

$$C = \frac{K_t}{K_l} = \left(\frac{t}{h}\right)^2 \left(\frac{L}{R}\right)^3 \left(\frac{L}{h}\right) \propto \left(\frac{t}{h}\right)^2 \left(\frac{L}{R}\right)^4 \quad (3.11)$$

The relative rigidity coefficient  $C$  has been used by several authors (5,7,41) as a definition of the range of applicability for a specific folded plate method. If the plate thickness-to-plate height ratio ( $t/h$ ) and the span-to-rise ( $L/R$ ) are small, the longitudinal deflection is small with respect to that of the transverse, and relative rigidity coefficient,  $C$  is much smaller. Therefore, the edges will remain in their position and the slab action prevails. This is the basic assumption for the plate theory neglecting joint displacements. However, if the  $t/h$  and the  $L/R$  are big, the longitudinal deflection is big with respect to that of the transverse ( $C$  is bigger) and effect of joint displacements cannot be ignored. Consequently beam action takes place and in the limiting case the structure behaves like an ordinary beam.

### 3.2 Range of Applicability for the Various Analysis Methods

Eq. (3.11) can be written as  $\left(\frac{L}{R}\right)^4 = k \left(\frac{h}{t}\right)^2$ , where  $k$  is a constant. (3.12)

In usual engineering practice, the folded plate structure has normally a limited range of the  $h/t$  ratio, 20 to 24 for reinforced concrete structures; therefore, the lower or higher limit of the  $L/R$  ratio may be developed by using Eq. (3.12) for the various analysis methods.

Whitney, Anderson, and Birnbaum<sup>(5)</sup> have described folded plate structures for small, intermediate and long structures by using Eq. (3.12), analogous to the classification

of short, intermediate and long columns based on the slender-ratio. These authors recommended the use of different analysis methods based on the L/R ratio as tabulated in Table 3.1:

Span-to-rise ratio L/R	Method of solution recommended
Small (L/R not described)	Folded Plate Theory Neglecting Relative Displacement
Intermediate (L/R < 10)	Folded Plate Theory Considering Relative Displacement
Long (L/R > 10)	Beam Theory designed by ultimate strength or working stress methods with the investigation for the effects of deflection and that of load on the end plate.

Table 3.1 Solution methods recommended by Whitney, et.al. for different values of the L/R ratio.

A similar classification was made of most of the previously tested models and prototype structures listed in the previous test data (Sec. 1.4.2) by Aldridge<sup>(7)</sup> (Fig. 3.1). The author based his study on a slightly modified version of the general equation (Eq. 3.12). The equation used was:

$$L/R = a \sqrt{h/t} \quad (3.13)$$

Where, a is a constant dependent upon the folded plate system. In this figure, the test structures are separated by two arbitrary dividing curves with  $a = 1.58$  and  $a = 2.00$ ,

which tends to distinguish the "beam" type failures from those of the "slab" type failures. The letters "L", "T", "DL" represent "beam", "slab" and "shear diagonal tension" failure respectively. Clearly the most of the previously tested structures fell into the intermediate range ( $L/R = 4$  to  $12$ ) with  $h/t$  ratios greater than 15. The effect of variations in span to rise ratios of folded plate structures was also studied by Calvo,<sup>(10)</sup> who reported that changes of transverse moment at some joints as high as 1700% for  $L/R$  of 19.6 compared with the basic transverse moment due to joint displacement calculated by the linear elastic plate theory.

(See page 41 for Figure 3.1 Dimensional Parameters and Collapse Mode)

### 3.3 Computer Study of Various Geometric Arrangements of Prototype Folded Plate Structures

The principal objective of this computer study was to find the effects of geometric parameters on the various shapes of ordinary folded plate structures. From this study a representative prototype structure was selected for a direct model test.

The prototype simply supported folded plate structures used in this study were:

1. 6-plates sawtooth unit (  Fig. 3.2.1),
  2. 6-plates hat unit (  Fig. 3.2.2,  Fig. 3.2.3),
- and

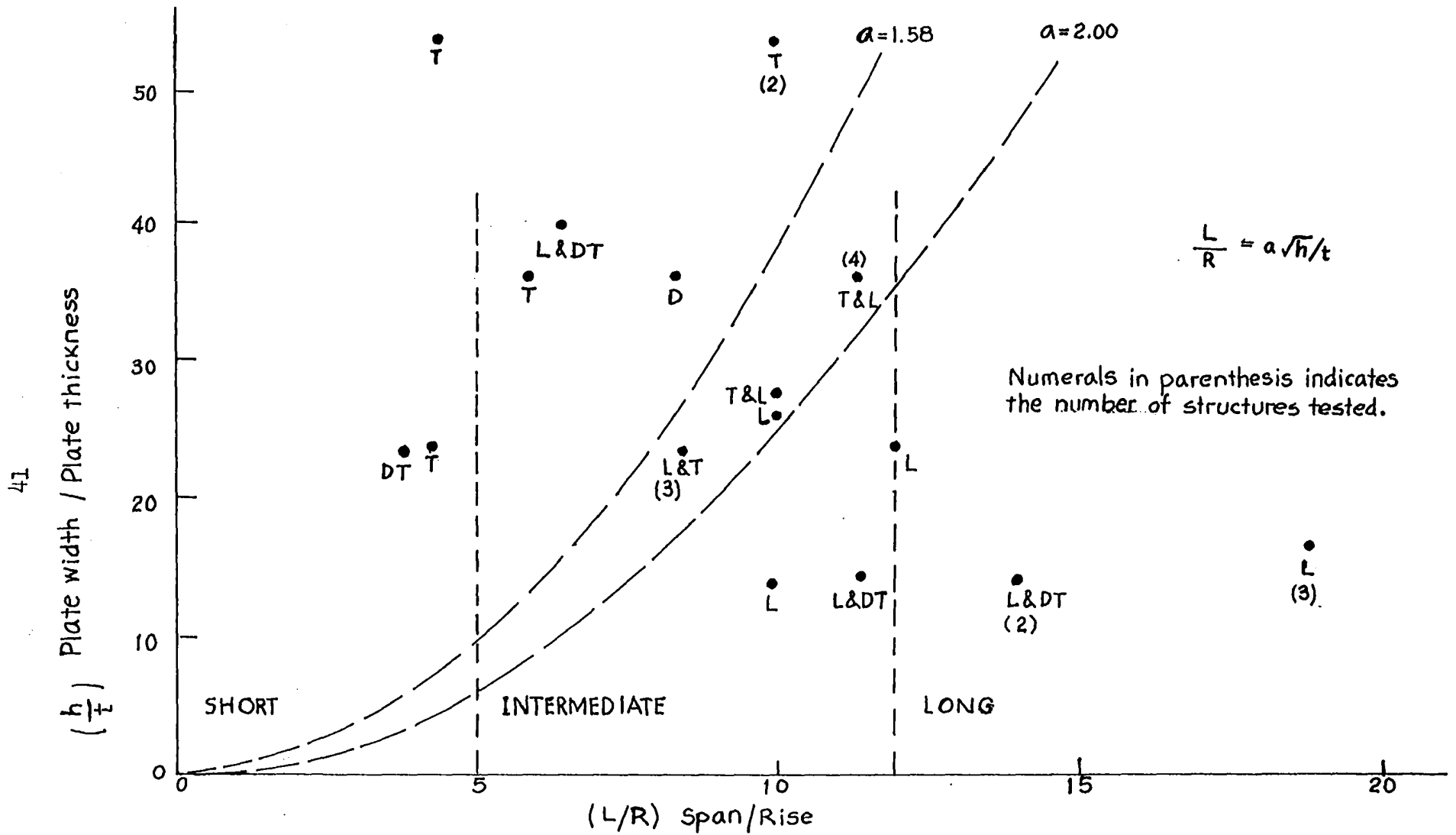


Figure 3.1 Dimensional parameters & collapse mode<sup>(7)</sup>

3. 8-plates unit ( Fig. 3.2.4) with the h/t ratio of 18, 19.2, 24 and 36, the L/R ratio between 2 and 46.8, and various lengths of cantilever edge plate.

All structures were symmetrical in geometry and loading (constant plate thickness of 3.75 in. or 4.0 in. with live load of 30 PSF on the horizontal projection) and were solved with Fortran computer programs named YIT3 (for 3-plates symmetrical) and YIT4 (for 4-plates symmetrical) (see Appendix B). These programs were originally written by Aldridge<sup>(7)</sup> and were later modified by the writer. These programs were developed using Yitzhaki's method<sup>(17)</sup> - one of the folded plate theories which considers the effect of joint displacements. The salient features of the forces (transverse moments and longitudinal stresses) versus the L/R are shown in Figures 3.3.1 to 3.3.8. Clearly all Figures 3.3.1 to 3.4 show that all curves are flat at the beginning and the ending indicating the slab action in first range, beam action in the last range and mixed action in middle range.

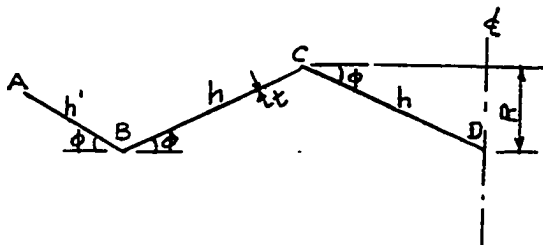
The pure beam action takes place when the L/R is infinite; however, beam action prevails when the  $L/R > 50$  for all structures.

Figures also show that curves with shorter edge plates scatter more indicating the disturbance caused by edge plates (see curves lalc, lald vs. la3c and la3d in

fig. 3.3.1). The influence of edge plate on range of slab action is also shown in the figures. For instance, in figure 3.3.1, range of slab action for structure la1 with  $h' = 1/2h$  is shown by the L/R ratio between 0 to 9 in compared to the L/R ratio between 0 to 15 with that of structure la3 with  $h' = h$ .

The effects of variation of  $\alpha_n$  and  $\phi_n$  in different types of cross section can be seen with comparison between figure 3.3.1 and 3.3.2. Curves in figure 3.3.2 scatter more and range of slab action becomes shorter than that of figure 3.3.1.

Strs.    la1,    la2,    la3  
           lb1,    lb2,    lb3  
           lc1,    lc2,    lc3  
           ld1,    ld2,    ld3




---

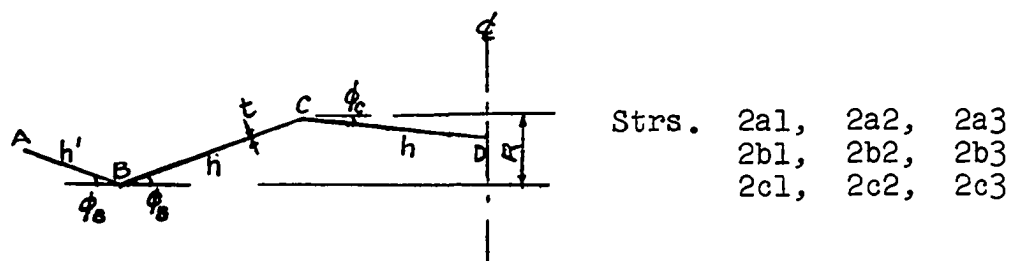
Descriptions of structures

---

Str.	t(in.)	R(ft.)	h(ft.)	$\phi$ (Degree)	h/t	R/t	h'(ft.)
la1							3
la2	4	2.052	6	20	18	6.2	4.5
la3							6
lb1							3
lb2	3.75	2.052	6	20	19.2	6.6	4.5
lb3							6
lc1							4
lc2	4	2.736	8	20	24	8.2	6
lc3							8
ld1							4
ld2	4	4	8	34	24	12.0	6
ld3							8
le1							6
le2	4	6	12	30	36	18.0	9
le3							12

---

Figure 3.2.1 6-Plates sawtooth unit




---

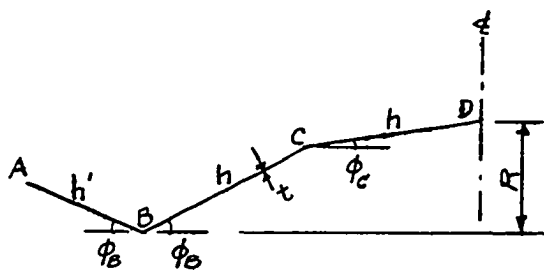
 Descriptions of structures
 

---

Str.	t(in.)	R(ft.)	h(ft.)	$\phi_B$ (Degree)	$\phi_C$ (Degree)	h/t	R/t	h'(ft.)
2a1								3
2a2	4	2.052	6	20	7.5	18	6.2	4.5
2a3								6
2b1								3
2b2	3.75	2.052	6	20	7.5	19.2	6.6	4.5
2b3								6
2c1								4
2c2	4	2.736	8	20	7.5	24	8.2	6
2c3								8

---

Figure 3.2.2 6-Plates hat unit ( )



Strs. 3a1, 3a2, 3a3  
 3b1, 3b2, 3b3  
 3c1, 3c2, 3c3

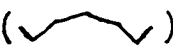
---

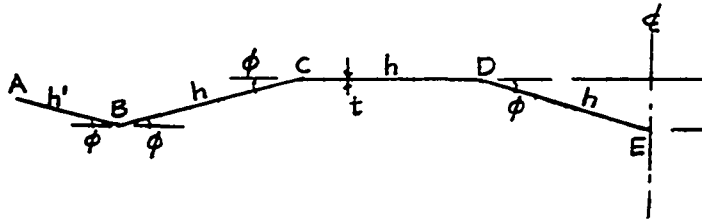
Descriptions of structures

---

Str.	t(in.)	R(ft.)	h(ft.)	$\phi_B$ (Degree)	$\phi_C$ (Degree)	h/t	R/t	h'(ft.)
3a1								3
3a2	4	2.835	6	20	7.5	18	8.5	4.5
3a3								6
3b1								3
3b2	3.75	2.835	6	20	7.5	19.2	9.6	4.5
3b3								6
3c1								4
3c2	4	3.780	8	20	7.5	24	11.35	6
3c3								8

---

Figure 3.2.3 6-Plates hat unit (  )



Strs. 4a1, 4a2, 4a3

Descriptions of structures							
Str.	t(in.)	R(ft.)	h(ft.)	φ(Degree)	h/t	R/t	h'(ft.)
4a1							4
4a2	4	2.736	8	20	24	8.2	6
4a3							8

Figure 3.2.4 Eight plates unit

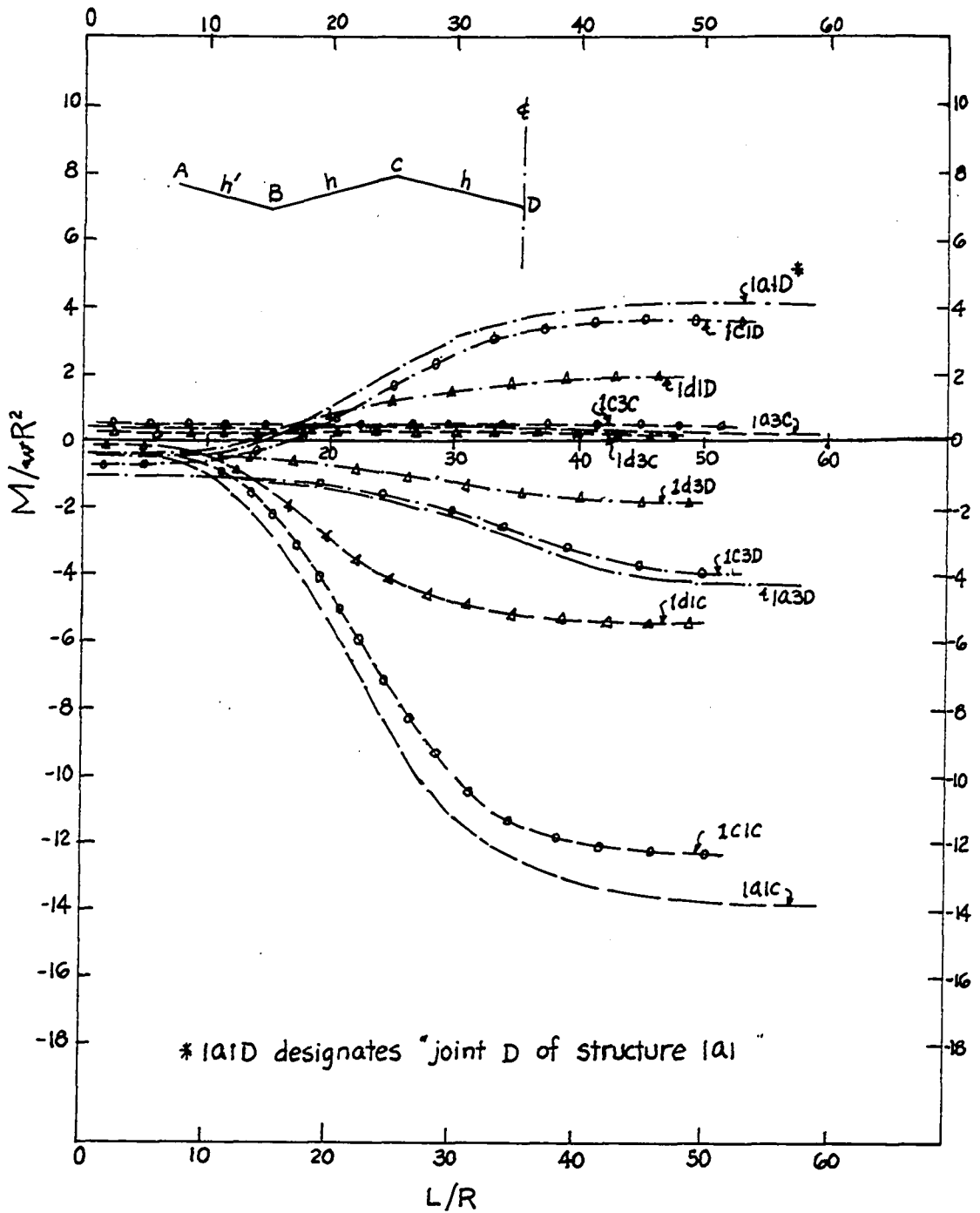


Figure 3.3.1  $M/wR^2$  vs  $L/R$ .  
Structures 1a1, 1a3, 1d1 and 1d3.

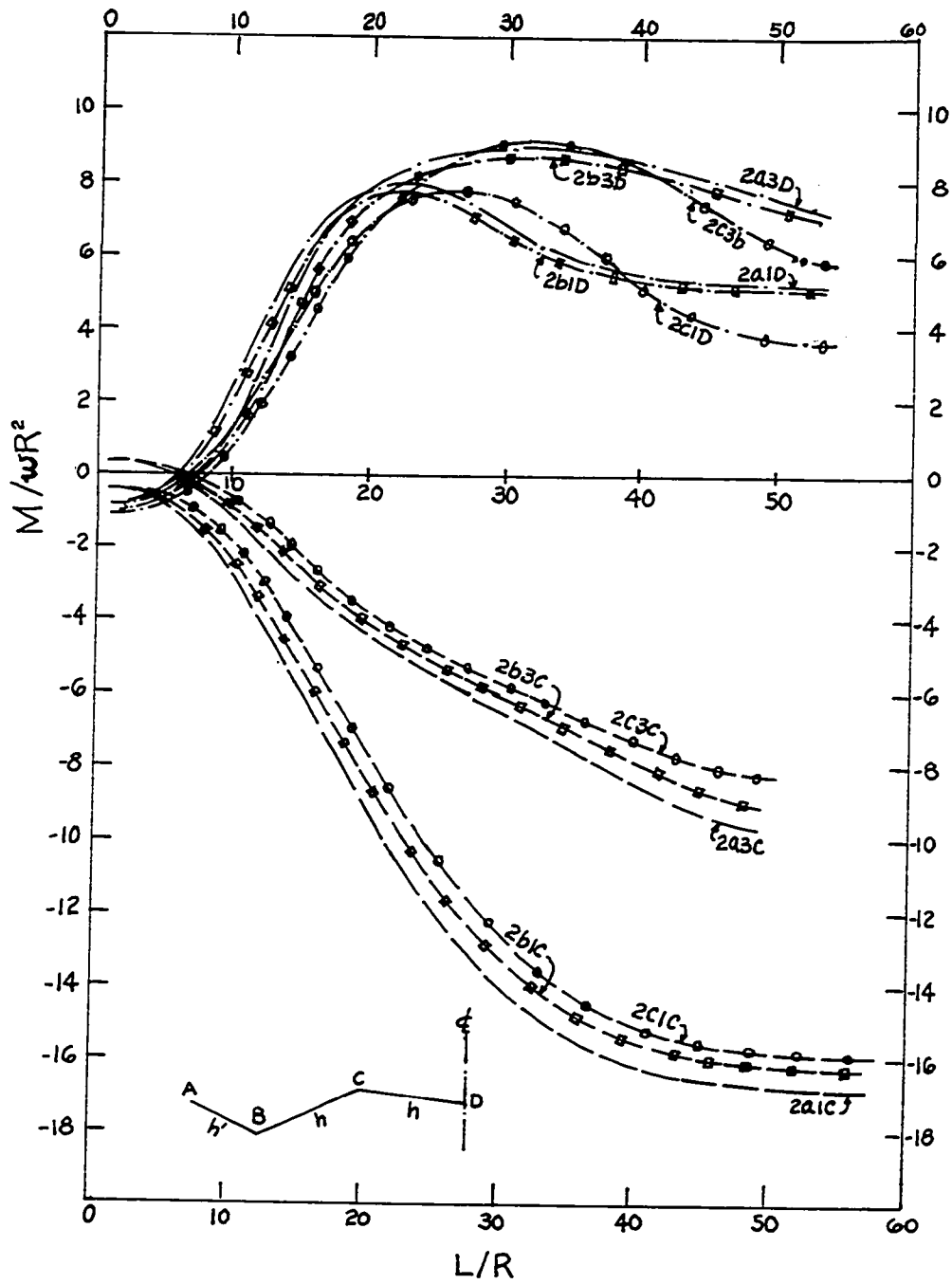


Figure 3.3.2  $M/wR^2$  vs  $L/R$ .  
Structures 2a1, 2a3, 2b1, 2b3, 2c1 and 2c3.

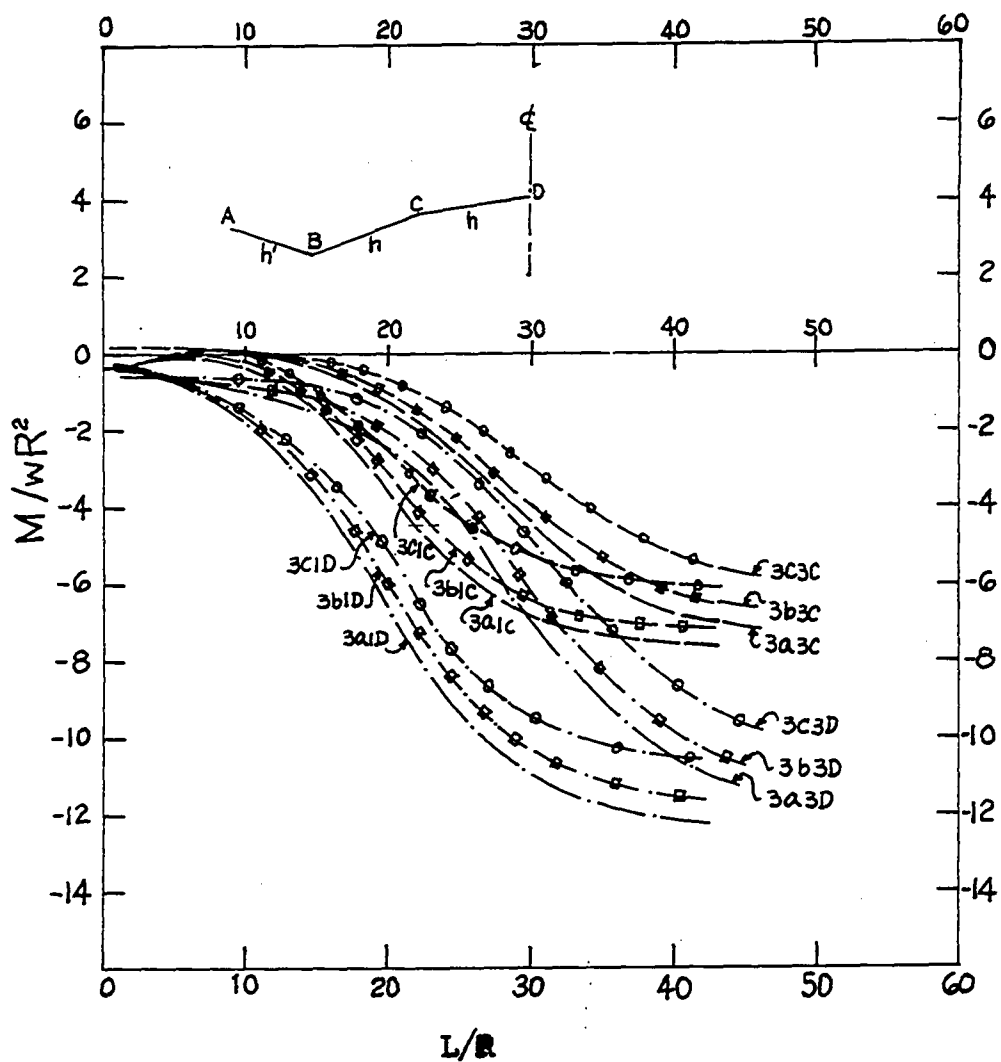


Figure 3.3.3  $M/wR^2$  vs  $L/R$ .  
Structures 3a1, 3a3, 3b1, 3b3, 3c1 and 3c3.

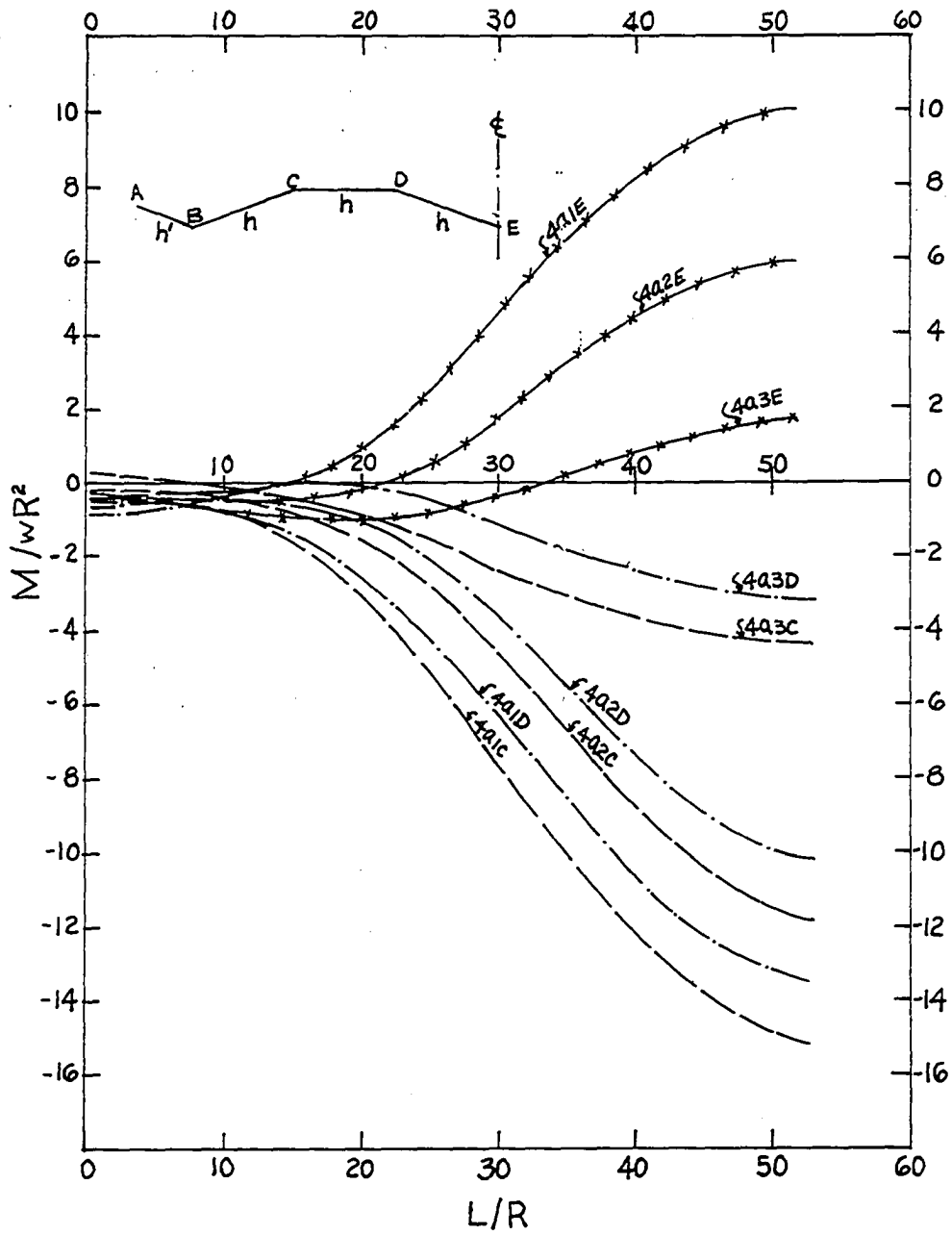


Figure 3.3.4  $M/wR^2$  vs  $L/R$ .  
Structures 4a1, 4a2 and 4a3.

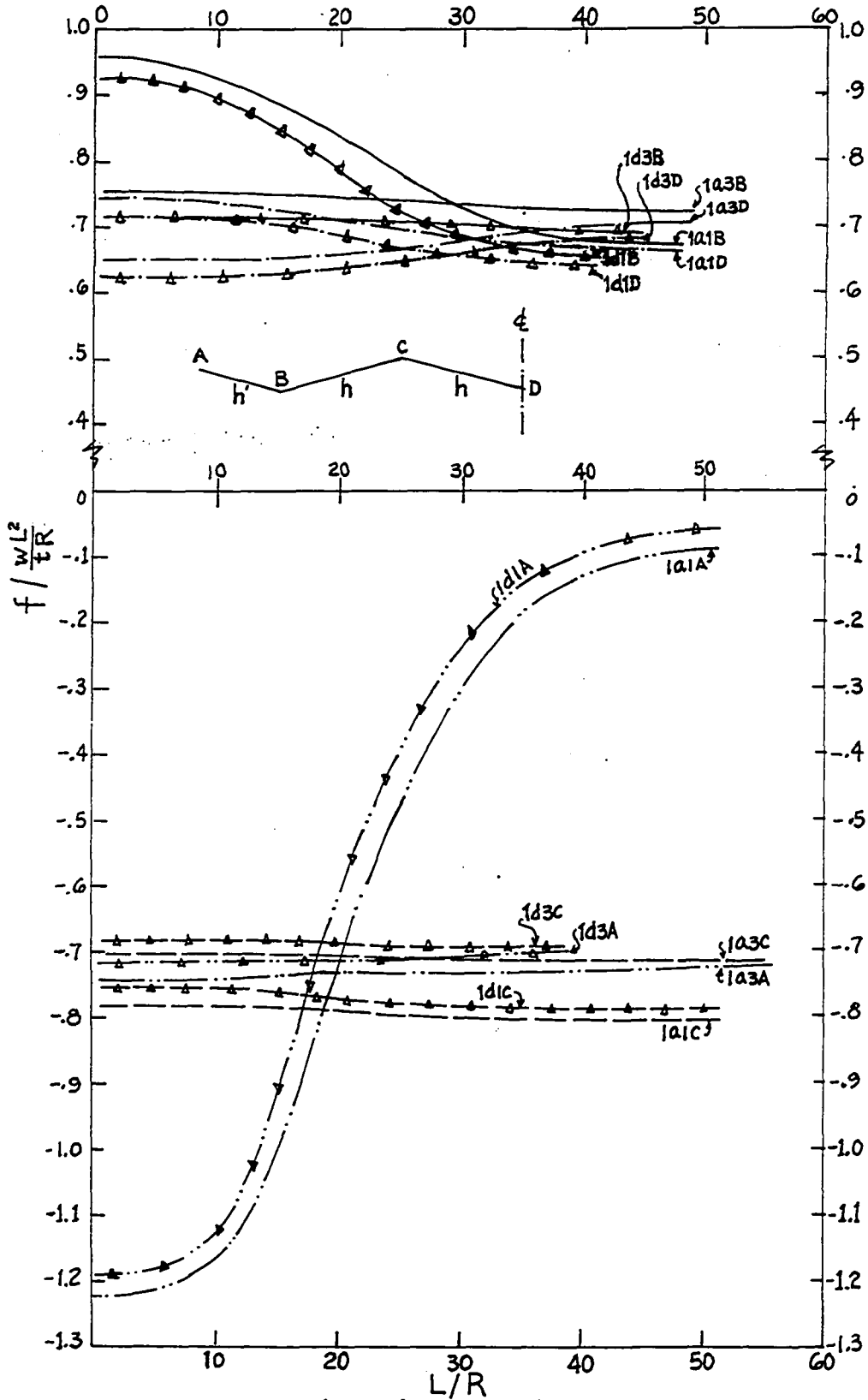


Figure 3.3.5  $f/(WL^2/TR)$  vs  $L/R$ .  
Structures 1a1, 1a3, 1d1 and 1d3.

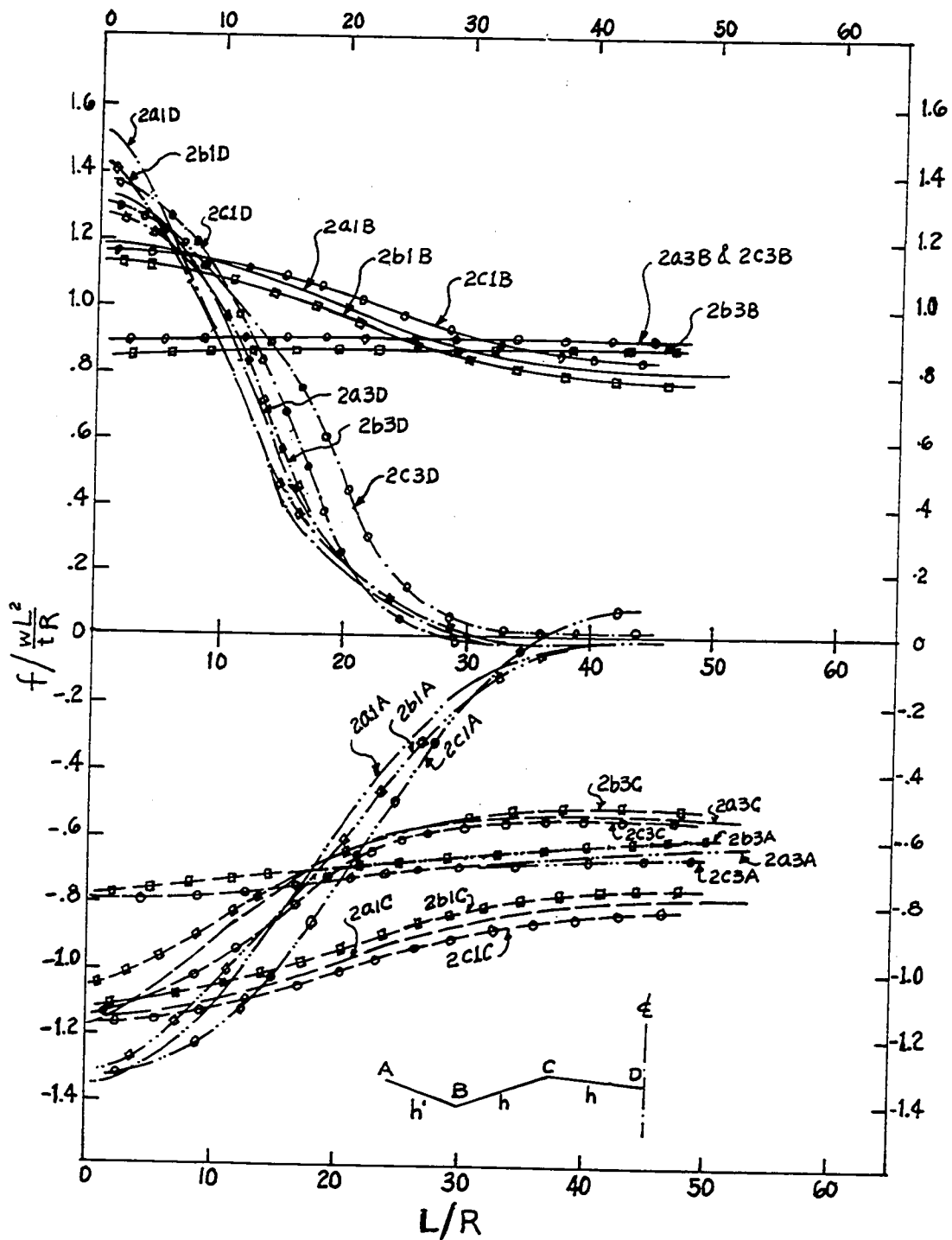


Figure 3.3.6  $f/(wL^2/tR)$  vs  $L/R$ .  
Structures 2a1, 2a3, 2b1, 2b3, 2c1 and 2c3.

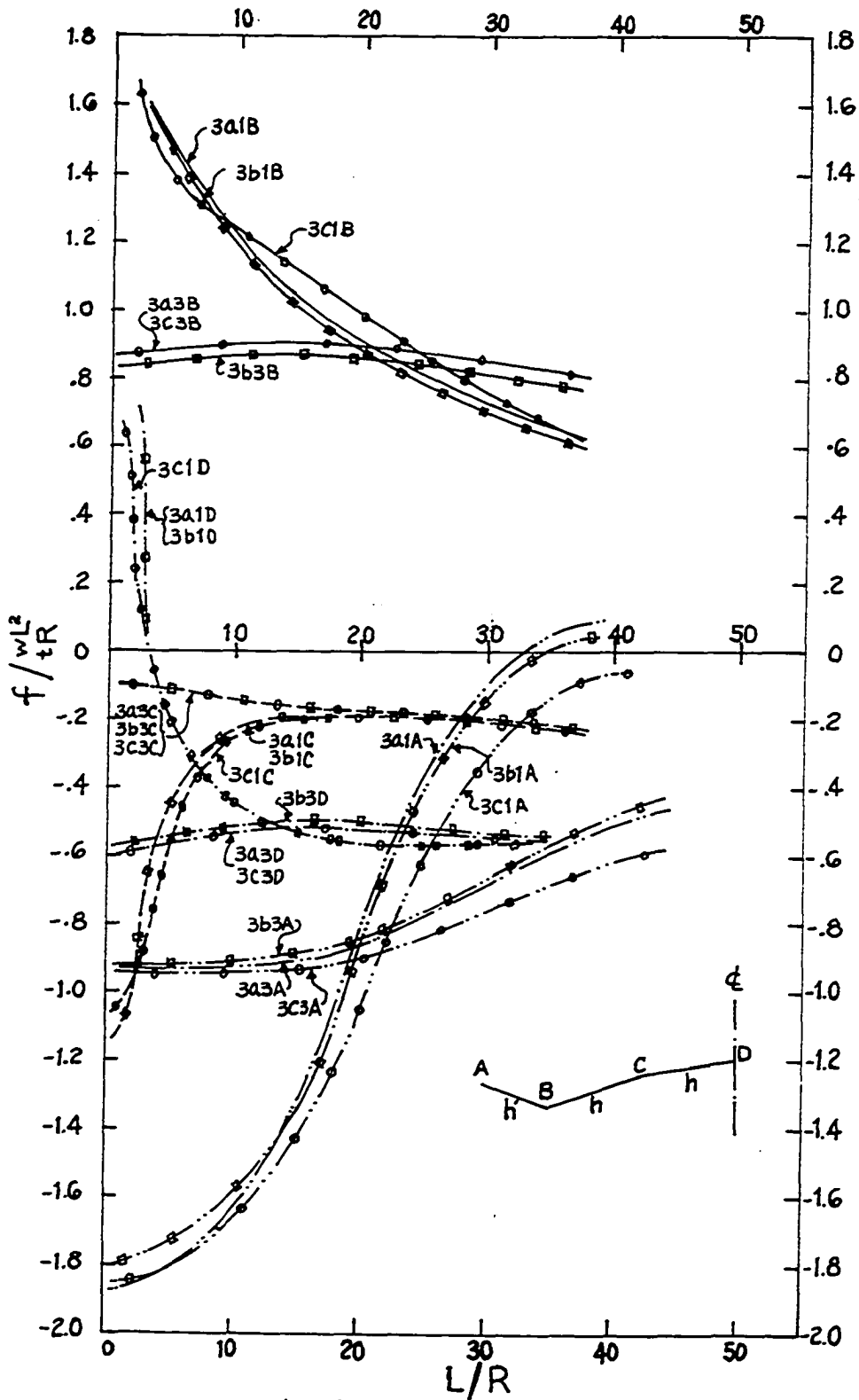


Figure 3.3.7  $f/(wL^2/tR)$  vs  $L/R$ .  
 Structures 3a1, 3a3, 3b1, 3b3, 3c1 and 3c3.

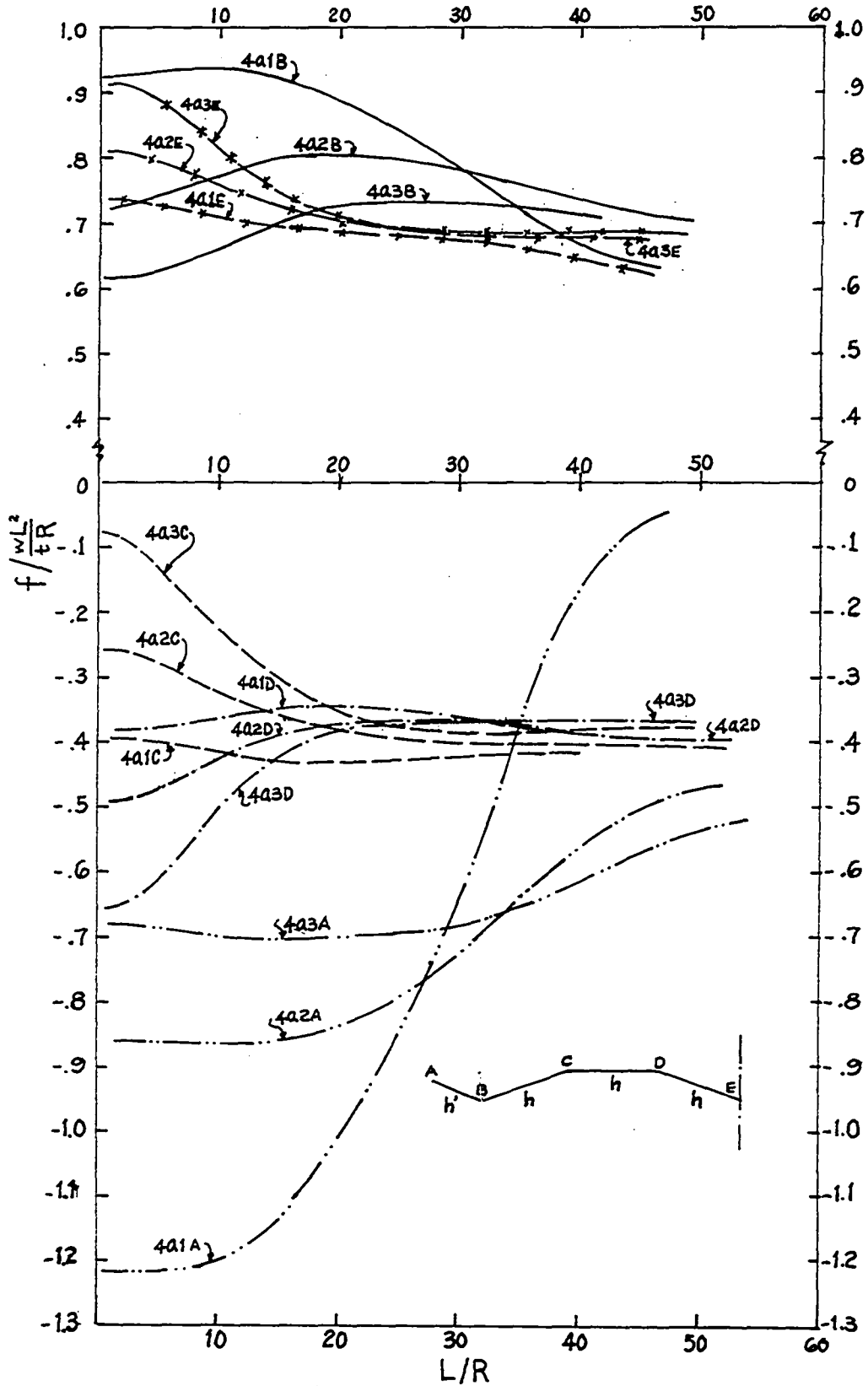


Figure 3.3.8  $f/(wL^2/tR)$  vs  $L/R$ .  
Structures 4a1, 4a2 and 4a3.

### 3.4 Conclusion

The results of the computer study may be summarized as follows:

(a) Common characteristics for all structures with a similar section ( $\alpha_n$ ,  $\phi_n$  are constant) are:

1. The slab action prevails for the high  $h/t$  and low values of  $L/R$ , and conversely beam (longitudinal) action prevails for the lower  $h/t$  and higher  $L/R$ . If  $L/R = \infty$ , the structures behave like an ordinary beam ( $M/wR^2$  and  $f/(wL^2/tR)$  are constant). However, the transverse moments are not zero. This will be called "pure beam action". This characteristic actually demonstrates the validity of Eq. (3.11) which expresses the relation between longitudinal and transverse rigidity.
2. The effects of edge plate cantilever are extremely significant. The slab action deviates more from the beam action in the shorter cantilever.

(b) For different types of cross section, the effects of variation of  $\alpha_n$  and  $\phi_n$  are significant. The slab action deviates more from beam action in the flat system (  ) with small angles  $\alpha_n$  and  $\phi_n$ . The ranges of slab and beam actions vary with the different types of section. The linear elastic solution methods related to the range of the  $L/R$  are tabulated in Table 3.4.

Structure	L/R	Recommended Method of Solution
6-plates sawtooth unit	Slab action range $L/R < 9$ for $h'/h < 3/4$ $> 15$ for $h'/h \geq 3/4$	The folded plate theory neglecting joint displace- ments
(  )	Mixed actions range $L/R \geq 9$ for $h'/h < 3/4$ $> 15$ for $h'/h \geq 3/4$	The folded plate theory considering joint dis- placements
6-plates unit	Slab action range $L/R < 4$ for $h'/h < 3/4$ $< 5$ for $h'/h \geq 3/4$	The folded plate theory neglecting joint displace- ments
(  )	Mixed action range $L/R \geq 4$ for $h'/h < 3/4$ $> 5$ for $h'/h \geq 3/4$	The folded plate theory considering joint dis- placements
6-plates unit	Slab action range $L/R < 6$ for $h'/h < 3/4$ $< 10$ for $h'/h \geq 3/4$	The folded plate theory neglecting joint displace- ment
(  )	Mixed action range $L/R \geq 6$ for $h'/h < 3/4$ $> 10$ for $h'/h \geq 3/4$	The folded plate theory considering joint displace- ment
8-plates unit	Slab action range $L/R < 7.5$ for $h'/h < 3/4$ $< 10$ for $h'/h \geq 3/4$	The folded plate theory neglecting joint displace- ment
(  )	Mixed action range $L/R \geq 7.5$ for $h'/h < 3/4$ $> 10$ for $h'/h \geq 3/4$	The folded plate theory considering joint displace- ment

Table 3.4 Solution Methods Recommended By  
Linear Elastic Methods

Where the  $L/R > 50$ , beam action prevails in all folded plate structures regardless of section and the beam theory

may be used for analysis and design. However, there is no way to determine transverse moments by this method unless some assumption is made for the determination of these moments. For example, a completely reasonable analysis method might include the beam method for longitudinal stresses and a one-way slab on unyielding supports for the transverse moments.

## CHAPTER IV

### ANALYSIS AND DESIGN OF THE TEST SPECIMEN

#### 4.1 General

Following careful comparison and evaluation of the results of the computer study of various geometric arrangements (Chapter III) a representative prototype structure (Fig. 4.1), which has ordinary dimensions (its existence in the form of real structures is obvious<sup>(5)</sup>), was selected for a direct model test (1/8 scale). This particular geometrical arrangement has not been previously investigated.

The selected prototype structure was first analyzed and designed by two different linear elastic methods -- the folded plate theory neglecting relative joint displacements and the folded plate theory considering relative joint displacements -- in accordance with the "ASCE Task Committee's Report"<sup>(1)</sup>, the "ACI Committee on Shell Structures"<sup>(2)</sup>, and "ACI 318-63, Building Code Requirements for Reinforced Concrete"<sup>(3)</sup> (Sec. 4.2.1 and 4.2.2). The results of the two different analyses and designs were compared and evaluated to choose the method feasible for actual construction (Sec.

4.2.3). The overall behaviors of prototype structure, moment-rotation and load-deflection responses, were then calculated by the "Program LDDFN" representing a nonlinear beam method (Sec. 4.3). Finally the selected prototype structure was scaled down (1/8 scale) to model proportions (Sec. 4.4.3).

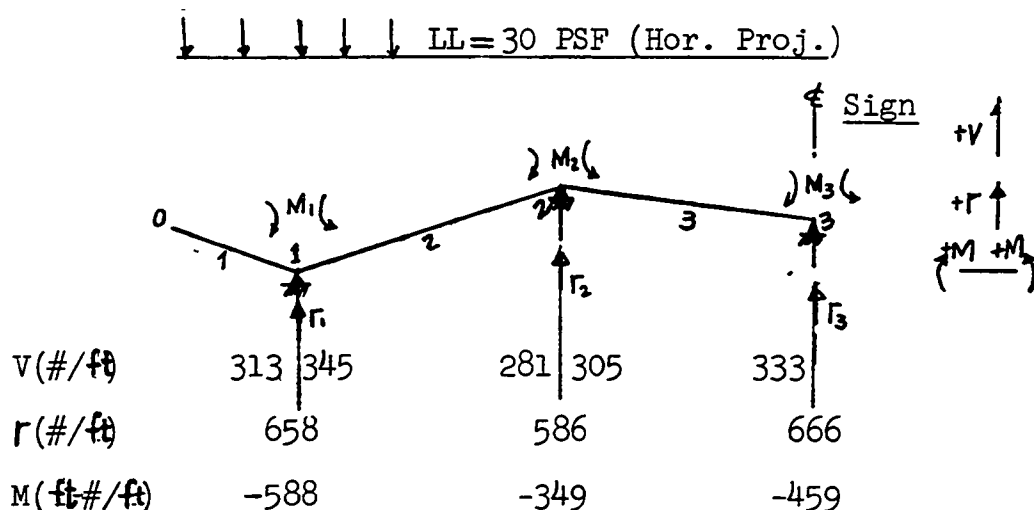
## 4.2 Prototype Structure Analysis and Design by Linear Elastic Methods

### 4.2.1 Analysis

The selected prototype structure with dimensions shown in Fig. 4.1 was designed for a live load of 30 psf uniformly distributed over the horizontal projection following the procedures listed in Sec. 2.1.

a. Basic Analysis (Folded plate theory neglecting displacements)

a.1 Transverse Slab Analysis:



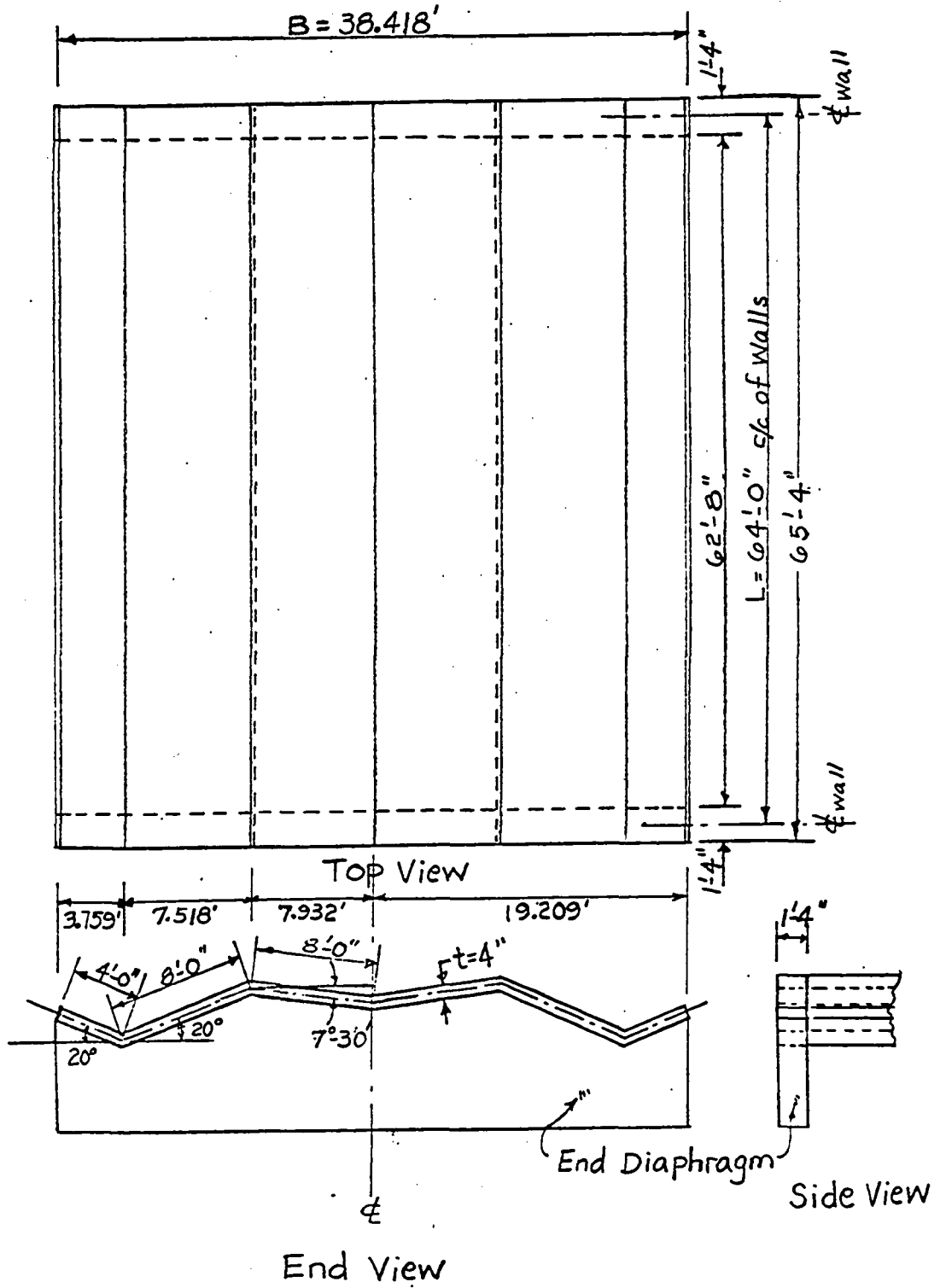
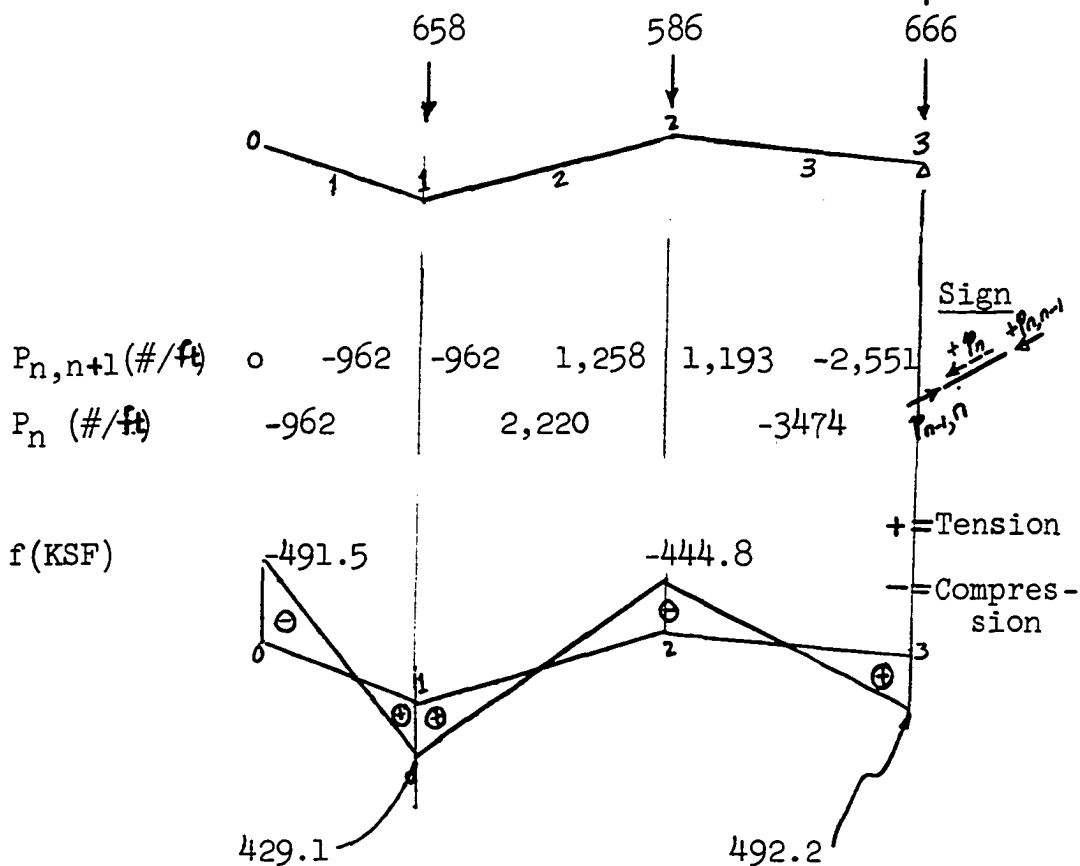
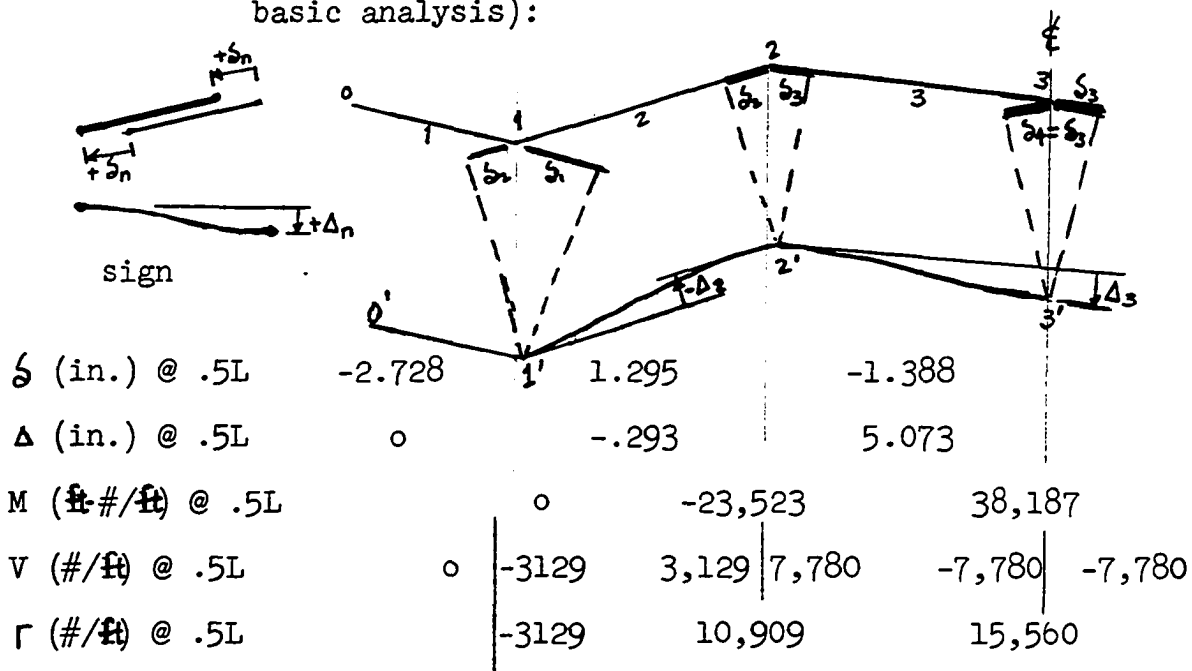


Figure 4.1 Prototype structure

a.2 Longitudinal Plate Analysis:

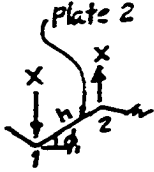


a.3 Longitudinal Plate Analysis \* (continued from the basic analysis):



The values,  $r_1$ ,  $r_2$  and  $r_3$  should not exist and would be brought to null by the following correction analysis.

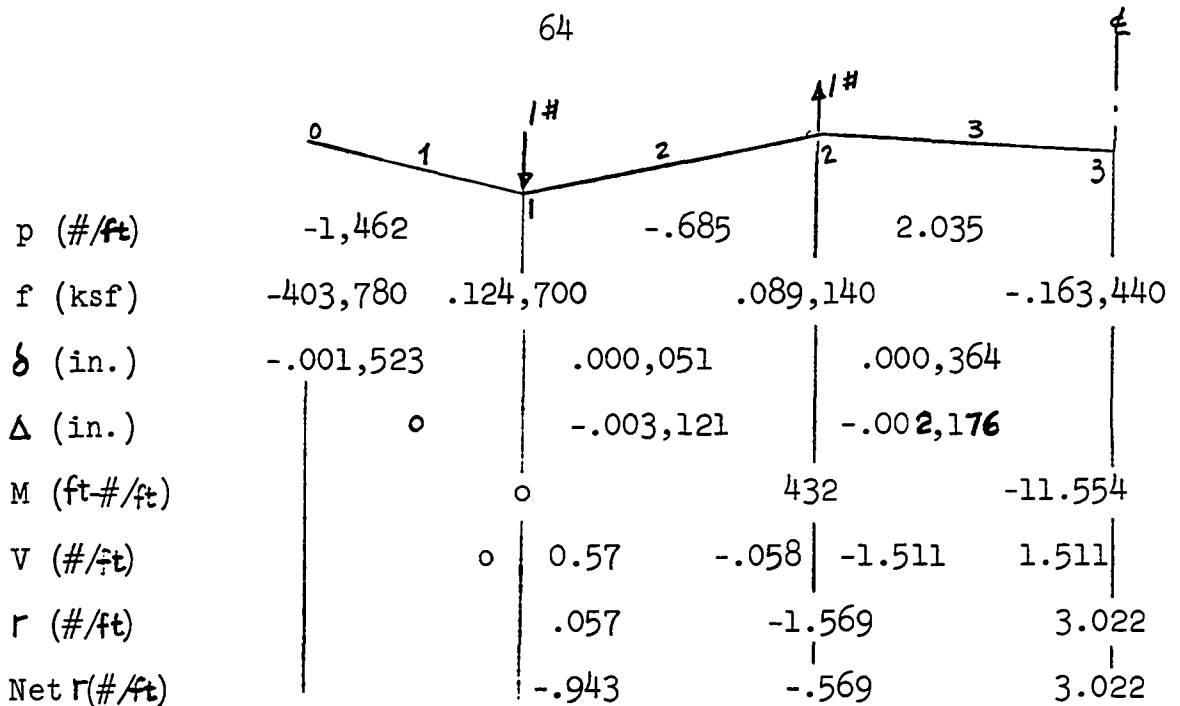
b. Correction Analysis

b.1 Due to "Virtual Couple,"  $Xh \cos \phi$ ,  at mid-span ( $.5L$ ). Instead of  $X$ , one unit load was used in this calculation, the results then multiplied by absolute value of  $X$ . Following the same preceding procedures,  $P_n$ ,  $f_n$ ,  $\delta_n$ ,  $\Delta_n$ ,  $M_n$ ,  $V_n$  and  $r_n$  at  $0.5L$  were calculated.

---

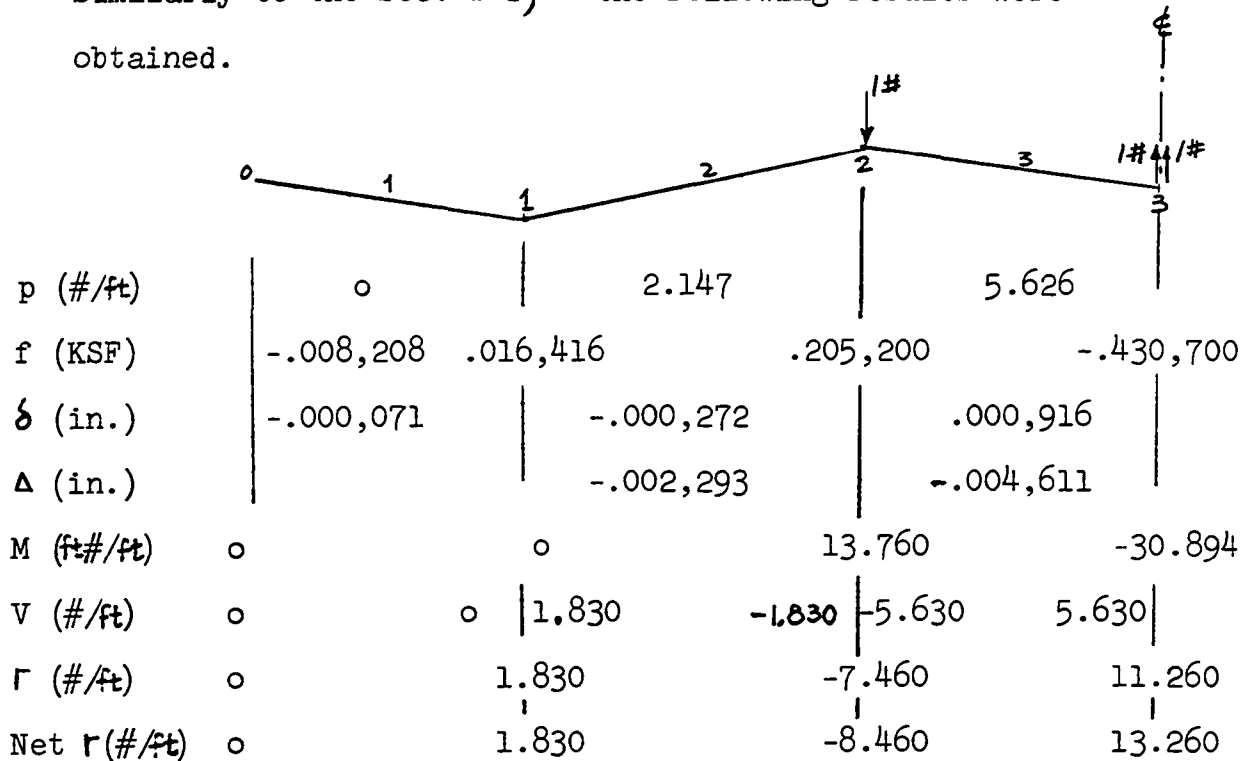
\*

The manipulations of this section were done only for the method which considers the effects of displacements.



b.2 Due to "Virtual Couple",  $y_h \cos \phi_2$  at  $0.5L$  in plate 3

Similarly to the Sec. b.1, the following results were obtained.



## b.3 Solution for x and y

Three equations of first order with two unknowns, x,y, were written by setting sum of reactions equal to zero at each joint.

$$-3,129 - .943x + 1.830y = 0 \quad (4.1)$$

$$10,909 - .569x - 8.460y = 0 \quad (4.2)$$

$$-15,560 + 3.022x + 13.260y = 0 \quad (4.3)$$

Solving for x and y from eqs. (4.1) and (4.2), yields

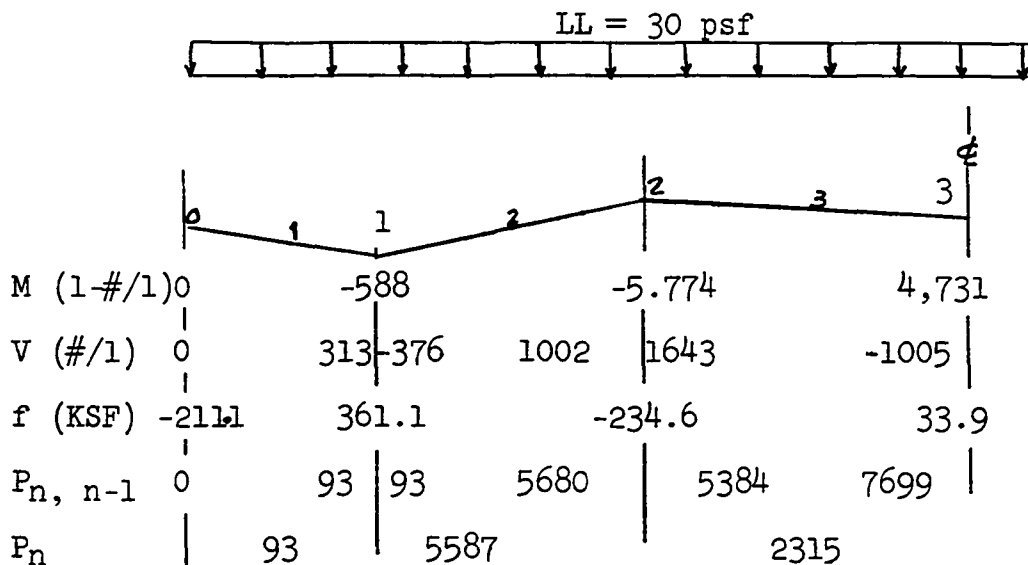
$$x = -722, \quad y = 1,338$$

Substituting in eq. (4.3) with x,y, yields

$$-15.560 - 2.181 + 17.741 = 0 \quad \underline{\text{OK}}$$

## c. Superposition

The final results with considering joint displacements = (Basic values) + (Corrections due to x) + (Corrections due to y). The final forces (M, V, f,  $P_{n,n-1}$  and  $P_n$ ) at .5L are shown below:



## 4.2.2 Design

## (a) General Data

Design method - Working stress design in accordance with "ACI Code 318-63"<sup>(3)</sup> and "ACI Committee 344"<sup>(2)</sup>

Concrete -  $W=150$  PCF,  $f'_c = 4,000$ psi,  $f_c = .45f'_c = 1,800$ psi  
 $n=8$ , allowable  $v = \begin{matrix} 70\text{psi} & \text{(no stirrup)} \\ 316\text{psi} & \text{(W/stirrup)} \end{matrix}$ , allowable  $u =$   
 $\begin{matrix} 287\text{psi} & \text{(top bars)} \\ 405\text{psi} & \text{(others)} \end{matrix}$

Reinforcement - Use #3 and #6 bars

$$f_y = 40,000\text{psi}, f_s = 20,000\text{psi}$$

## (b) Design coupled with "folded plate theory neglecting relative joint displacements"

## b.1 Transverse slab design

Given:  $t=4$  in.,  $d=3.3125$  in. with  $1/2$  in. covering,

$$\text{Max Neg. Mom.} = 588 \text{ } 1\text{-\#}/1,$$

$$\text{Max Pos. Mom.} = 171 \text{ } 1\text{-\#}/1, \text{ Max. shear} = 345 \text{ } \#/1$$

$$\text{Design: Max. } A_s \text{ req'd.} = \frac{.588}{(1.435 \times 3.3125)} = .124 \text{ sq. in.}$$

Use #3 @  $10-1/2$  in. c/c -  $A_s$  provided = .13 sq. in.

Actual  $v \leq 9$ psi ok

## b.2 Longitudinal plate design - the following calculations were based on the results at mid-span

plate #1,  $A_s$  req'd. = 6.46 sq. in.,  $A_s$  provided =

$$6.6 \text{ sq. in. } W/15\text{-\#6}$$

$$A'_s \text{ req'd.} \gg 47.6 \text{ sq. in.}, A'_s \text{ provided} \gg$$

$$47.6 \text{ sq. in. } W/108\text{-\#6}$$

$V$  max. = 228psi, use #3 @ 18 in. stirrups

plate #2,  $A_s$  req'd. = 13.69 sq. in.,  $A_s$  provided = 13.7 sq.  
in. W/31-#6

$A'_s$  req'd. >> 11.60 sq. in.,

$V$  max. = 3.2psi, Use #3 @ 5" c/c stirrups in end  
quarter span

plate #3,  $A_s$  req'd. = 18.37 sq. in.,  $A_s$  provided = 18.48 sq.  
in. W/42-#6

$A'_s$  req'd. >> 12.74 sq. in.

$V$  max. = 455psi > 405psi, use #3 @ 1-3/4 in. c/c  
in end quarter span

Obviously the negative reinforcement layout was impossible --  
for instance, 108 - #6 bars are required to put in the dis-  
tance of 48.9" in the plate #1, -- unless the solid steel  
section were used in place of reinforcement bar.

(c) Design coupled with "folded plate theory considering  
relative joint displacements

c.1 Transverse slab design (at mid-span)

joint 1,  $A_s$  req'd. = .124 sq. in., #3 @ 10-1/2 provided

$A_s = .13$  sq. in.

joint 2,  $A_s$  req'd. = .48 sq. in., #3 @ 2-5/8" provided

$A_s = .503$  sq. in.

joint 3,  $A_s$  req'd. = .255 sq. in., #3 @ 5-1/4 provided

$A_s = .250$  sq. in.

Max  $V = 41.4$ psi

## c.2 Plate design (at mid-span)

Plate #1,  $A_s$  req'd. = 8.0 sq. in., 19-#6 provided  $A_s$   
= 8.4 sq. in.

$A'_s$  req'd. = .21 sq. in., 1-#6 provided  $A_s$   
= .44 sq. in.

Max.  $V$  = 99psi Use #3 @ 18 in. through  
whole plate

Plate #2,  $A_s$  req'd. = 14.8 sq. in., 34-#6 provided  $A_s$   
= 14.9 sq. in.

$A'_s$  req'd. = .71 sq. in., 2-#6 provided  $A_s$   
= .88 sq. in.

Max  $V$  = 464psi, Use #3 U @ 3 in. in end quarter  
span

Plate #3,  $A_s$  req'd. = None, 1#-6 provided  $A_s$  = .44 sq. in.

$A'_s$  req'd. = 6.25 sq. in., 14-#6 provided  $A_s$   
= 6.17 sq. in.

Max  $V$  = 74psi, Use #3 @ 18 in. through whole  
plate

Reinforcements at  $1/8L$  and  $3/8L$  were obtained in similar  
way and their layouts are shown in Sec. 4.5.

#### 4.2.3 Comparison of the Results of Two Different Linear Elastic Methods

The summary of reinforcements required in the two  
different analysis methods are shown in Table 4.1:

Reinforcement in pounds		
Analysis method	Theory neglecting joint displacements	Theory considering joint displacement
Transverse Reinf.	1.703	7.166
Long. Reinf.	>>32,371	12,300
Stirrup	2,385	2,982
Temp. & Shrinkage	1,028	1,067
<u>Total</u>	<u>&gt;&gt;37,487</u>	<u>23,515</u>

Table 4.1 Reinforcement quantity comparison between analyses neglecting and considering relative joint displacement

Clearly reinforcement required is less in the transverse direction but much more in the longitudinal direction calculated by the theory neglecting relative joint displacements as compared with that of the theory considering relative joint displacements. Total required reinforcement is much less with the theory considering relative joint displacements. Moreover, it was impossible to lay out the longitudinal reinforcement obtained by the analysis neglecting relative joint displacements in 4-inch plates.

Therefore, the folded plate theory considering relative joint displacements was chosen to build a model for tests.

#### 4.3 Overall Behaviors of the Selected Prototype Structure -- by "Nonlinear Inelastic Beam Theory"

By using the longitudinal reinforcements requirements

calculated with the theory considering relative joint displacements, the load-deflection and responses of the selected prototype structure were obtained by the "Program LDDFN" based on the nonlinear inelastic beam theory. The results are shown on Fig. 4.5. These responses will be used in Chapter V to compare with the actual responses of the direct model tested.

#### 4.4 Model

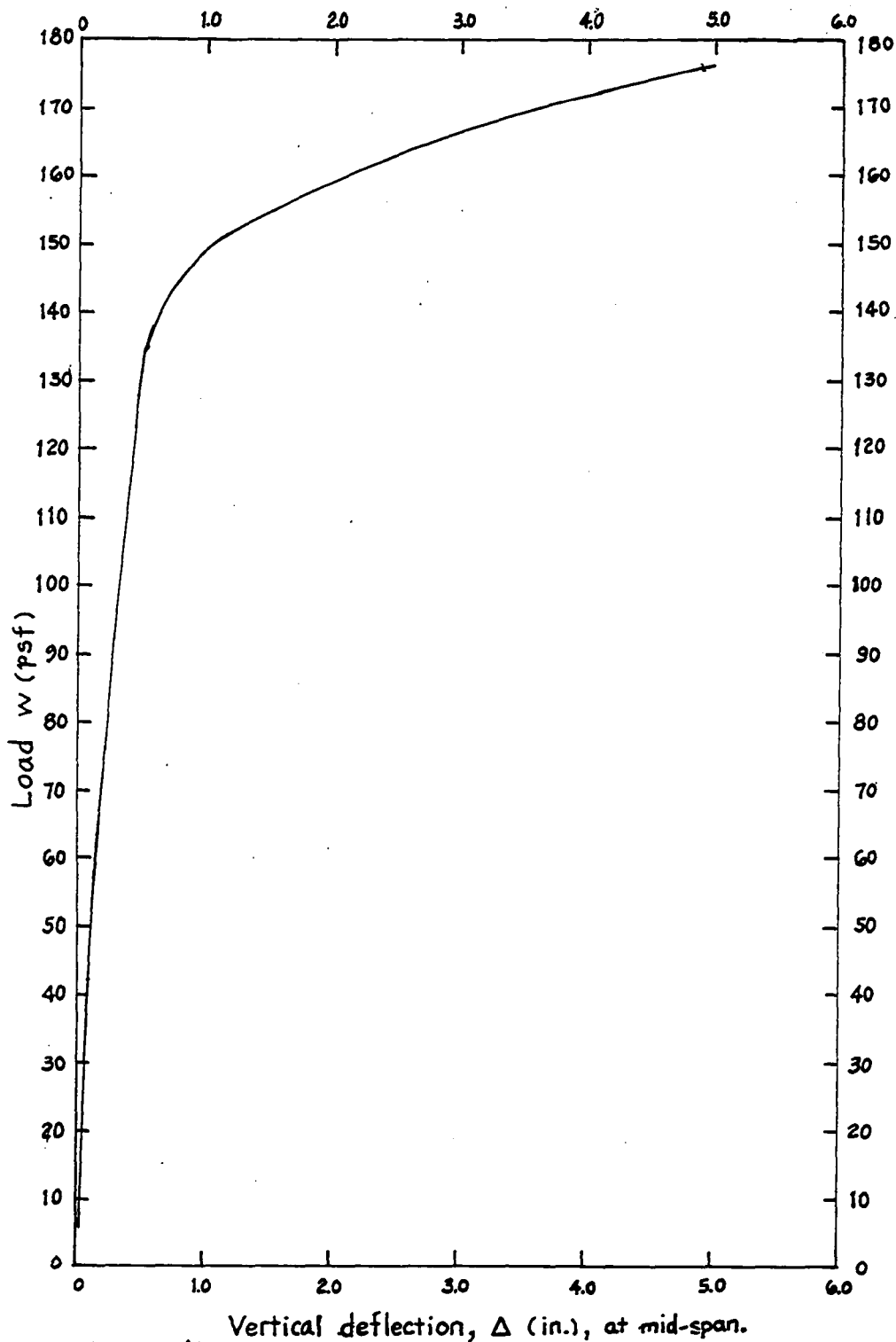
##### 4.4.1 General

A model structure may be defined as a small scale physical replica of some prototype structure which can be used experimentally to predict the behaviors of the prototype structure.

In the past forty years a great deal of work has been done in the development of concepts and applications of the use of models for structural engineering purposes as aids for design purposes or research purposes. (54)

Throughout the entire range of loading, the actual response of a structural system to applied loads is little understood due to the complexity of the real material properties and the methods of analysis. Thus the engineer has been forced to work with ultimate tests of models loaded to collapse.

Without question, the testing of the large numbers of prototype structural systems would be impractical as well



Vertical deflection,  $\Delta$  (in.), at mid-span.  
Figure 4.5 Load-deflection curve of the model by  
'Program LDDFN' .

as expensive. As a consequence, direct modeling technology has received a large measure of attention in recent years, and the concept of using a reduced scale model to predict prototype behavior has been fairly widely accepted as a sound basis for structural research purposes. In general, the reliability of the use of models in structural research (55,56,57,58,59,60,61,62,63,64, 65,66) has been well established

The methods of structural model testing are generally classified into two categories, "Indirect" and "Direct" methods. The "Indirect" method employs the Müller-Breslau principle for the physical determination of influence lines or surfaces for the desired forces (moment, shear, reaction, etc.). Therefore, the principle of superposition must be utilized and the requirements on model materials are not restrictive. The "Direct" method is subclassified into "Direct elastic method" and "Direct inelastic method". In the "Direct elastic method", the structure may be subjected to nonlinear geometric effects such as in beam-column behavior and shell buckling. It is used for determining elastic stress distributions within a shell or across a section of a beam-column, and other actions not readily amenable to mathematical approaches. On the other hand, the "Direct inelastic method" attempts to accurately duplicate behavior of prototype structure through all loading stages up to and including failure, cracking, inelastic buckling

and crushing of concrete.

This study is concerned solely with the "Direct inelastic method", to achieve true modeling of a concrete structure reinforced with steel with its fixed modulus. A true model is a model structure in which there is no distortion of stress-strain similitude between prototype and model structures.

In those instances where true modeling cannot be achieved, alternate similitude requirements must be employed. The effects of the resulting distortions are discussed in detail in references 7,56, and 57.

#### 4.4.2 Direct Inelastic Model Analysis

In the direct inelastic method of analysis all of the important dimensions of the prototype are reduced by an arbitrary geometrical scale factor  $S$ . Then stresses, strains, moments, deflections, etc. in the prototype structure may be determined from observations of the model when it is subjected to the appropriate scale loadings (7,54,55, 57)

The theory of dimensional analysis can be utilized to derive the following set of requirements for true models reinforced with steel neglecting the effect of creep, shrinkage, strain rate, temperature, age, etc.:

1.  $d_m = d_p / s$  (linear dimension)
2.  $\delta_m = \delta_p / s$  (deflection)

3.  $e_m = e_p$  (strain)
4.  $\nu_m = \nu_p$  (Poisson's ratio)
5.  $E_m = E_p$  (elastic modulus)
6.  $f_m = f_p$  (critical stresses in compression, tension,  
or any combination thereof)
7.  $W_m = W_p/s$  (dead load per unit area)
8.  $q_m = q_p$  (uniform load per unit area)
9.  $P_m = P_p/s^2$  (concentrated load)
10.  $r_m = r_p/s$  (uniform load per unit length)

The subscripts p and m refer to prototype and model respectively, and the factor S is a geometrical scale factor defined as the ratio of the prototype linear length to the corresponding model linear length.

Equation 6 follows from Equations 3 and 5. This requirement is further substantiated by the fact that tensile strengths of model and prototype structures must be identical if tensile cracking is to initiate at corresponding points in the model and the prototype structures. It also implies that the failure criterion of model and prototype structures be identical.

#### 4.4.3 The Selected Prototype versus Model Correlations

The geometrical linear scale factor (s) selected for this study was 1/8, and the variables in the model were scaled down in accordance with correlations listed in Table 4.2.

Variable in model = K x (Variable in prototype)	
Variable	K
d (Linear dimension)	1/8
$\delta$ (deflection)	1/8
e (strain)	1
$\nu$ (Poisson's ratio)	1
E (elastic modulus)	1
f (stresses)	1
w (dead load per unit area)	1/8
q (uniform load per unit area)	1
p (concentrated load)	1/64
r (uniform load per unit length)	1/8

Table 4.2 Correlations between model and prototype structures

#### 4.4.4 Microconcrete

The linear scale factor (1/8) was applied in attempt to scale the aggregate gradation of the assumed prototype concrete mixture (Fig. 4.2 and 4.3). The resulting concrete mixture - defined herein as microconcrete -- was reasonably scaled replica of the mixture which was used for the standard 6" x 12" cylinders with the exception of the finer particles.

The specific gravity of the aggregate was found to be 2.59 and 2.51 for portions finer than #4 and the 3/4 in.

standard sieves, respectively. Absorption ranged from 1.125 to 1.79%.

Tests were performed to determine the stress-strain characteristics of the prototype concrete and the microconcrete mixture including the determination of Poisson's Ratio, and the results are shown in Fig. 4.4. The instrumentation consisted of four SR-4 wire strain gages (Baldwin-Type A7) mounted two each in series vertically and horizontally and four dial gages with 0.001" least reading as shown in Fig. 4.3.

The following constants are used in the proportioning of the mixture by weight for the microconcrete and the prototype concrete:

(a) For Microconcrete,

Water/Cement (W/C) = 0.55

Total Aggregate/Cement (A/C) = 3.57

(b) For Prototype,

Water/Cement = 0.55

Total Aggregate/Cement = 6.25

Type III Portland Cement was used to allow early form removal, and Plastiment was added to the mixture in quantities ranging from 3 to 4 ounces per sack of cement depending on the average temperature and relative humidity on the day of casting for shrinkage control and to retard the setting of the cement. Curing was effected by spraying with hyrocode resin curing compound.

U. S. Bureau of standards sieve size

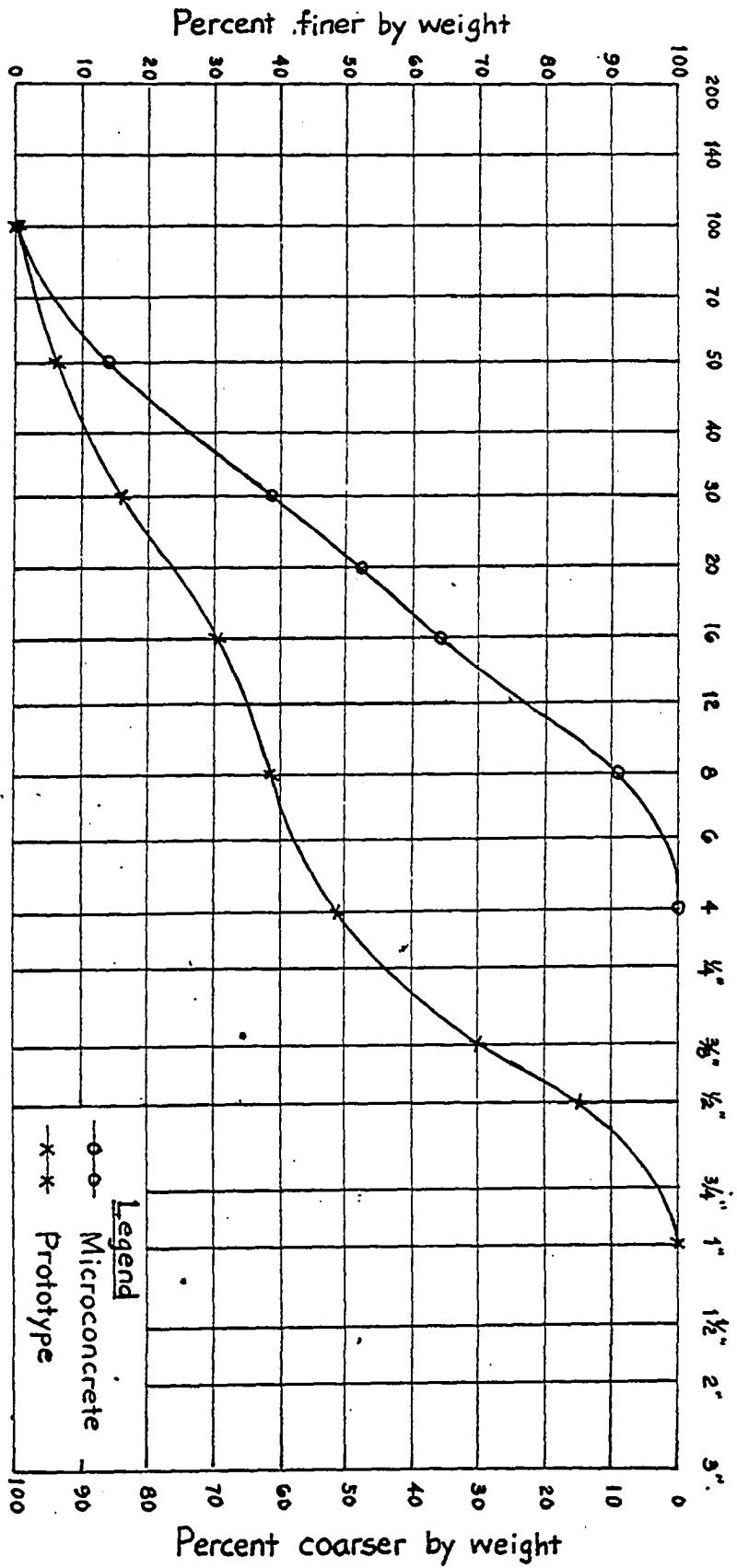


Figure 4.2 Summary of aggregate gradations

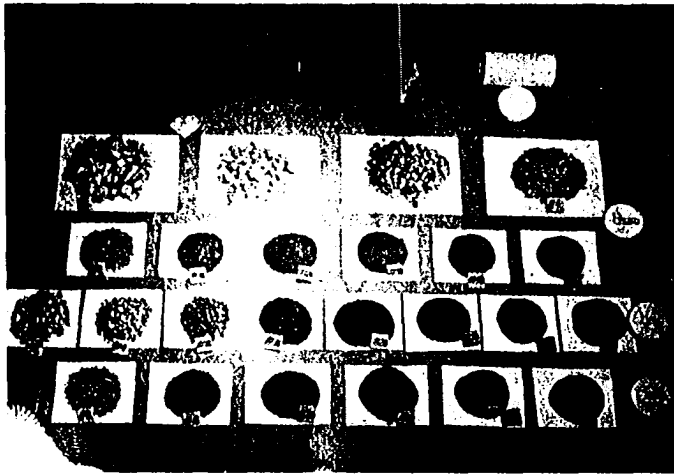


Figure 4.3a-Aggregates and cylinder molds.

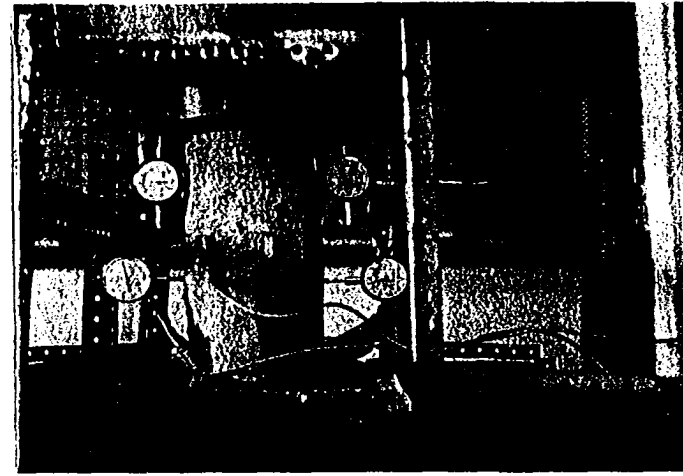


Figure 4.3b-Strain instruments for concrete.

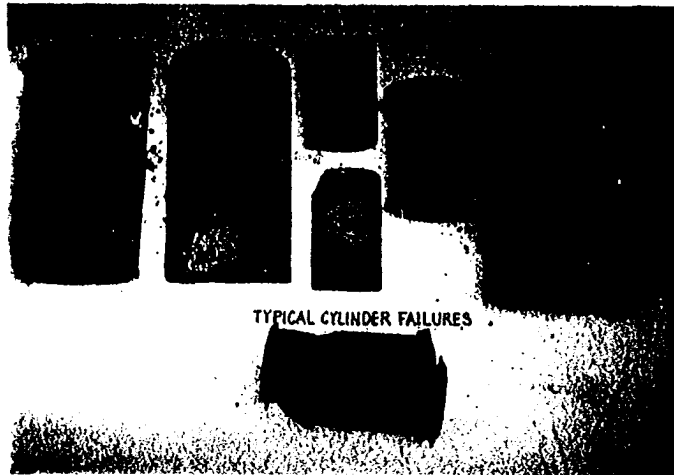


Figure 4.3c-Typical cylinder failures.



Figure 4.3d-Typical wire tensile test specimens.

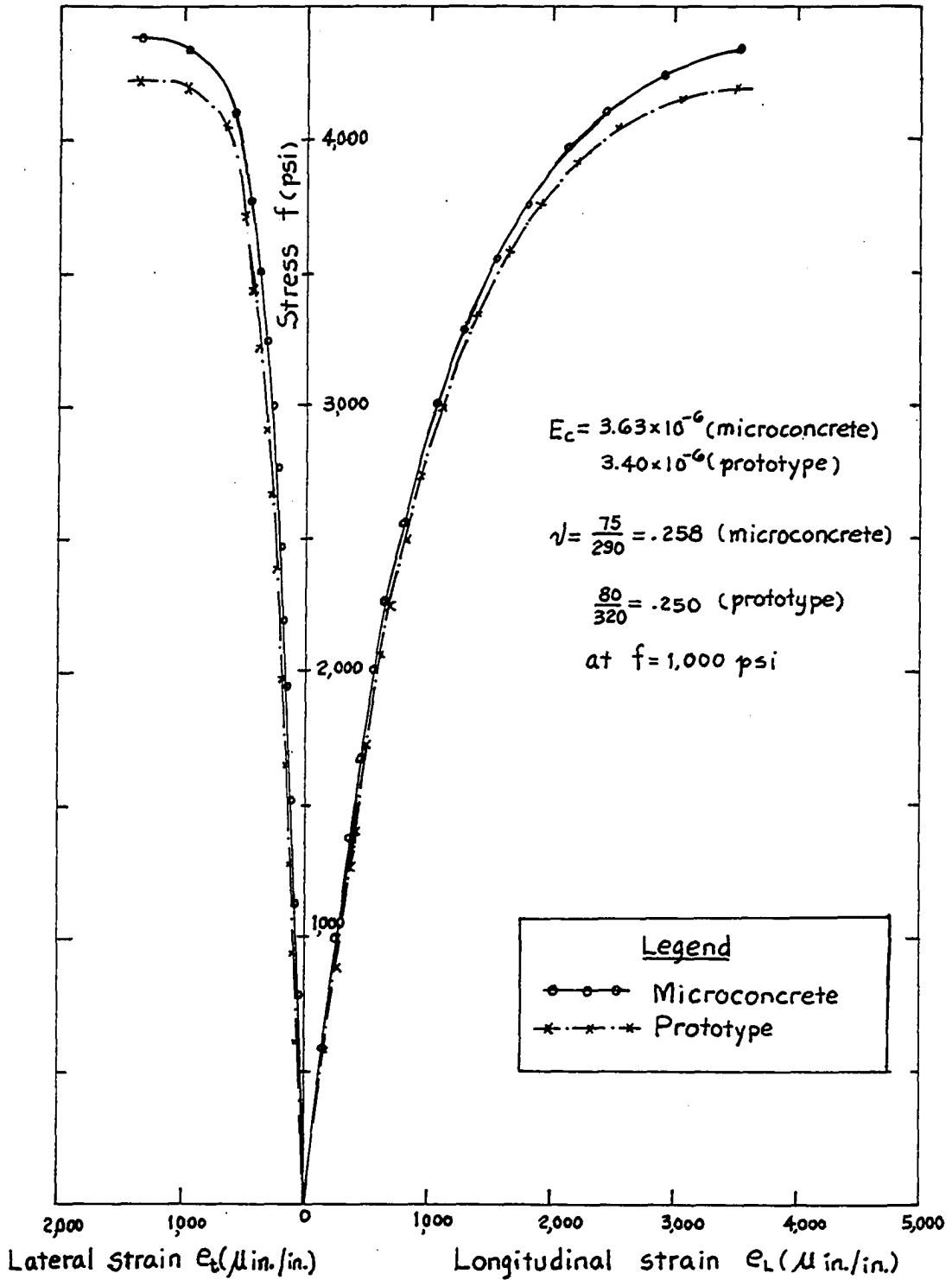


Figure 4.4 Stress-strain curves for prototype and microconcrete

Eight cylinders (six for compression strength test and two for splitting tensile strength test) and seven cylinders (five for compression strength test and two for splitting tensile strength test) of microconcrete and prototype concrete respectively were tested following the procedures of ASTM test methods C192, C496 and C39. The results of the cylinder tests are shown in Table 4.3.

The results of the tests are summarized as follows:

(a) Poisson's Ratio - 0.258 for microconcrete, 0.250 for prototype concrete at 7 days at 1000psi.

(b) Compression strength - 4,360psi for microconcrete, 4,190psi for prototype concrete at 7 days.

(c) Splitting tensile strength - 547psi for microconcrete, 508psi for prototype concrete at 7 days.

To sum up, the mechanical properties of the microconcrete were found to be in good agreement with those of a prototype concrete. It was concluded that the mechanical correlations ( $\nu$ , E and f) between model and prototype structure shown in Table 4.2 were considered valid.

#### 4.4.5 Model Reinforcement

The soft black annealed steel wires, AISI designation C1008, were used for modeling of reinforcing bars of the prototype -- No. 6 bars modeled by SWG13 0.0915" in diameter, and No. 3 bars modeled by SWG18 0.0485" in diameter. The steel wires -- SWG13 and 18 -- were rusted to provide better

bonding in the model. The mechanical properties were determined from tests on 2" gage length of wires (Fig. 4.3d) made with the Instron testing machine. The principal mechanical properties for the wires (Table 4.4) were found to be:

- 1) For SWG13, lower yield point= 28.3Ksi  
ultimate strength= 47.1Ksi  
% of elongation =35%
- 2) For SWG18, lower yield point = 33.0Ksi  
ultimate strength = 44.7Ksi  
% of elongation = 26.7%

The representative stress-strain curves are shown in Figure 4.6.

The pullout Bond tests were not performed. However, other investigators <sup>(7,67)</sup> had shown that the wires could be fully developed by the microconcrete by embedment lengths of roughly 25 diameters. Thirty diameters were used in this study.

#### 4.5 Summary

A selected prototype structure designed with the folded plate theory considering relative joint displacements was scaled down to model proportions by direct linear scaling (1/8 linear scale factor). Certain conditions of material compatibility were investigated. The detail drawings of the model are shown in Figure 4.7.

Concrete	Age at time of test (days)	Weight		Compressive strength			Split cylinder strength		
		No. of cyls.	w (pcf)	$f'_c$ (psi)	No. of cyls.	Coef. of var. V(%)	$f'_{sp}$ (psi)	No. of cyls.	Coef. of var. V(%)
Microconcrete	7	8	146.4	4360	6	6.9	547	2	1.3
Prototype	7	7	150.6	4190	5	5.3	508	2	3.9

Table 4.3 Summary of cylinder tests.

Wire	No. of test	Yield point		Ultimate strength		Percent elongation	
		$f_y$ (ksi)	$V$ (%)	$f_u$ (ksi)	$V$ (%)	$e$ (%)	$V$ (%)
SWG 18	16	33.0	1.6	44.7	1.2	26.7	0.1
SWG 13	15	28.3	8.8	47.1	1.7	35.0	9.2

Table 4.4 Summary of mechanical properties of model steel.

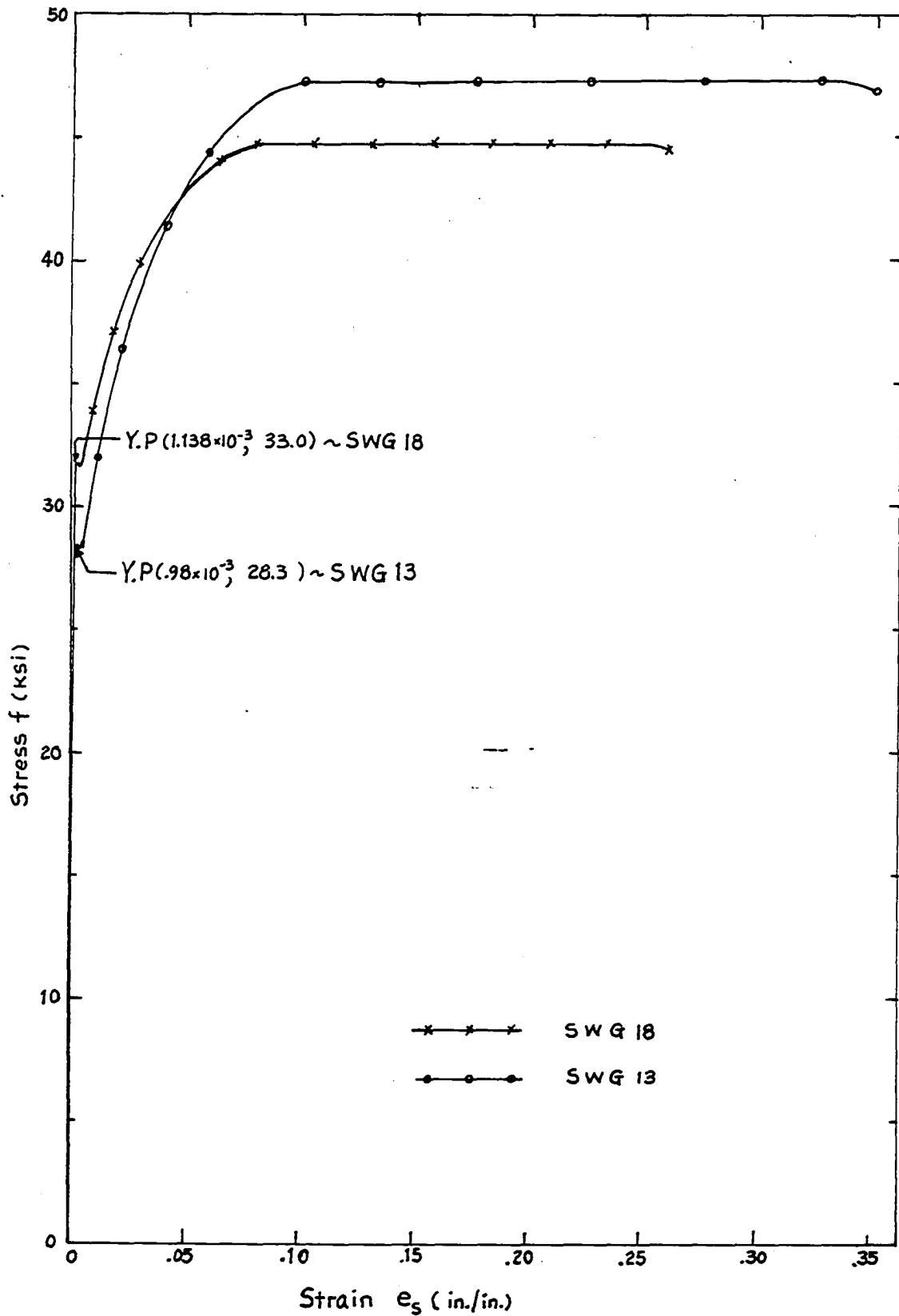


Figure 4.6 Stress-strain curves for model reinforcements.

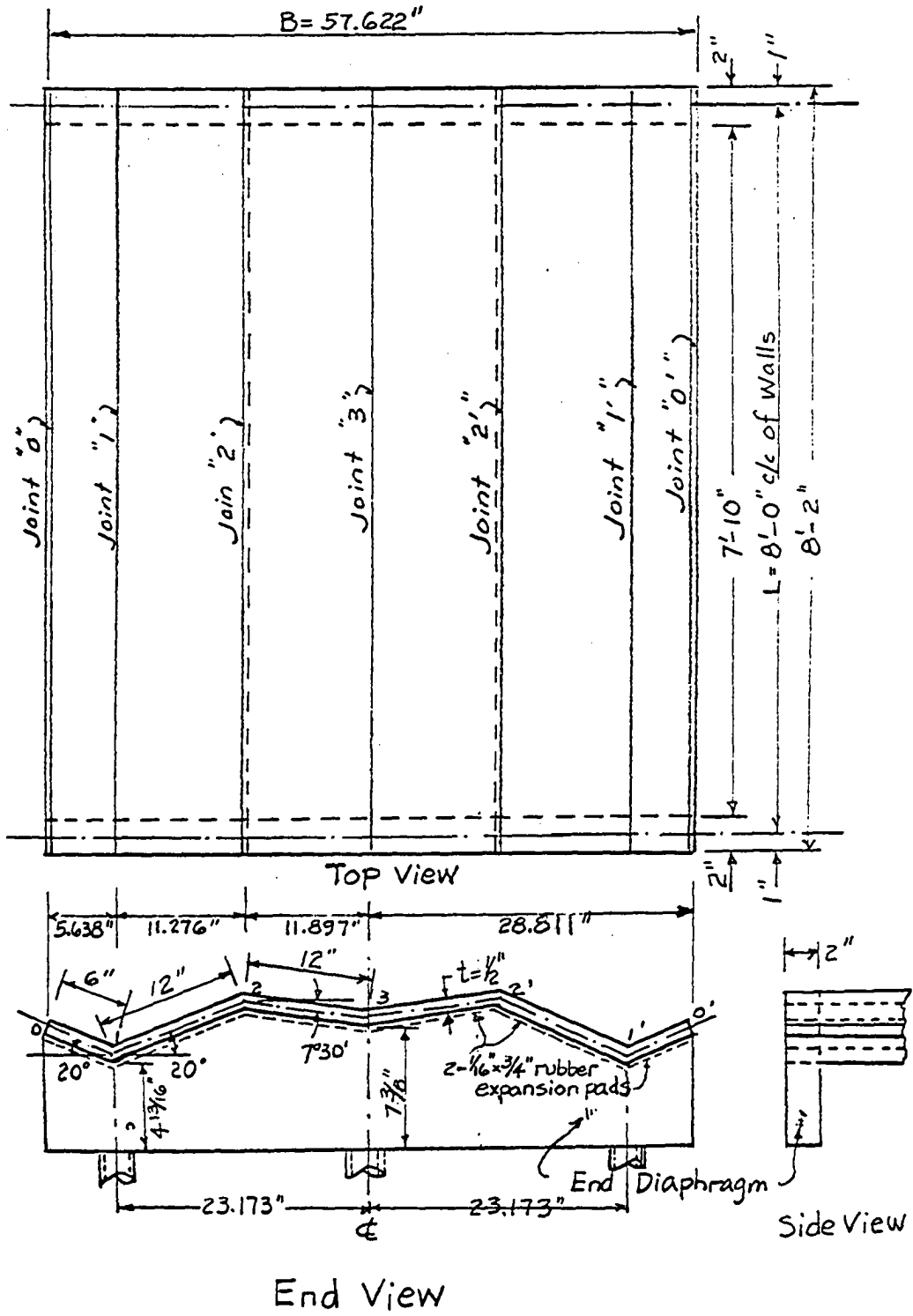


Figure 4.7a Model structure

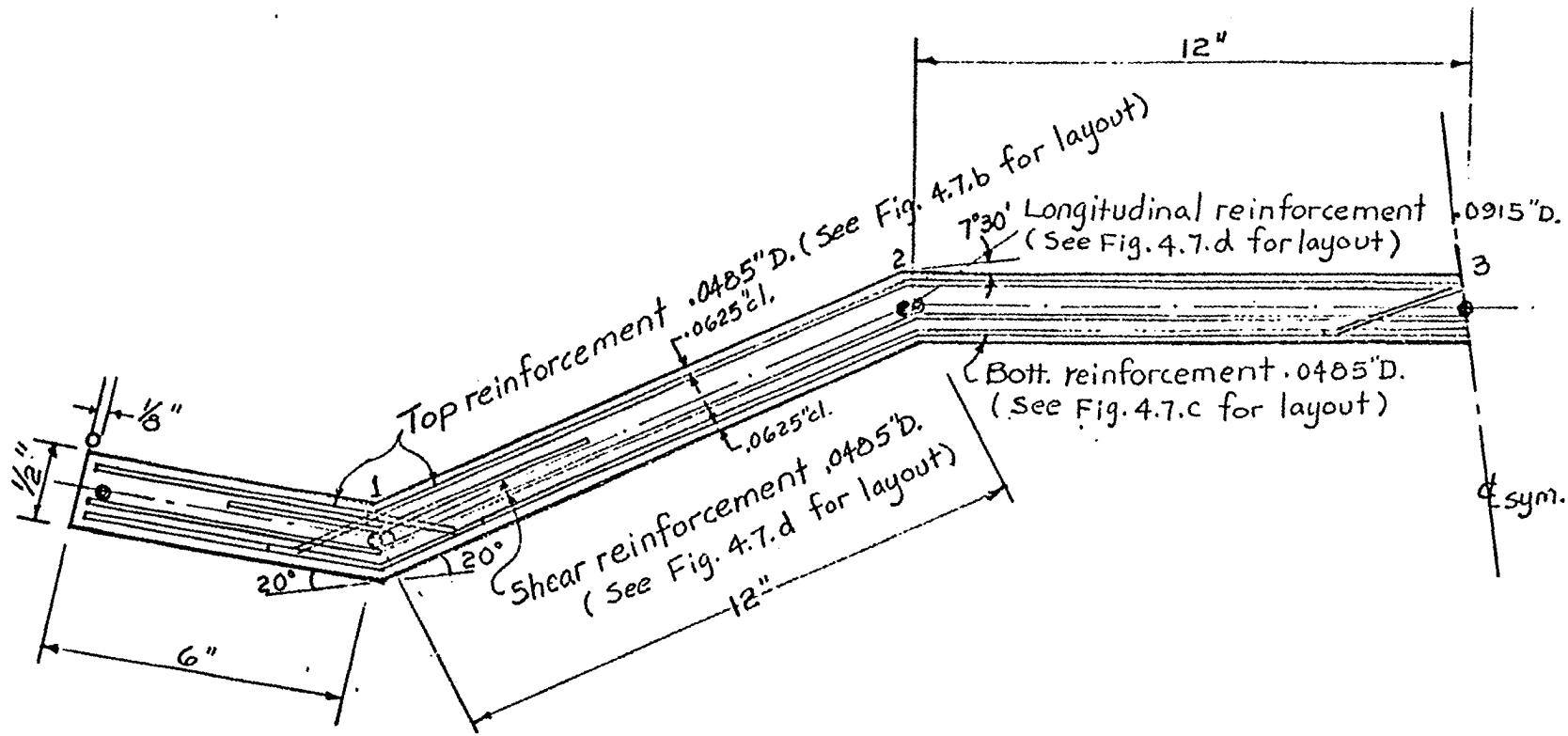


Figure 4.7b. Half cross-section of model

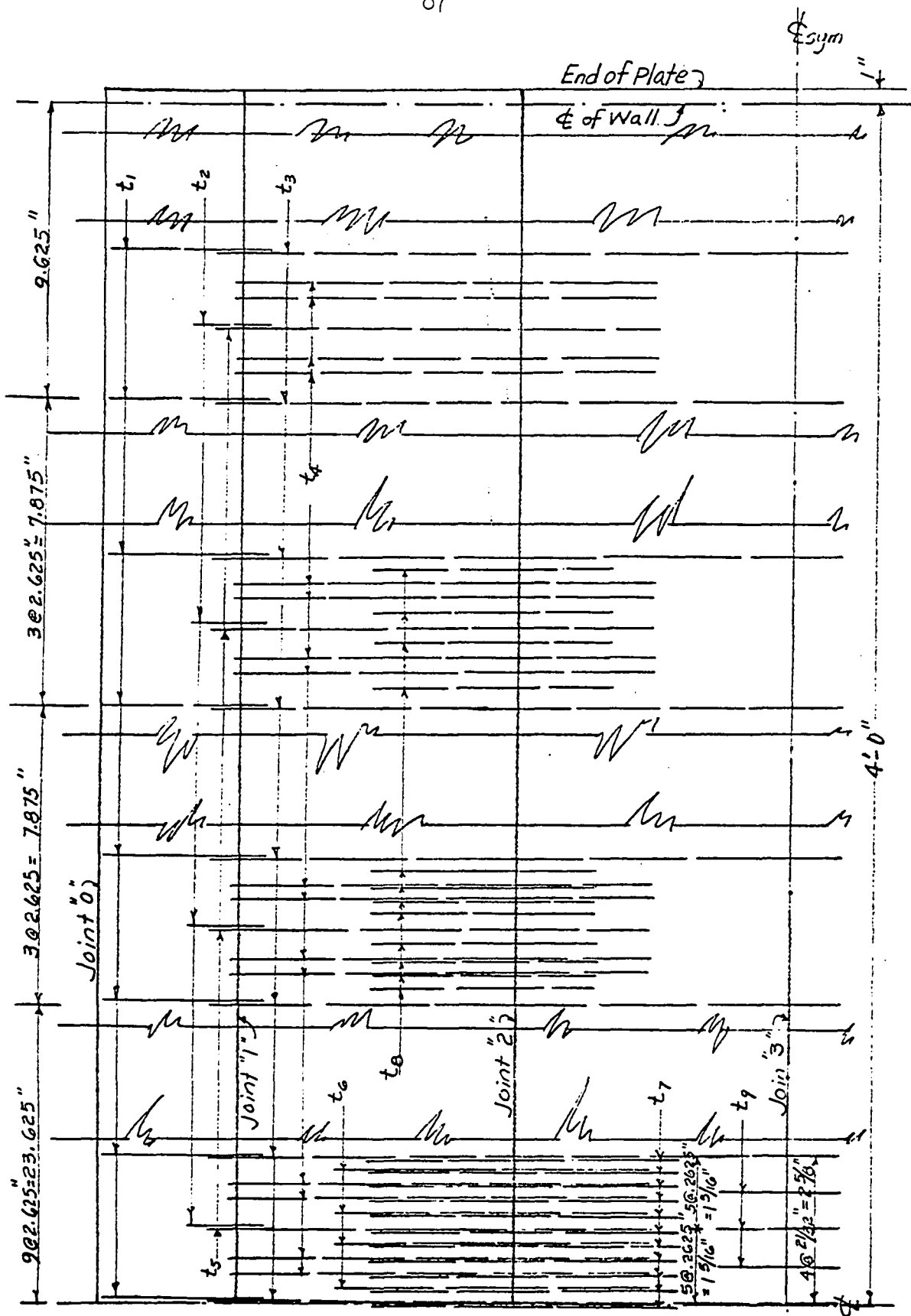


Figure 4.7c Top reinforcement layout (See Fig. 4.7.f for detail)



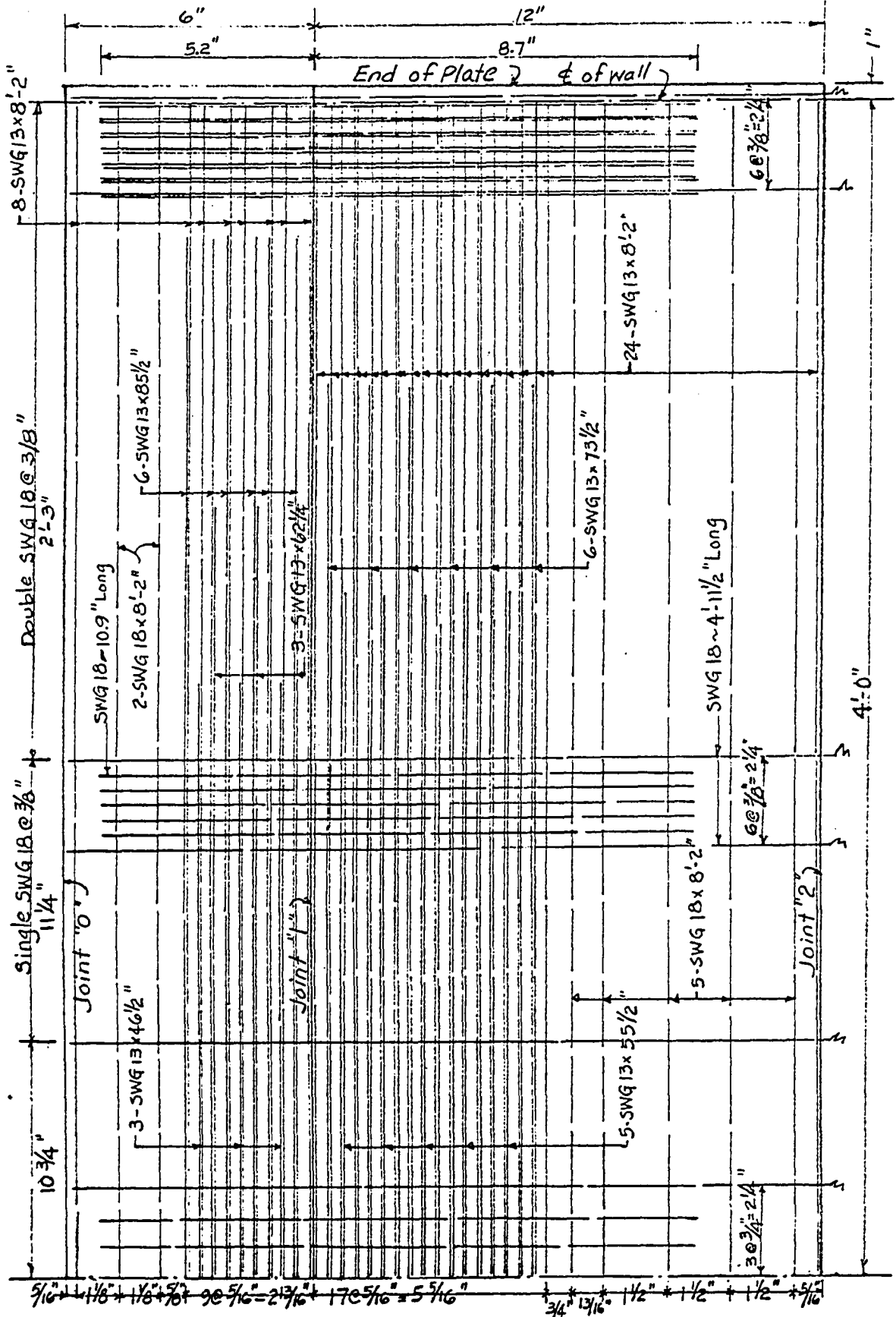


Figure 4.7e Longitudinal and stirrup reinforcements layout for Plates #1 and #2

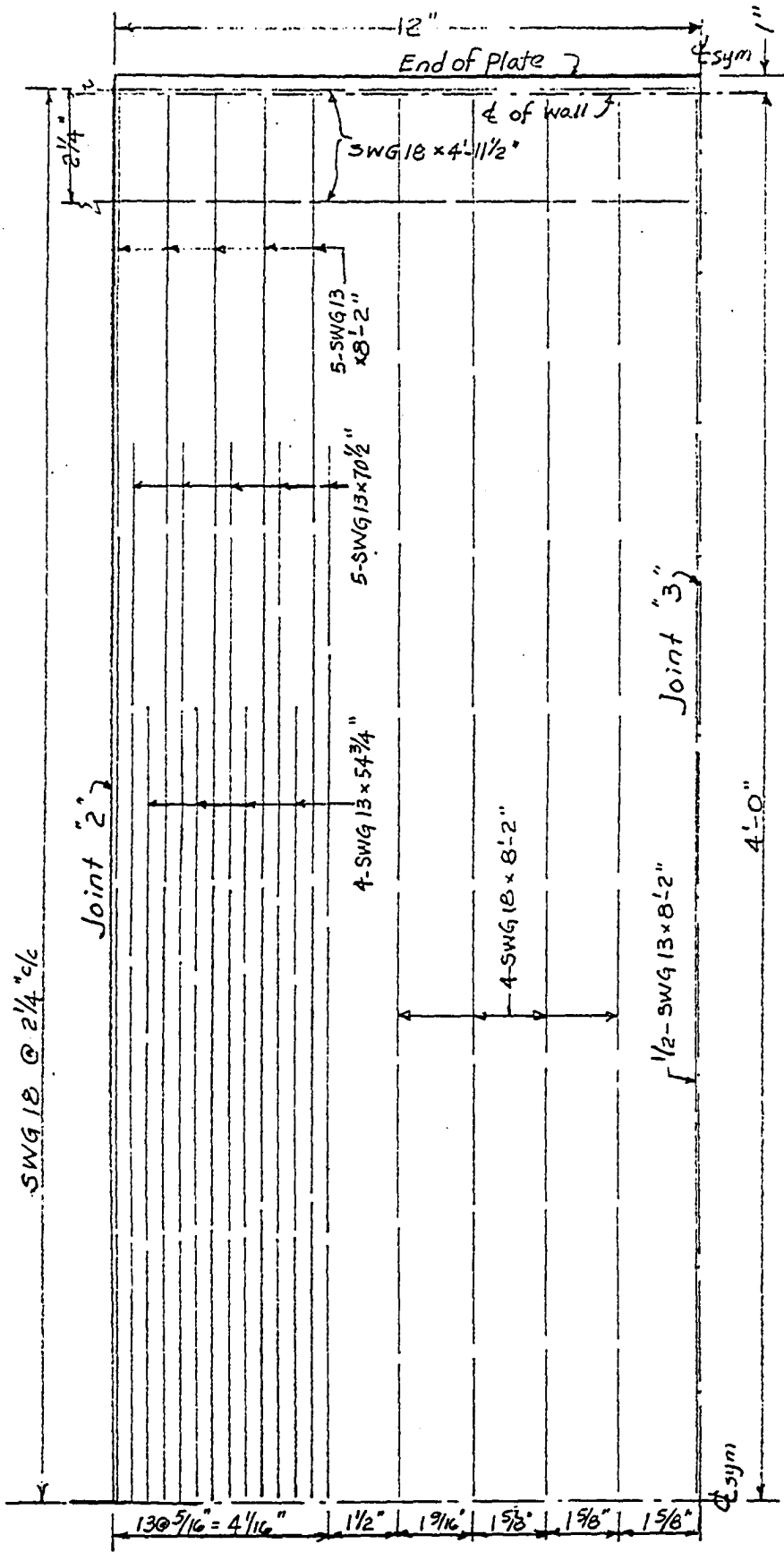


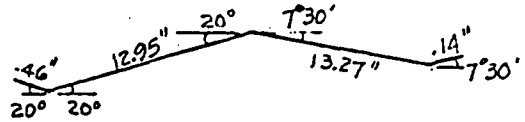
Figure 4.7f Longitudinal and stirrup reinforcements layout for Plate #3



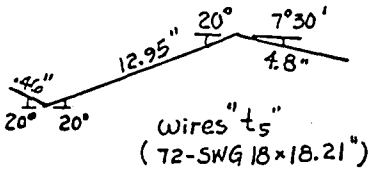
Wires "t<sub>1</sub>"  
(78-SWG 18 x 7.16")



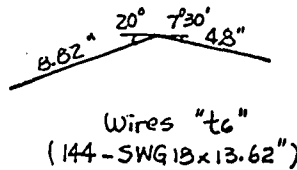
Wires "t<sub>2</sub>"  
(72-SWG 18 x 4.71")



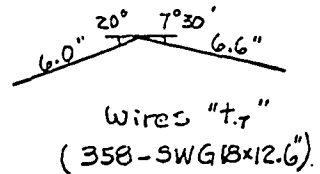
Wires "t<sub>3</sub>"  
(78-SWG 18 x 26.52")



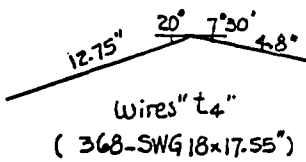
Wires "t<sub>5</sub>"  
(72-SWG 18 x 18.21")



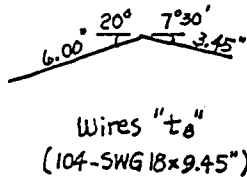
Wires "t<sub>6</sub>"  
(144-SWG 18 x 13.62")



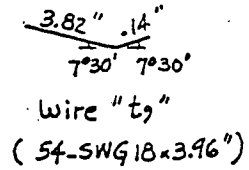
Wires "t<sub>7</sub>"  
(358-SWG 18 x 12.6")



Wires "t<sub>4</sub>"  
(368-SWG 18 x 17.55")

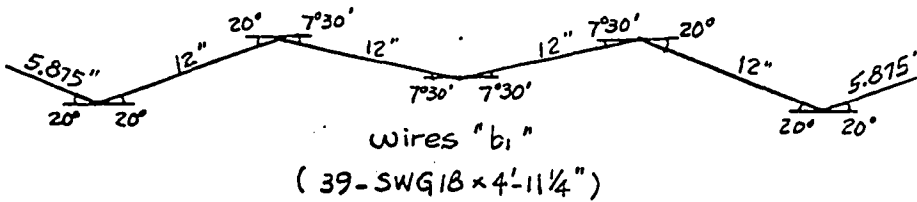


Wires "t<sub>8</sub>"  
(104-SWG 18 x 9.45")

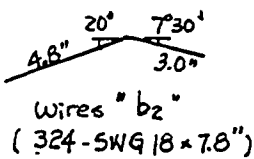


Wire "t<sub>9</sub>"  
(54-SWG 18 x 3.96")

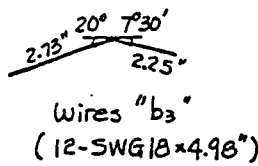
Top reinforcements



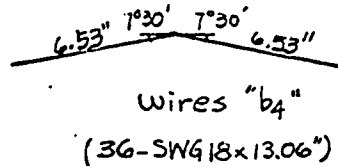
Wires "b<sub>1</sub>"  
(39-SWG 18 x 4'-11 1/4")



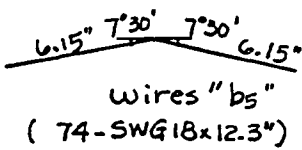
Wires "b<sub>2</sub>"  
(324-SWG 18 x 7.8")



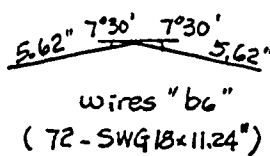
Wires "b<sub>3</sub>"  
(12-SWG 18 x 4.98")



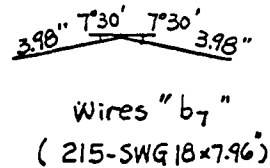
Wires "b<sub>4</sub>"  
(36-SWG 18 x 13.06")



Wires "b<sub>5</sub>"  
(74-SWG 18 x 12.3")



Wires "b<sub>6</sub>"  
(72-SWG 18 x 11.24")



Wires "b<sub>7</sub>"  
(215-SWG 18 x 7.96")

Bottom reinforcements

Figure 4.79 Top and bott. reinforcement details

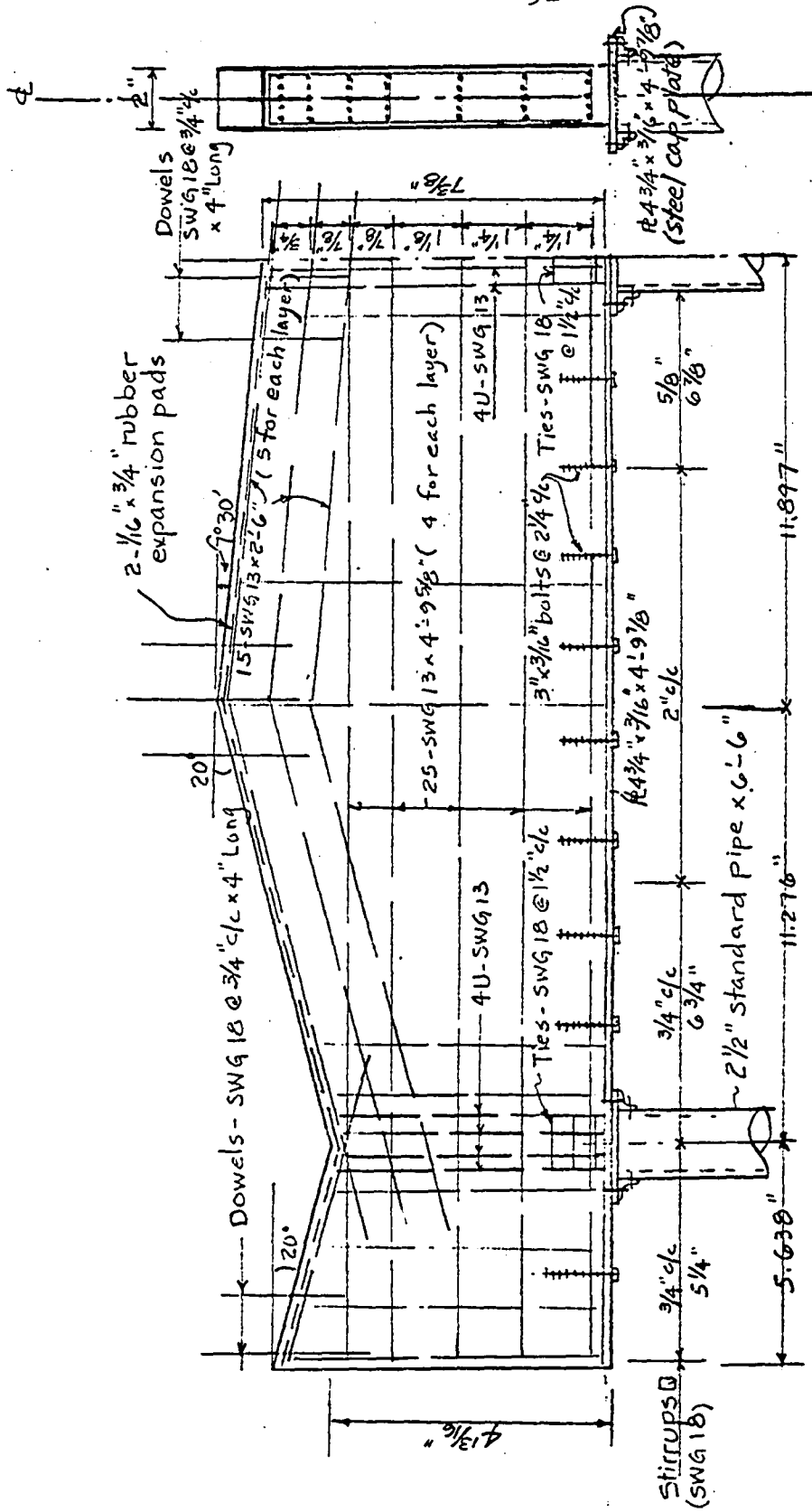


Figure 4.7h Details of end diaphragm.

## CHAPTER V

### CONSTRUCTION AND TESTING OF MODEL STRUCTURE

#### 5.1 General

The reliability of the analysis and design methods for the structure based on the classical concepts of linear elastic behavior of materials were to be investigated by a direct model test.

One 1/8 scale simply supported reinforced micro-concrete model folded plate (Sec. 4.7) was constructed and loaded monotonically to collapse with uniform load, applied on the horizontal projection through a "whiffle-tree" system. (Figure 5.1c and 5.1d).

The model structure was simply supported on two end diaphragms cast separately from the model. The diaphragms were rigidly connected to six 2½" standard steel pipes -- three pipes for each end diaphragm -- which were mounted on a 3' x 1.5' x 18' reinforced concrete dummy beam. (Figure 5.1c).

Deflections along the ridge lines, strains, and cracking of the model structure were recorded to obtain the

overall behavior of the model structure and from these results the reliability of the analysis and design methods for the structure were to be evaluated.

Preceding the test of the model structure, the "whiffle-tree" loading system was varified by independent testing. (Figure 5.1a).

## 5.2 Construction of Model Structure

### 5.2.1 Supporting Frames - Substructures (Figures 5.1c and 5.2a)

Supporting frames consisted of (a) one 3' x 1.5' x 18' reinforced concrete dummy beam, (b) end diaphragm supporting frames, and (c) two reinforced concrete end diaphragms.

#### (a) 3' x 1.5' x 18' Reinforced Concrete Dummy Beam

This beam, made of 2500 psi concrete reinforced with intermediate grade steel, was a basic supporting frame for the model structure and was also used as a loading frame. This beam was provided with an opening at the center line to accomodate a cable which passed through the beam and a 20-ton hydraulic ram. The ram was used to apply load by pushing against the underside of the beam. (Figure 5.1b).

#### (b) End Diaphragm Supporting Frames

Each frame consisted of 3-2 $\frac{1}{2}$ " x 6'-6" standard steel pipes with a bolt connecting steel cap plate (PL 4 3/4" x

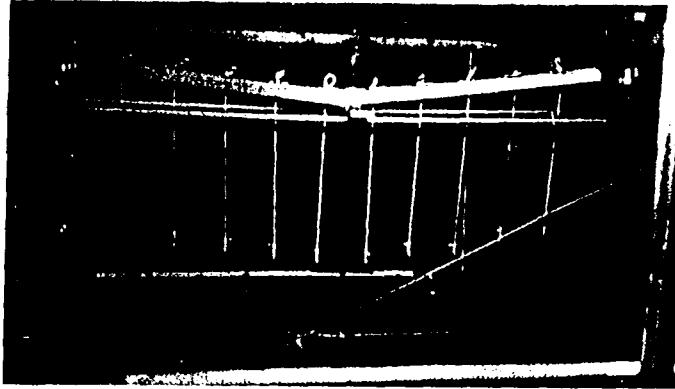


Figure 5.1a-Verification of loading system.

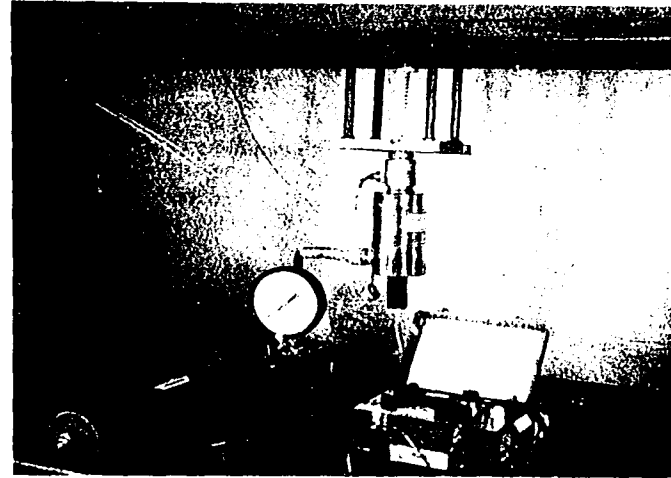


Figure 5.1b-Hydraulic ram, load cell, pump, chair, chucks etc.

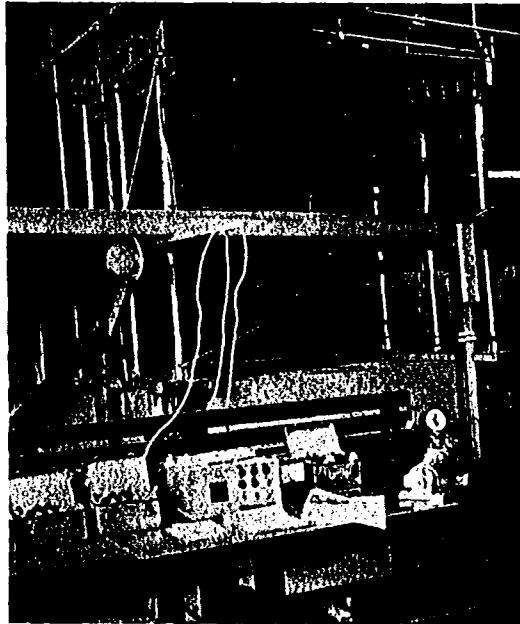


Figure 5.1c-Model, supporting frame, whiffle-tree, and strain gage monitoring equipment.

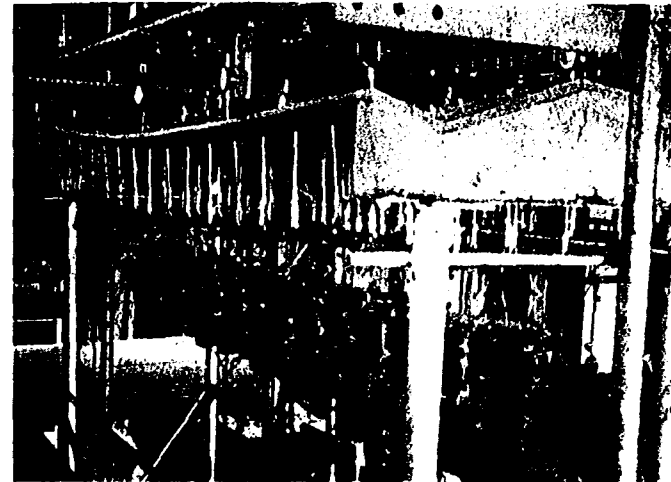


Figure 5.1d-Deflection of the model.



Figure 5.2a-End diaphragm steels and dowels.

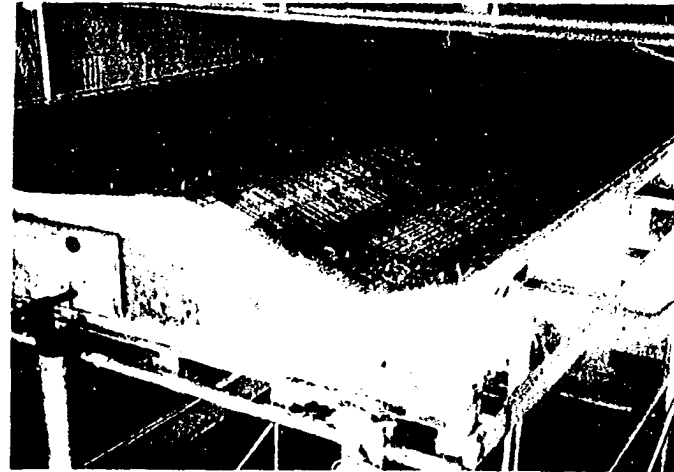


Figure 5.2b-Model steel cages for plates.

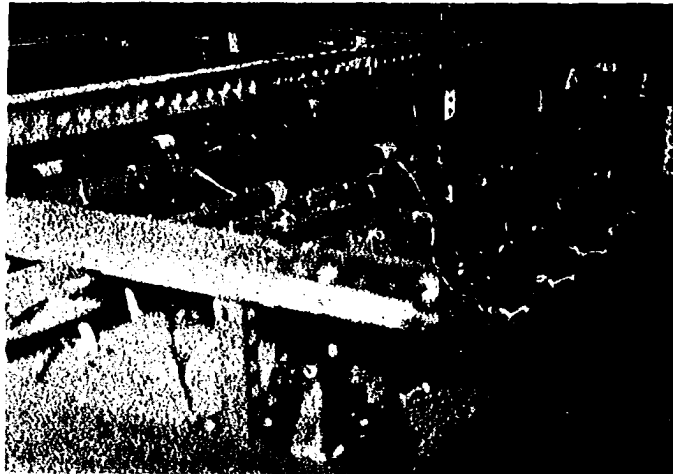


Figure 5.2c-Layout of strain gages on microconcrete surface.

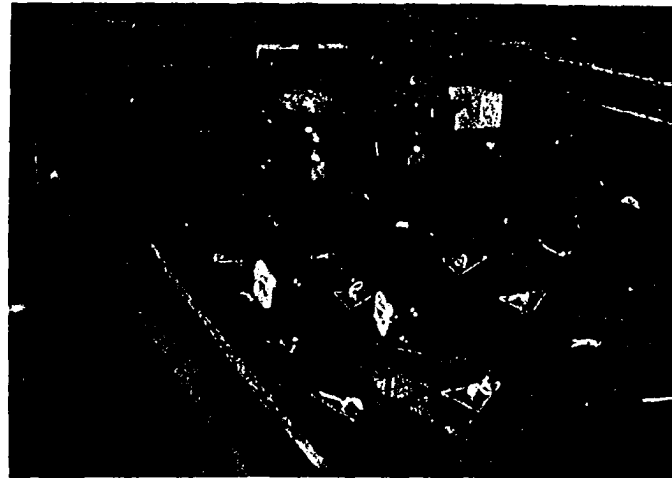


Figure 5.2d-Instruments for measuring deflections.

3/16" x 4' -9 7/8") on top (Figure 4.7h and 5.2a) and the lower ends of the pipes were bolt connected to the dummy beam.

(c) Two Reinforced Concrete End Diaphragms

The wire reinforcing cage for these diaphragms was made of SWG 18 and 13 and was fabricated in place on the steel cap plates by brazing at random locations. Details are shown in Figure 4.7h and Figure 5.2b.

The same mixture used in the microconcrete (described in the Sec. 4.4.4) was used in casting the end diaphragms two days in advance of the model casting. The compressive strength of 3 cylinders was 3,800 psi at age 7 days.

Plexiglas was chosen as formwork material because: (1) the nonbonding and smooth surface produced smooth surfaces on the model for easy location of initial cracking during the test, and (2) the characteristic transparency enabled the elimination of honeycombing. The individual Plexiglas pieces were "welded" together with ethylene dichloride ( $\text{CH}_2\text{CHCl}_2$ ).

The principal purpose of this study was to evaluate the currently recommended analysis and design methods of a simply supported folded plate structure. Consequently, the end diaphragms were designed with a large safety factor (4.0) in order to circumvent a possible detail failure.

#### (d) Elastic Hinge Type Construction Joints

Special consideration was given to the construction joints to meet the boundary condition of simple support which is a key assumption for the analysis and design in this study. The end plates of the model had to be free to rotate longitudinally but able to resist the shears along the plate edge parallel to the end diaphragms transmitted from the plates to the end diaphragms. Construction joints also had to meet the criteria of the ACI Code<sup>(3)</sup> for actual construction.

Rubber pads coupled with a single line of dowels of SWG 18 were used because of: (1) its elastic characteristics -- providing the elastic hinge in the longitudinal direction --, and (2) its high resistance against sliding and compression. Single dowels were placed along the center line of the end diaphragms by using 4" SWG 18 wires at 3/4" c/c extending 2" into plates and end diaphragms according to the requirements of the ACI Code. Two 1/16" x 3/4" rubber pads were placed on both sides of the dowels along the joints (Figure 4.7h). This type of hinged joint performed very well during the test and are shown in the Figures 5.3d and 5.3e.

### 5.2.2 Model Structure

#### (a) Formwork

As described in the Sec. 5.2.1c, Plexiglas braced with 1" x 2" lumber strips and intermediate diaphragms of

1/2" plywood was used for the formwork. Galvanized wood screws were inserted vertically from the bottom side of the Plexiglas plate in order to form access holes through the model plates for nylon strips which applied the point loads. These vertically mounted screws were preset to extend 1/2" normal to the upper plate-surfaces of the model to provide control points for screeding purposes to help establish the desired thickness of microconcrete.

The forms were constructed in 3 sections for ease of removal after the microconcrete hardened and were aligned and cambered 1/8" in the middle section by means of adjustable steel belts connecting the intermediate diaphragms which were separated by 1" x 1" x 1" neoprene rubber pads.

#### (b) Reinforcement (Wire) Cage Fabrication

Fabrication of the wire cage was completed by brazing at random locations in three phases: (1) transverse positive moment steel, (2) longitudinal plate and diagonal tension steel, and (3) transverse negative moment steel (see Figures 4.7 and 5.2b) on a control form made of plywood with the same dimensions as used in the form for the model. The bar spacings in the transverse and longitudinal directions were controlled by drawing lines on the form, and the bar spacing and cover distances in the normal direction to the plate were controlled by reinforcement chairs made of suitable sized wire. The fabricated wire cage was then placed in the

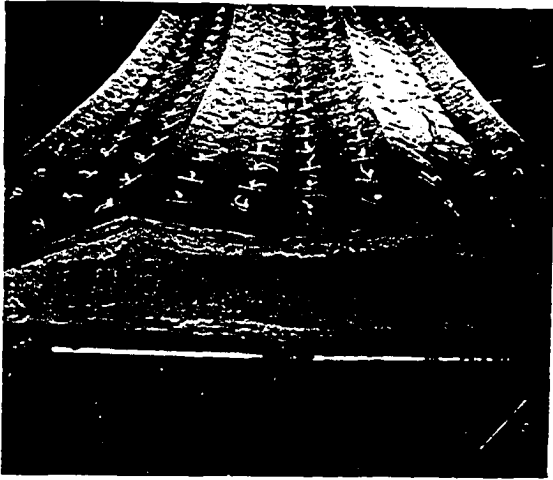


Figure 5.3a-Top view of the model after testing.

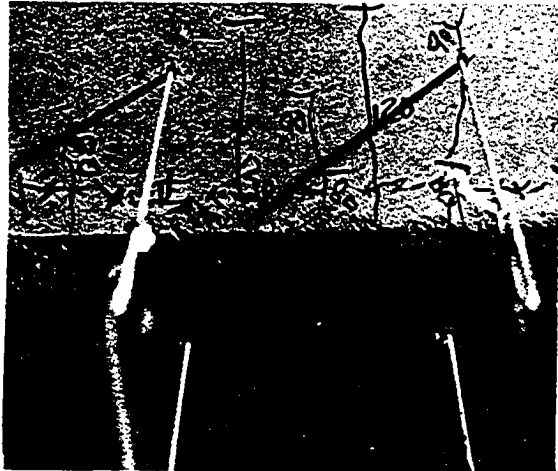


Figure 5.3b-Typical cracking due to longitudinal action and concrete crushing at bottom ridge line 1 of the model.



Figure 5.3c-Cracking of plates along the inside face of the end diaphragm.

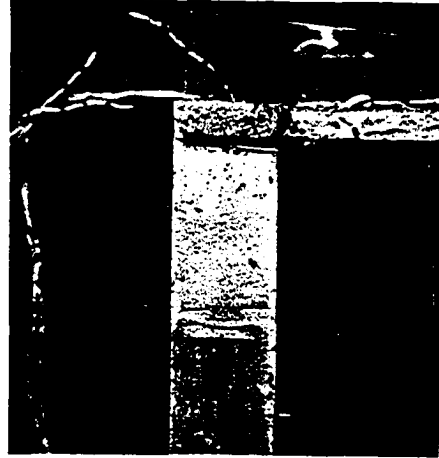


Figure 5.3d-Rotation of plates at support of the model.

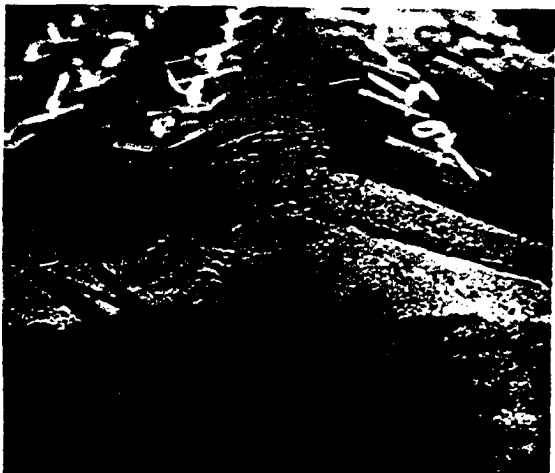


Figure 5.3e-Typical cracking along the ridge line 2' at the end of plates due to slab action.

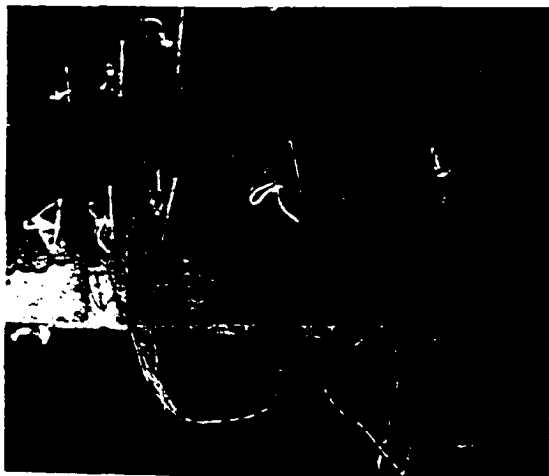


Figure 5.3f-Typical cracking due to a combination of longitudinal, transverse and diagonal stresses.

Plexiglas form and was held in its proper position by the wood screws described in the previous subsection (Sec. 5.2.2a).

(c) Casting of Model Plates

Two days after the end diaphragms were cast, the model plates were cast from the microconcrete mixed by hand as described in Sec. 4.4.4. Three small vibrators were applied to the form until no visible air bubbles were found by observation through the transparent Plexiglas form. Curing was effected by spraying the models after the finishing operation with hydrocide resin curing compound. Quality control for the model concrete was maintained by testing ten 3" x 6" microconcrete cylinders which were cured in the same manner and maintained in the same environment as the model structure. Seven compression and three split cylinder tests were made on the day of the model test (7 days after casting). The test results are shown in Table 5.1:

Cylinder size (in.)	Age at time of test (days)	Compressive strength			Split cylinder strength		
		fc' (psi)	No. of cyls	V (%)	fsp (psi)	No. of cyls	V (%)
3" x 6"	7	4,270	7	.67	477	3	2.12

Table 5.1 Summary of model quality control cylinder tests

Plexiglas form and was held in its proper position by the wood screws described in the previous subsection (Sec. 5.2.2a).

(c) Casting of Model Plates

Two days after the end diaphragms were cast, the model plates were cast from the microconcrete mixed by hand as described in Sec. 4.4.4. Three small vibrators were applied to the form until no visible air bubbles were found by observation through the transparent Plexiglas form. Curing was effected by spraying the models after the finishing operation with hydrocide resin curing compound. Quality control for the model concrete was maintained by testing ten 3" x 6" microconcrete cylinders which were cured in the same manner and maintained in the same environment as the model structure. Seven compression and three split cylinder tests were made on the day of the model test (7 days after casting). The test results are shown in Table 5.1:

Cylinder size (in.)	Age at time of test (days)	Compressive strength			Split cylinder strength		
		fc' (psi)	No. of cyls	V (%)	fsp (psi)	No. of cyls	V (%)
3" x 6"	7	4,270	7	.67	477	3	2.12

Table 5.1 Summary of model quality control cylinder tests

## (d) Design versus As-Built Dimensions

As-built vertical distances (measured through loading holes) were measured before the test of the model and are shown in Table 5.2 in accordance with "code schema for as-built dimensions" shown in Figure 5.4. A summary of the thicknesses of the model plates is shown in Table 5.3. Overall as-built thickness of the model plates was 0.531", and the ratio of measured average thickness to design thickness was 1.06.

As expected, there were only minor variations in the dimensions. However, calculations of capacities were based on the actual measured values.

## (e) Discussion

Honeycombing was limited to small diameter voids on the formed surfaces; however, the brazed connections caused some discolorations of the bottom surfaces of the model plates.

## 5.3 Load Testing System

## 5.3.1 General

Several commonly used loading systems in testing folded plate model structures are: (1) water loading system, (30) (2) brick or concrete block loading system,<sup>(24,27)</sup> (3) sand bag loading system<sup>(28,47,50)</sup> and (4) "whiffle-tree" loading system.<sup>(7,26,57)</sup> A water loading system was used

L		D <sub>N</sub>		D <sub>S</sub>		L'			D' <sub>N</sub>			D' <sub>S</sub>		
		R <sub>1</sub>	R <sub>2</sub>	R <sub>3</sub>	R' <sub>3</sub>	R' <sub>2</sub>	R' <sub>1</sub>	a <sub>1</sub>	a <sub>2</sub>	a <sub>3</sub>	a' <sub>3</sub>	a' <sub>2</sub>	a' <sub>1</sub>	
98 1/16	2 3/16	2 3/16	2 1/16	2 1/16	98 1/16	2 1/8	2 1/16	2 1/8	2 1/16	2 1/8	2 1/16	2 1/8	2 1/16	
9/16	2 9/16	1 1/2	1 1/2	2 1/2	1/2	5 11/16	11 7/8	11 7/8	11 7/8	11 13/16	11 13/16	11 5/16	5 1/16	
1/2	2 5/8	1 7/8	1 7/8	2 7/16	1/2	W 57 7/8						5 3/4		
Diaphragm														
South														
North														
Vertical distance through loading holes														
A														
B														
C														
D														
E														
E'														
D'														
C'														
B'														
A'														
1	.495	.619	.479	.485	.487	.518	.522	.496	.534	.525				
2	.536	.607	.453	.433	.433	.544	.540	.510	.577	.512				
3	.517	.548	.470	.480	.450	.500	.550	.515	.573	.564				
4	.490	.500	.480	.512	.470	.510	.590	.505	.571	.550				
5	.498	.507	.526	.512	.517	.542	.629	.555	.548	.535				
6	.507	.527	.580	.605	.503	.508	.595	.550	.610	.525				
7	.507	.558	.614	.638	.506	.512	.608	.573	.650	.609				
8	.517	.521	.644	.618	.506	.533	.601	.600	.650	.649				
8'	.644	.538	.667	.586	.597	.548	.604	.576	.658	.614				
7'	.564	.571	.644	.603	.573	.585	.605	.538	.650	.594				
6'	.610	.640	.611	.589	.540	.561	.611	.546	.650	.620				
5'	.528	.501	.546	.545	.503	.529	.640	.627	.650	.580				
4'	.533	.557	.524	.534	.550	.636	.650	.556	.650	.547				
3'	.538	.458	.496	.554	.520	.602	.633	.584	.650	.554				
2'	.542	.500	.477	.559	.584	.615	.578	.527	.651	.550				
1'	.543	.476	.486	.523	.516	.520	.551	.509	.542	.551				

Table 5.2 As-built dimensions (Inches).

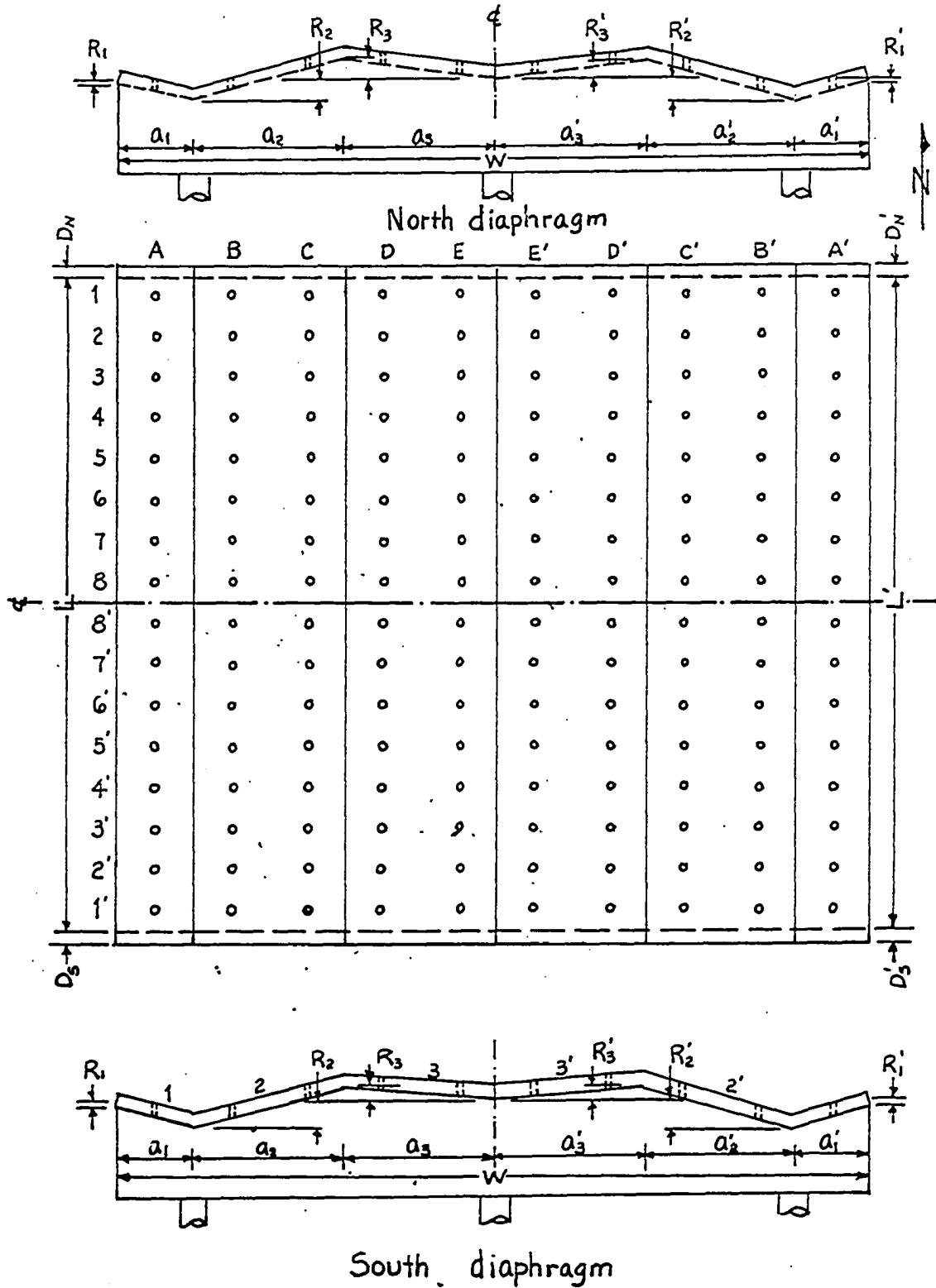


Figure 5.4 Code schema for as-built dimensions.  
 (See Table 5.2 for as-built dimensions).

in the relatively small model test by Enami.<sup>(30)</sup> However, the frame provided resistance to translation and rotation of the end diaphragms. A brick (or concrete block) loading system was used successfully by Chacos and Scalzi<sup>(24)</sup> on a small model. This system is not practical for relatively large models. Sand bag loading has been employed in the relatively large model or prototype test,<sup>(28)</sup> even though uniformly distributed load is hardly obtained. The most practical and popular system to provide uniform loading is the "whiffle-tree" system. The soundness of this loading system has been reported by several authors.<sup>(7,26, 57)</sup> As mentioned in Sec. 5.1, the "whiffle-tree" system was used in this study.

### 5.3.2 "Whiffle-tree" Loading System

This system can provide either concentrated loads or uniform loads (simulated by many discrete points). In this study a 160 point tension type loading system was used. The "whiffle-tree" was composed of simple beams connected (carefully articulated) with steel ropes or nylon wires. In this study each of the 160 load points was distributed to the plate surface by means of three hard neoprene rubber pads (1/4" x 1/4" x 1/4") glued to 2" x 2" x 2" x 3/16" Plexiglas pieces. The first layer (with open hooks in the beams) was connected to the 2" x 2" x 2" x 3/16" Plexiglas pieces with 400 pound nylon strings which provided flexibility to the loading system to eliminate lateral restraint. The

Plate	1	2	3	3'	2'	1'	Overall	Overall $\frac{t_{meas.}}{t_{design}}$
No. of holes	16	32	32	32	32	16	160	1.06
t(in)	.532	.512	.565	.526	.506	.502	.531	
V(%)	7.45	8.10	5.55	5.28	9.58	5.61	7.89	

Table 5.3 Summary of model plate thickness.

remainder of the layers were connected by wire ropes. Longitudinally 16 identical transverse units were brought by simple beam connections to a single point where a pull type hydraulic ram was used to apply load to the model structure (See Figure 5.1 for "whiffle-tree" beam connections). The "whiffle-tree" device was supported by 10-1/2" standard pipes spanning between the supports and a movable table until the time for the model test. This arrangement allowed the application of the dead weight of the loading device onto the model structure in small increments.

### 5.3.3 Design and Verification of "Whiffle-tree" Loading System

The "Whiffle-tree" was designed for 55 pounds per loading point (1/3 of 55 pounds per rubber pad). The salient features of the system are shown in Figure 5.1. Each transverse unit of the "whiffle-tree" was load tested prior to installation.

In order to check the reliability of the loading system, two simple span reinforced concrete beams, one with a single transverse unit "whiffle-tree", the other with two transverse units, were designed for 55 pounds per loading point and tested (Figure 5.1a). The results of the tests (Table 5.4) indicated that the loading system could be used successfully for the model test.

A 20 ton center hole hydraulic ram with a 2.5 in. stroke was used to apply load. This ram was controlled

by a pressure pump equipped with a 10,000 psi pressure gage. The applied load (hydraulic pressure) was monitored by both the pressure gage and a self-temperature compensating center hole load cell which had been previously calibrated.

Total travel of the lowest point of the "whiffle-tree" where load was applied was expected to be between 7" and 8". Rechuck devices, consisting of a loading chair and two chucks, were used to apply load continuously (Figure 5.1b).

#### 5.3.4 Performance of Loading System

The loading system performed without incident throughout the test.

### 5.4 Instrumentation

#### 5.4.1 General

Instrumentation for the test was designed to obtain overall responses, (1) load-deflection and (2) load-strain of the model during the test.

#### 5.4.2 Deflection System

The deflections, vertical and horizontal were obtained from observations of 0.001" least count dial gages mounted on a fixed bridge with sliding tracks which allowed the dials to move freely horizontally. The details of the deflection measuring device are shown in Figure 5.2d.

Beam No.	Width (in.)	Depth (in.)	Span (in.)	p (%)	Application of loads	Yield $M_{test}/M_{calc.}$
1	4"	1.5	61.75	3.3	10 @ 5.75" c/c longitudinally only	.995
2	10	1.5	61.75	2.6	10 @ 5.75" c/c longitudinally 2 @ 6" transversely	1.17

Table 5.4 Summary of dimensions and test results of the beams for verification of "Whiffle-tree" loading system

Vertical deflections were measured at end diaphragms, mid-span and selected quarter-span points along the ridge lines of the model and horizontal deflections were measured at joints 0, 1, 2 and 3 at mid-span for each load increment. Dial gage layout for deflection measurement is shown in Figure 5.5.

#### 5.4.3 Strain System

Wire strain gages (SR-4) were installed on the longitudinal reinforcement (SWG 13) and the microconcrete surface to measure longitudinal and transverse strain respectively. Strains were monitored with a servo-balance strain indicator and two twenty channel switch and balance units.

##### (a) Microconcrete Strain System

Twelve SR-4 paper base wire strain gages were installed transversely on the microconcrete surface on the South-East quarter section of the model along ridge lines (Figure 5.5). However, transient temperature and humidity conditions rendered all but four of the twelve gages ineffective.

##### (b) Longitudinal Strain System

Twelve SR-4 paper base wire strain gages were installed on the longitudinal SWG 13 steel wires. Two SWG 13 wires were brazed together to have a surface wide enough for mounting the gages. Waterproof epoxy resin was used to

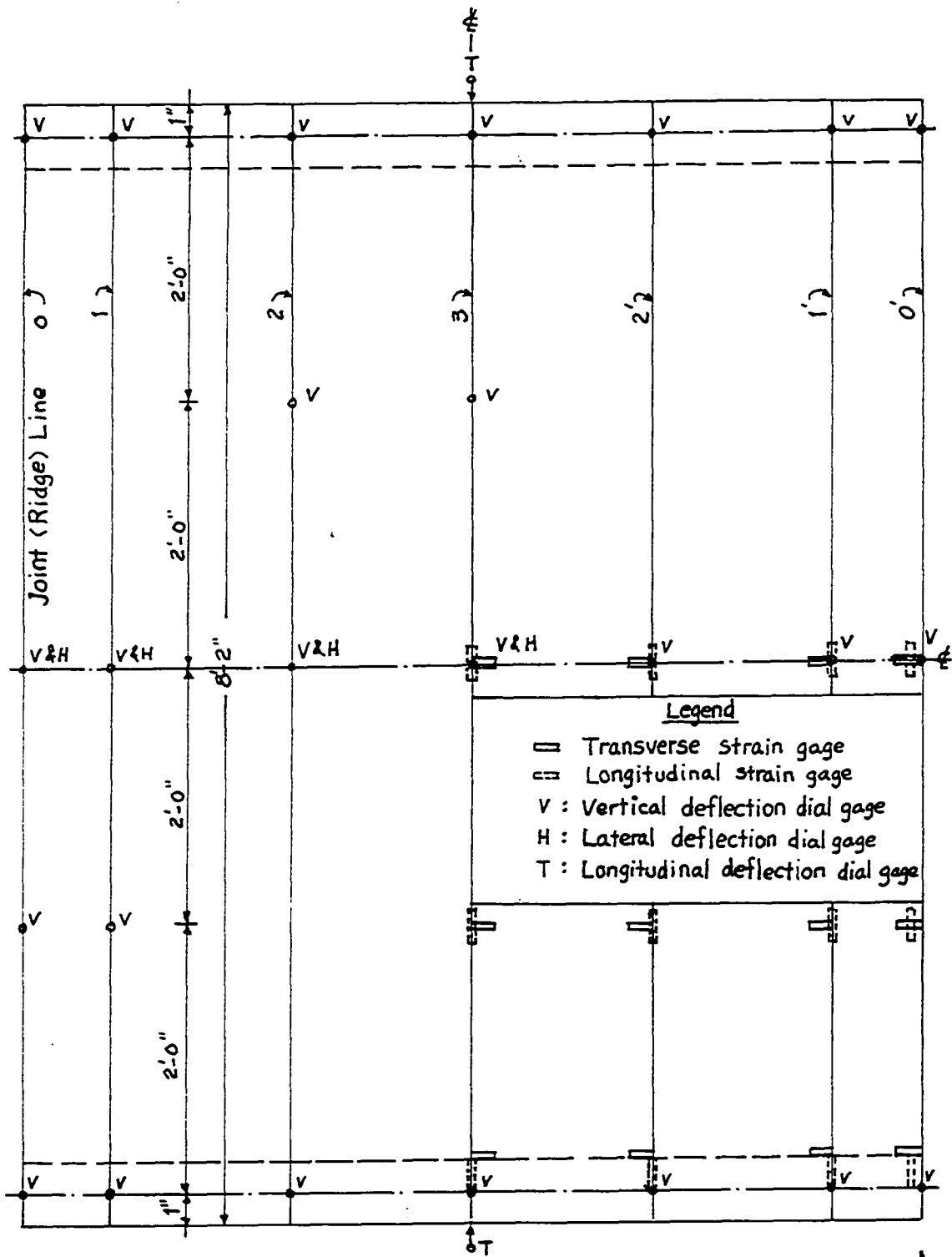


Figure 5.5 Layout for strain and deflection dial gages.

insulate and waterproof the gages before the model was cast. All of the gages performed satisfactorily during the test. The strain gage layout is shown in Figure 5.5. The effects of the brazed connections on the material properties of the wires were studied and found to be negligible (Table 5.5).

### 5.5 Description of the Model Test

At age of 7 days the model was loaded to failure. The weight of "whiffle-tree" was applied to the model in small increments by connecting the transverse units to the model while the longitudinal unit was supported by a table, then the supported table was removed. After the entire "whiffle-tree" system, including the hydraulic ram, was connected to the model, the ram, which was monitored by a pressure gage and a load cell, was used to apply load in 10 psf increments.

After application of each loading increment, the load was maintained constant as vertical and horizontal displacements and strains were recorded. Cracking of the top and bottom surfaces of the model plates was observed and marked for each load increment. As expected the ram had to be rechucked twice. However, the test lasted only two hours and the effects of creep during the test were considered insignificant. As described in Sec. 5.2.1 and 5.3.5, the elastic hinge joints and the "whiffle-tree" loading system performed satisfactorily. The maximum

Wire	No. of Test	Yield point		Ultimate strength		Elongation	
		$f_y$ (ksi)	V (%)	$f_u$ (ksi)	V (%)	e (%)	V (%)
SWG 13	8	28.25	7.91	46.54	1.52	.335	6.74

Table 5.5 Summary of mechanical properties of model reinforcement with brazed connections

load supported by the model was 135 psf. The results of the test are shown in Figure 5.6.

## 5.6 Analysis and Discussion of the Test Results

The response of the model is analyzed and discussed in terms of cracking, load-strain, load-deflection and collapse in the following sections. The theoretical responses of the model were obtained with the mean dimensions of the model as built.

### 5.6.1 Cracking and Load versus Strain Responses

The cracking of the plates of the test model were observed on the top and bottom surfaces of the model. The general development of this cracking for various stages of the loading is shown in Figures 5.6g and 5.6h.

The first visible cracks occurred at a load (DL + LL) of 90.5 psf. which is slightly higher than the design load (85.7 psf); however, load-strain response showed that the cracking load was 83.5 psf (see  $S_{1M}$  and  $C_{2E}$  in Figure 5.7a and 5.7c respectively). These cracks (Figure 5.3, 5.6g and 5.6h) were of two distinct types: (1) transverse cracks across (normal to) the bottom ridge lines 1 and 1' at mid-span caused by the longitudinal stresses, (2) longitudinal cracks at ends of the plates along the top ridge lines 2 and 2'. These cracking responses indicated that for loads up to the service load the model behaved very closely in a manner predicted by the folded plate theory

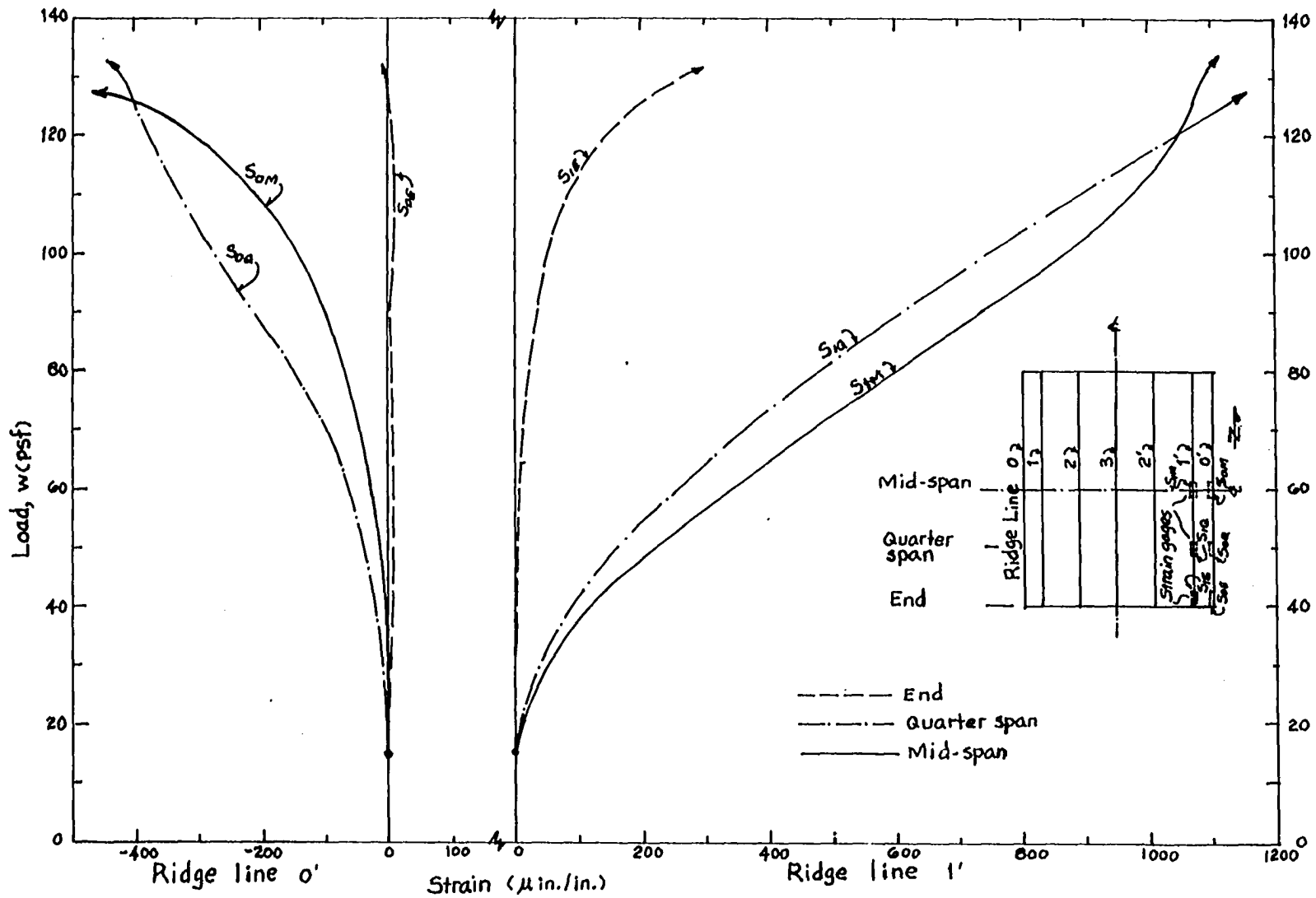


Figure 5.6a Longitudinal strain on the steel (Initial reading taken w/transverse "whiffle-tree" unit on the model) - ridge lines 0' and 1'.

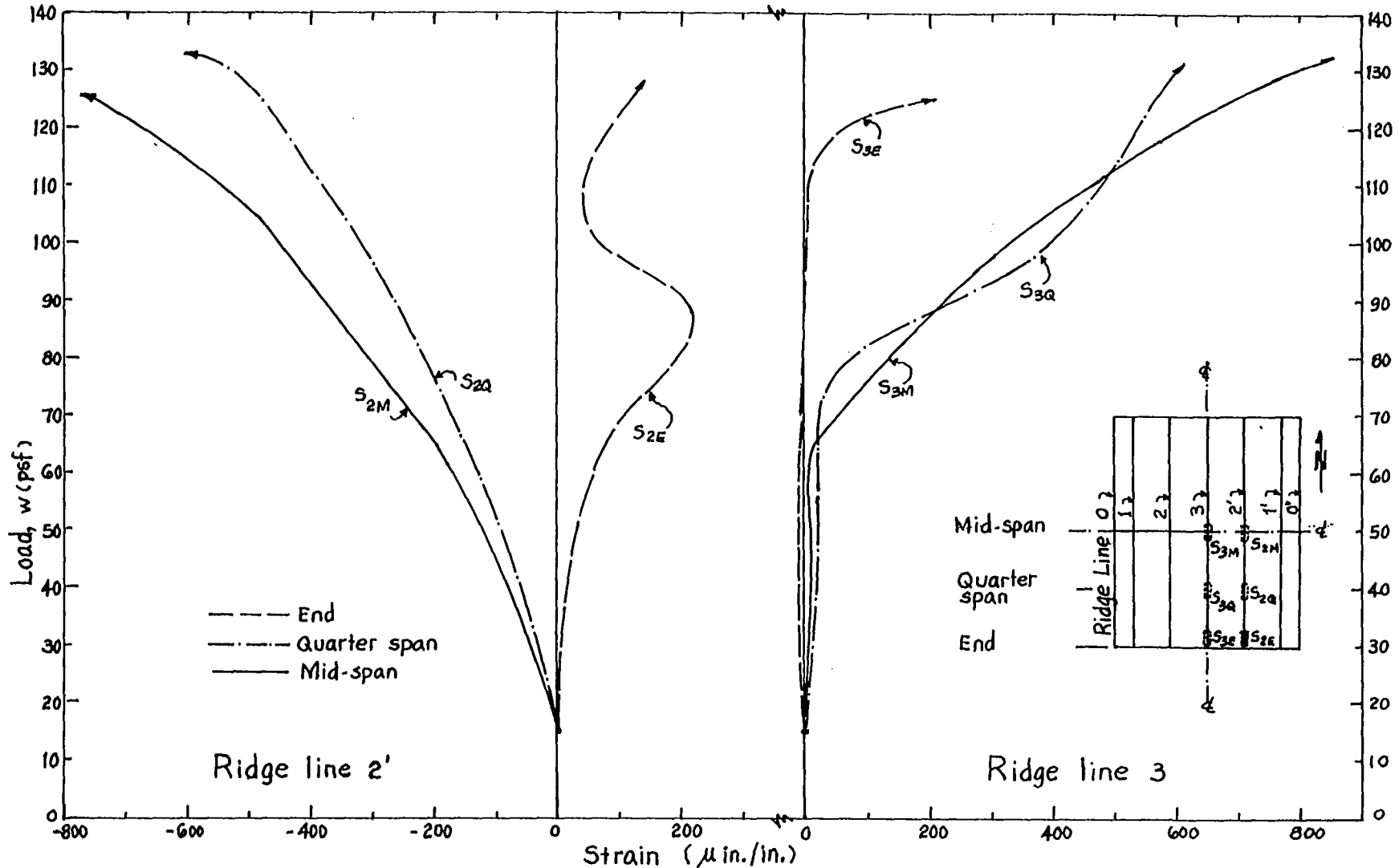


Figure 5.6b Longitudinal strain on the steel (Initial reading taken w/transverse 'whiffle-tree' unit on the model)-ridge lines 2' and 3.

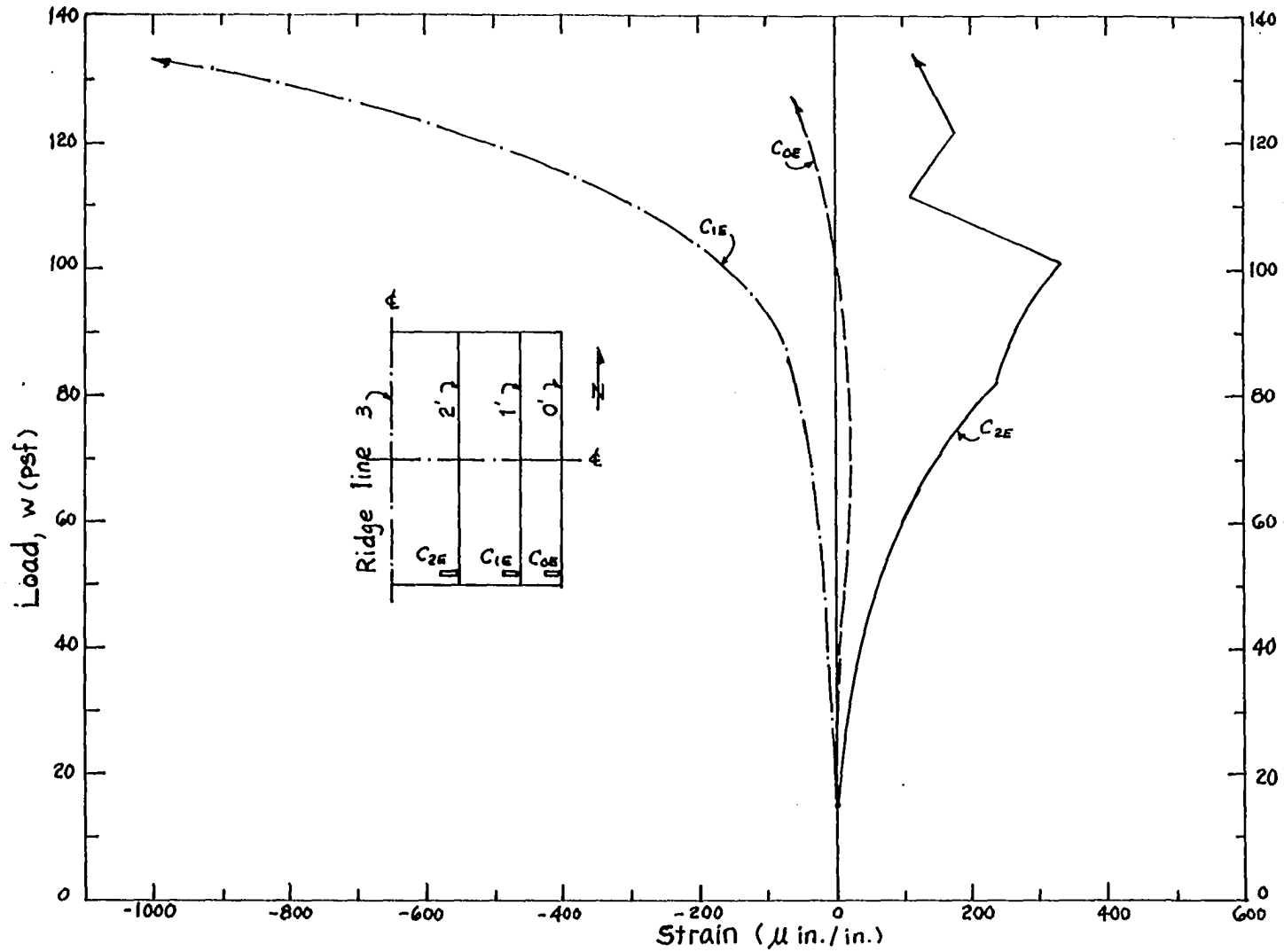


Figure 5.6c Transverse strain on the top surface of the model (Initial reading taken w/ transverse 'whiffle-tree' unit on the model).

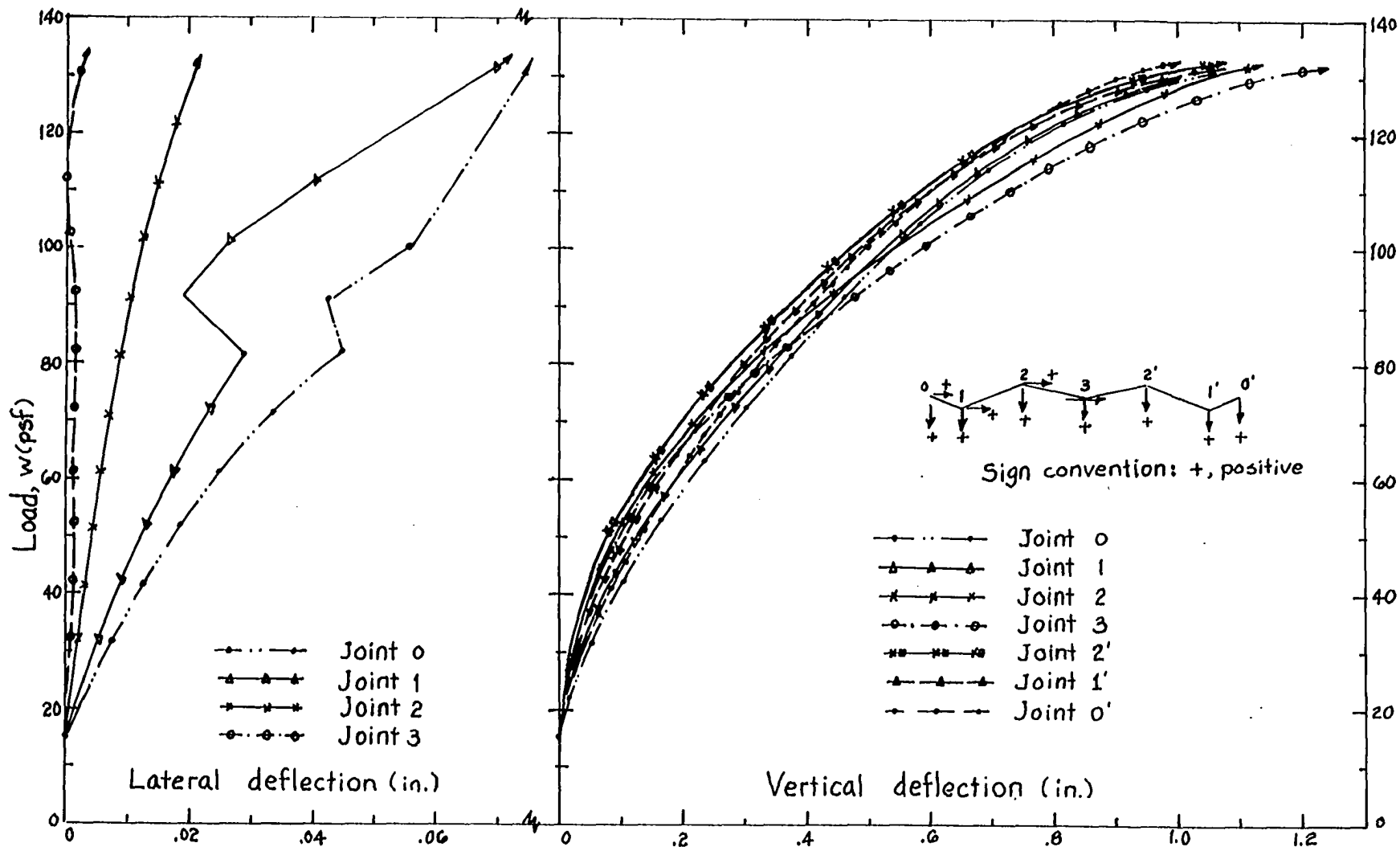


Figure 5.6d Deflection at mid-span (Initial reading taken w/transverse "whiffle-tree" unit on the model).

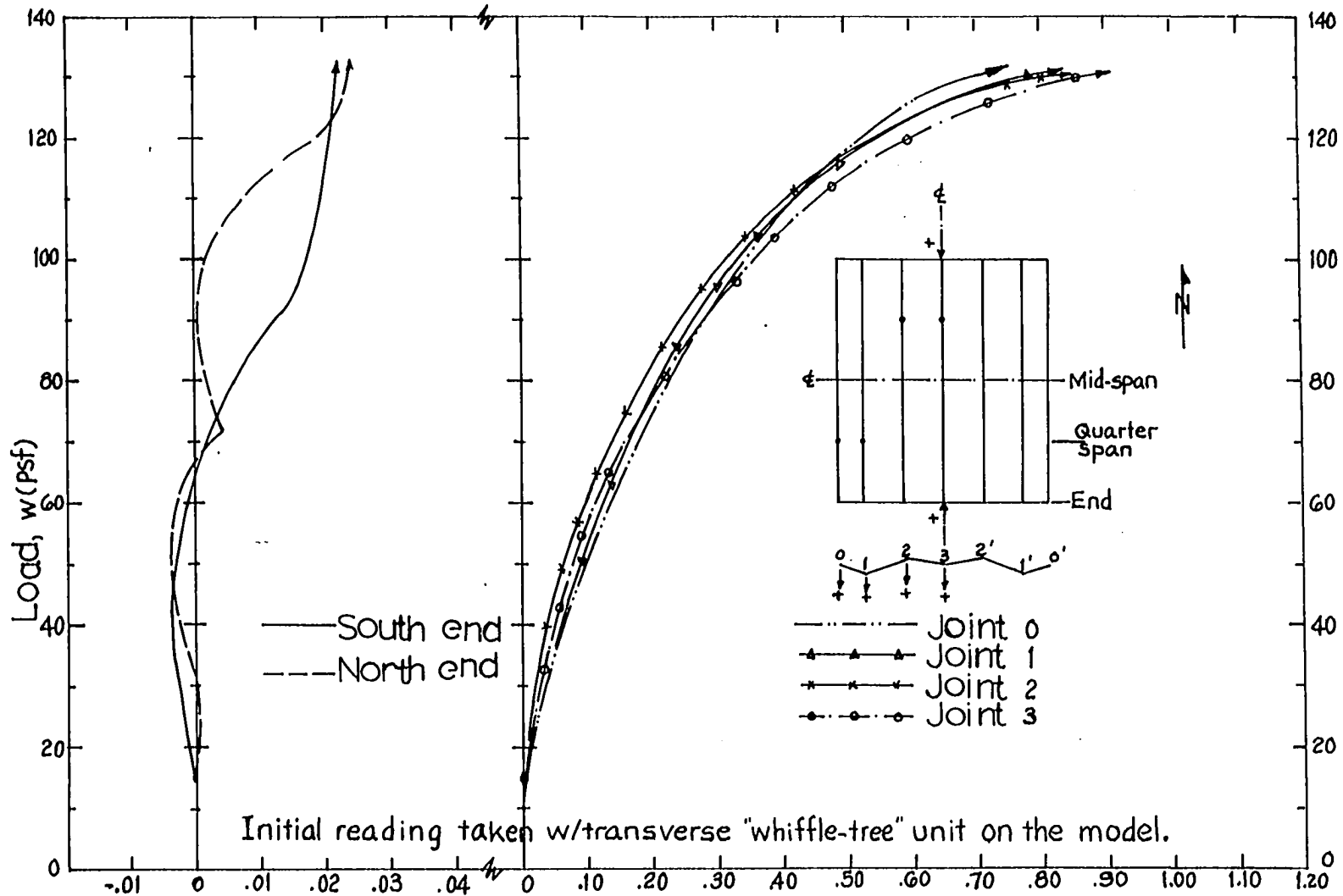


Figure 5.6e Longitudinal deflections at end diaphragms(in.).

Figure 5.6f Vertical deflections at quarter span(in.).

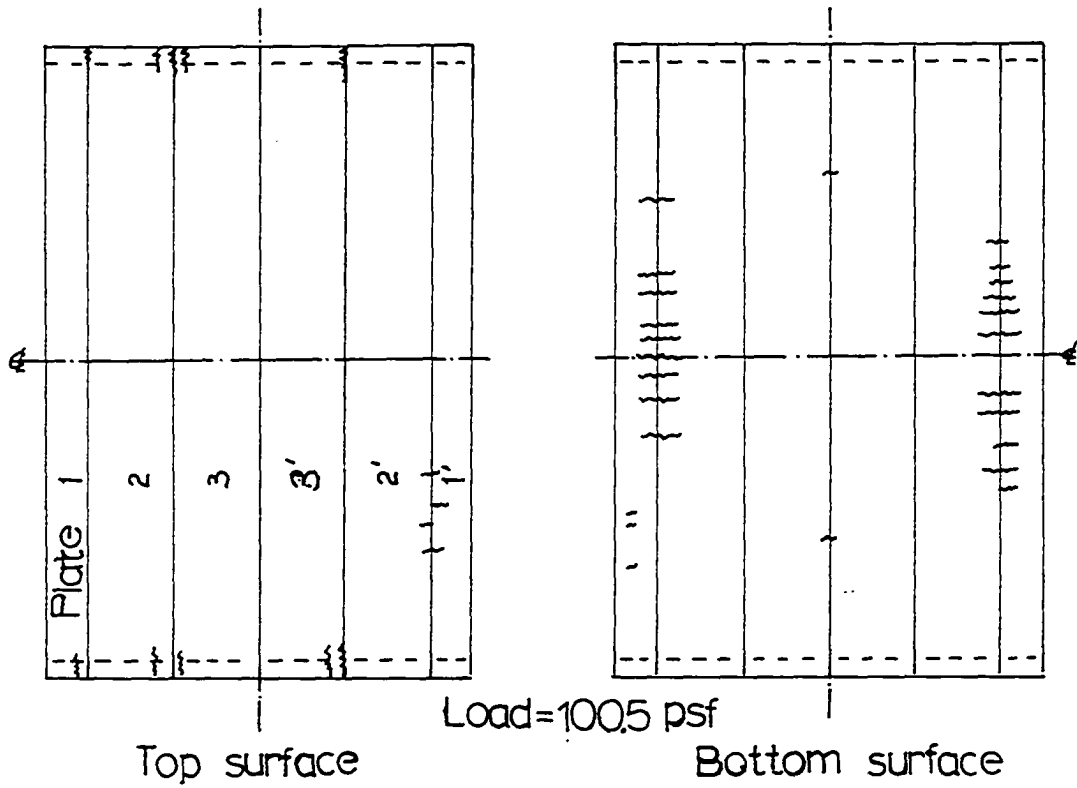
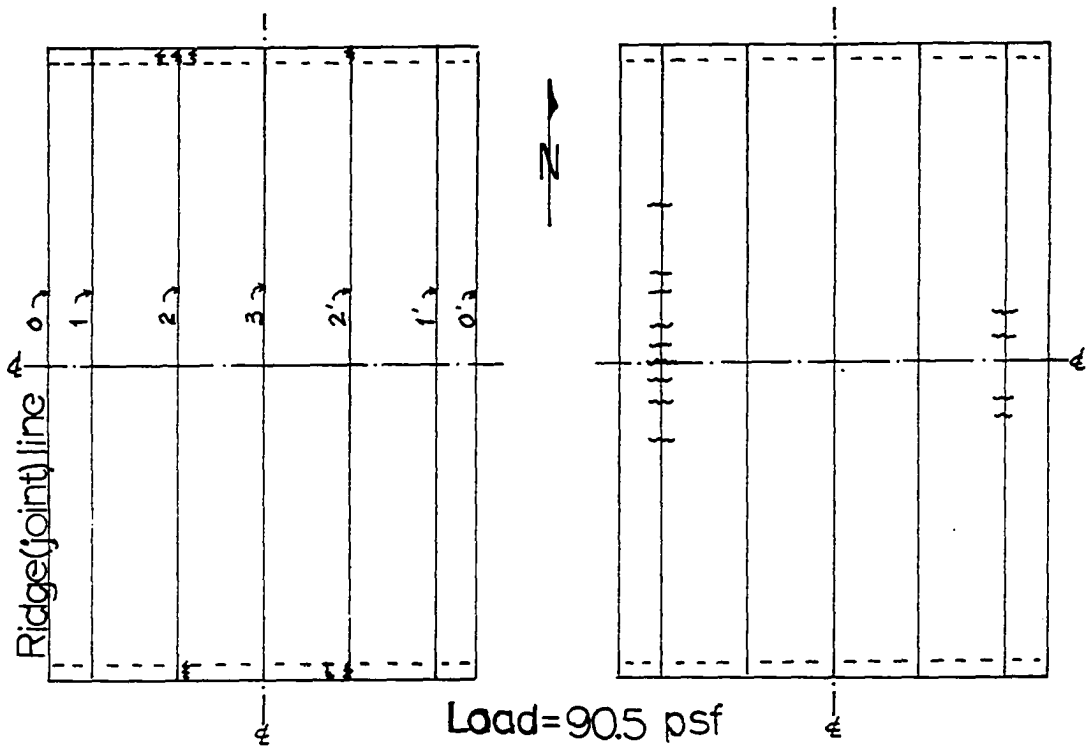


Figure 5.6g Cracking

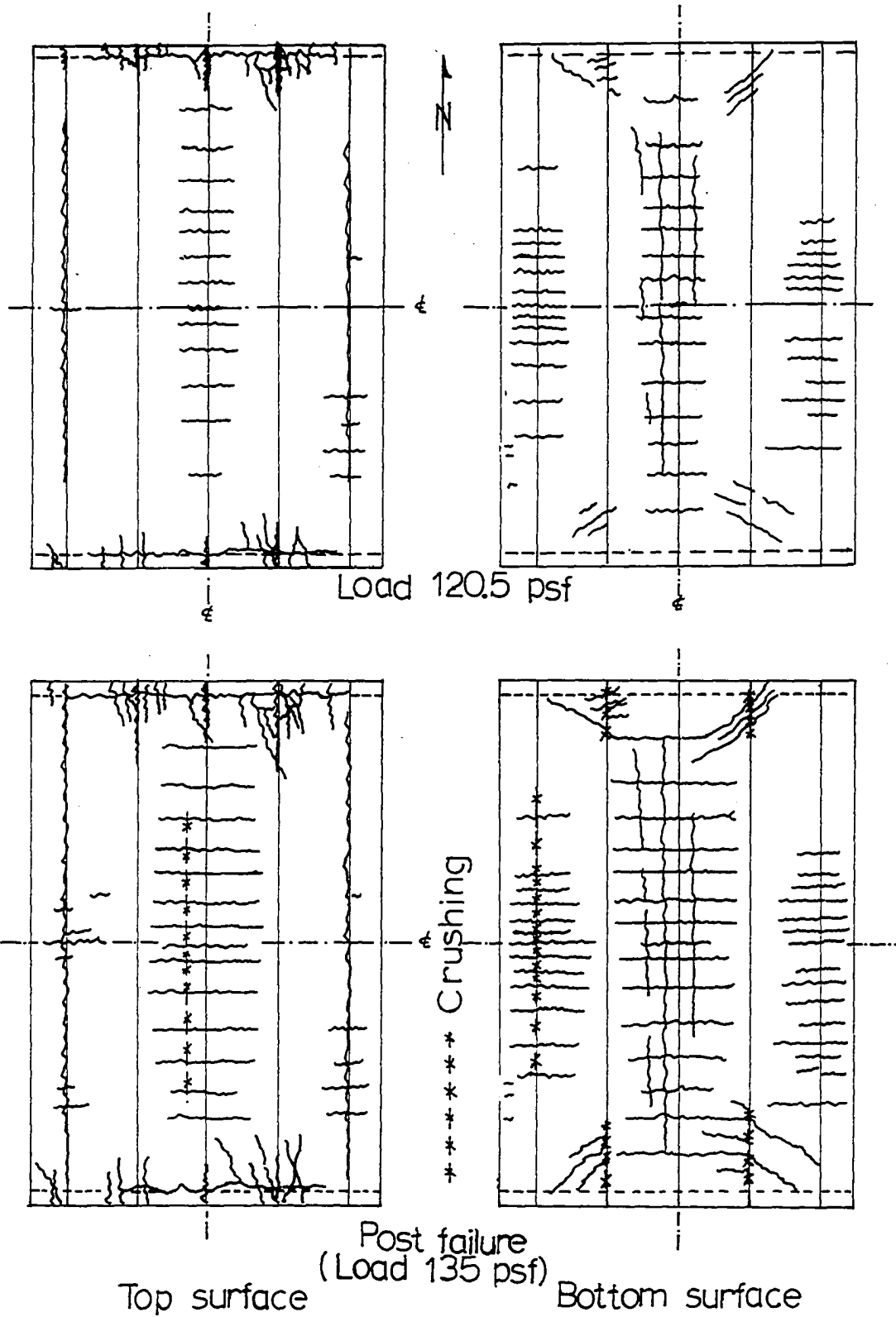


Figure 5.6h Cracking

considering the relative joint displacements. As the load increased, all these cracks widened and became more numerous. At 100.5 psf load (94 psf shown in the curve SlQ) new cracks appeared: (1) transverse cracks at quarter span across the top and bottom ridge line 1' and the bottom ridge line 3, and at mid-span across the top ridge line 1, (2) longitudinal cracks at ends of the plates along the top ridge line 1. At 120.5 psf load transverse cracks appeared almost entire span across the top and bottom ridge line 3 and on the top inside four plates along the inside faces of the end diaphragms, longitudinal cracks appeared on the bottom surface of plates near the ridge line 3 and along the top ridge lines 1 and 1', and diagonal cracks appeared near the supports on the top and bottom surfaces of plates. The longitudinal crushing of concrete along the bottom ridge line 1 and on the top plate near the ridge line 3 began to appear at a load of 130.5 psf.

Three separate ranges were observed in the load-tensile strain responses: (a) the first range, up to load of approximately 60 psi, has steep slope which flattens gradually and the concrete has not cracked, (b) second range, up to yield strength, has nearly linear but flatter slope, and the concrete has cracked, and (3) the last range up to collapse is a nonlinear zone and the slope decreases sharply and approaches zero.

The three separate ranges appeared in the load-strain curves such as  $S_{1M}$  and  $S_{3Q}$  are apparently the characteristics of the reinforced concrete structure. Since the reinforced concrete structure is heterogeneous, nonisotropic, and inelastic, its properties are very complex and subjected to change as the applied load increases. In the first range, with an uncracked section the concrete prevails and the characteristics of the curves are nearly same as that of plain concrete. Steel characteristics dominate in the second range and the curves are fairly straight in this range. It is very interesting to observe that the slope at the yielding strength level increases instead of decreasing. This particular phenomena can be explained as follows: At this stage plastic hinging begins to develop, and the elastic resistance resists that change, thus an excess external force is required to make this transition possible. Like steel, which has transition range between the elastic and plastic ranges, there is a transition range in the reinforced concrete structure. The only difference is that the concrete which is far away from the plastic status at this stage alters the transition curve slightly. This occurs since at the moment of the change, the steel has lost momentum and the properties of the concrete prevail; therefore, the curve is similar to that of plain concrete in this short transition range. The third range is an inelastic range, and the steel prevails as with the normal cracked section.

From the load-strain curves it was obvious that the longitudinal stresses at the supports were negligible up to yielding load. These indicated that the elastic hinge type construction joints provided satisfactorily the simple support boundary conditions. It was noted that the opening of the joints at the ends of the plates was about  $3/8$ " at the maximum capacity load (Figure 5.3e). The yield point load determined from the load-strain curve was 108 psf (corresponding to  $e_y = 975 \times 10^{-3}$  in./in. in the curve  $S_{1M}$  of the Figure 5.7a). The plate load variations at  $1/2L$  and  $1/4L$  along the same ridge lines were obtained from the load-strain responses and compared with that of the design load in Table 5.6. The comparison showed that there were significant differences at the ridge lines 0' (edge plate end) and 3 (flat ridge). These responses indicated that the disturbance of the edge plate and the influence of the parameter (angle between the plates), as described in Chapter III, were significant.

The transverse strain at end of the model across the ridge line 1 ( $C_{1E}$ ) was negative instead of the positive value obtained by calculation. This contradiction caused by torsional bending as a result of warping at the support induced by longitudinal strain as seen during the test, indicated that the assumption of the insignificant torsion effect in the elastic linear plate theory was incorrect. The abrupt change in the slope of the curve  $S_{2E}$  indicated

that the plate joints 2 and 2' at end where the concrete deteriorated were the most critical places. This phenomena was caused by the higher local stress due to warping on the end of the model.

The load, obtained from the load-strain response, for various stages -- cracking, yielding -- were compared with that of the design and also with the value obtained from the nonlinear inelastic beam theory as shown in Table 5.7. The test results showed that the linear elastic theory predicted very closely for loads up to the working load level and the nonlinear beam theory predicted closely at yielding load level.

#### 5.6.2 Load versus Deflection Response

The load-deflection responses of the model were compared, Figure 5.7d through 5.7g, with theoretical load-deflection responses predicted by (a) folded plate theory considering relative joint displacement -- linear elastic theory -- and (b) a nonlinear inelastic beam theory.

##### (a) The Characteristics of the Load deflection Responses of the Test Model

The characteristics of the load-vertical deflection responses were similar to that of the load-tensile strain responses, and again there were three separate ranges as described in the previous section. The deflections of symmetrically located stations such as ridge lines 0 and 0'

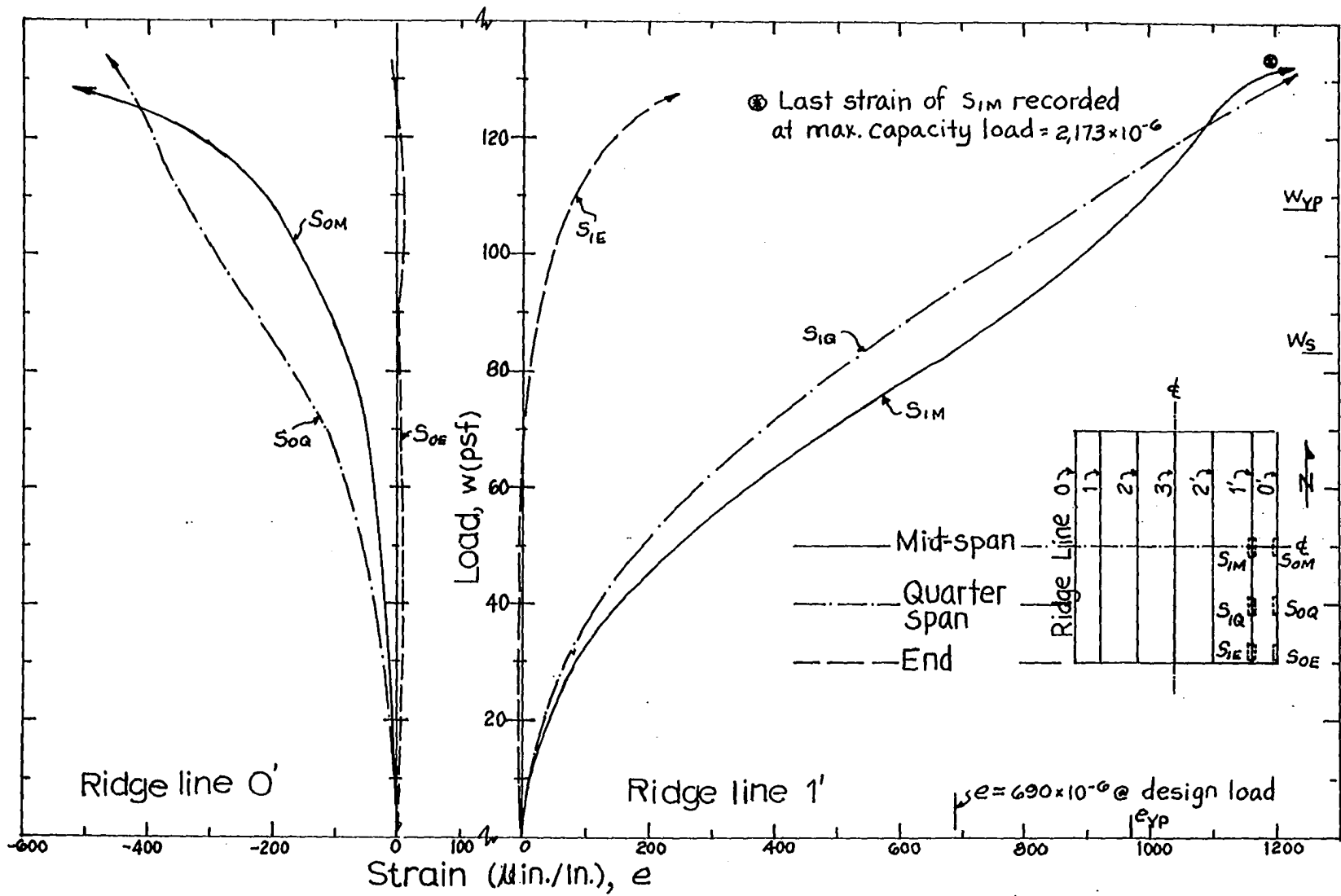


Figure 5.7a Longitudinal strains on the steels - ridge lines 0' and 1'

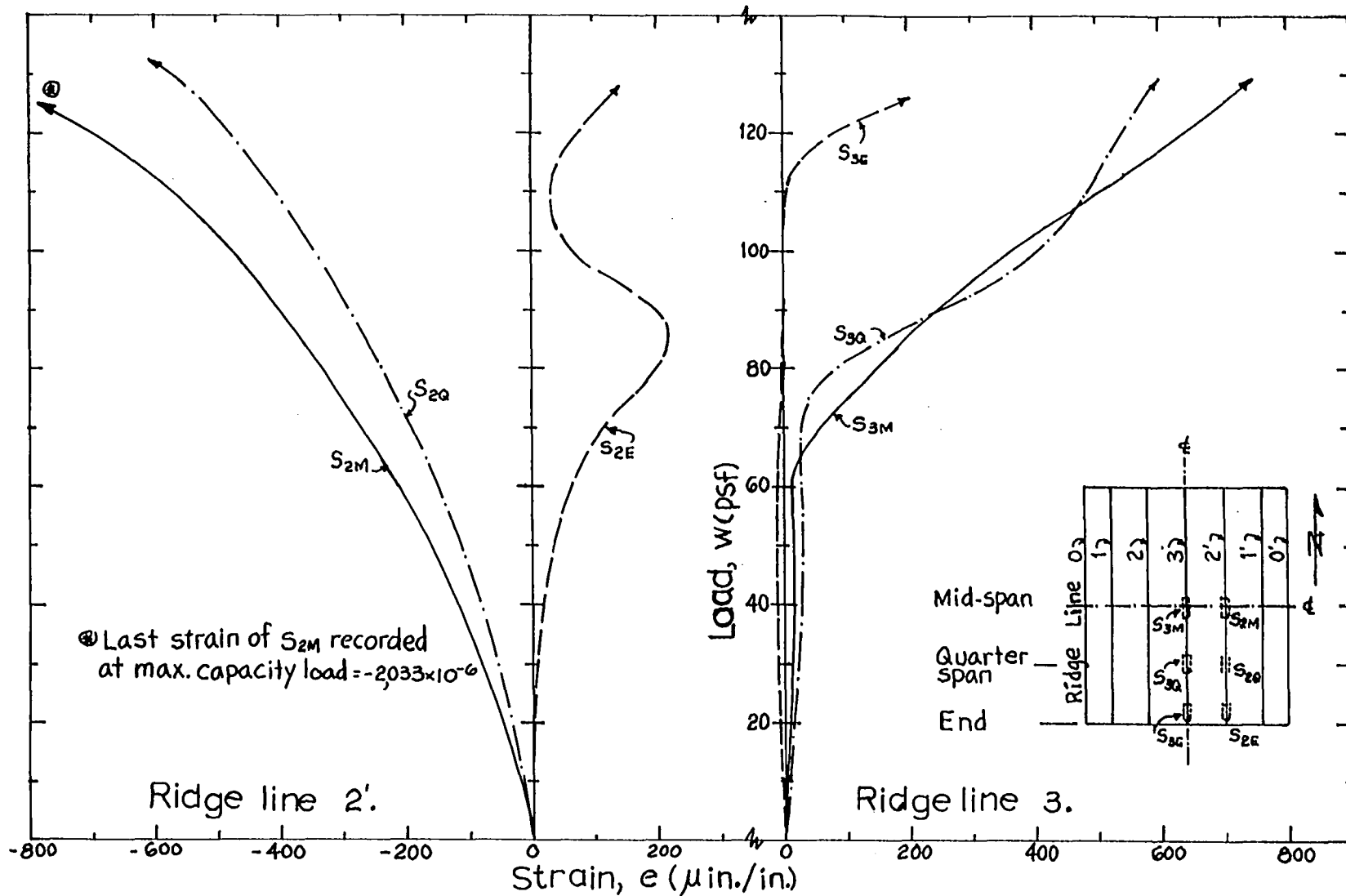


Figure 5.7b Longitudinal strains on the steels—ridge lines 2' and 3

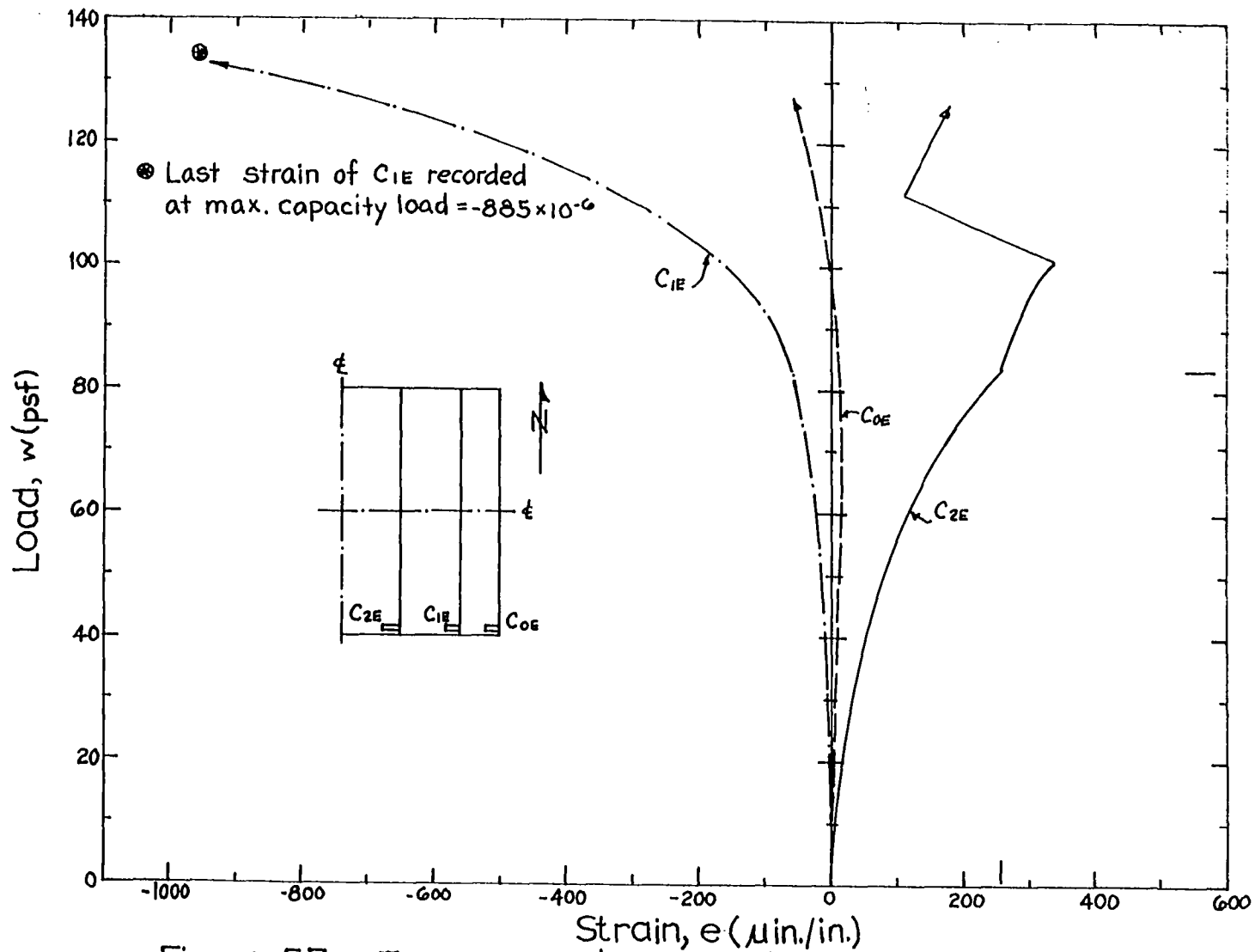


Figure 5.7c Transverse strains on the top surface of the model

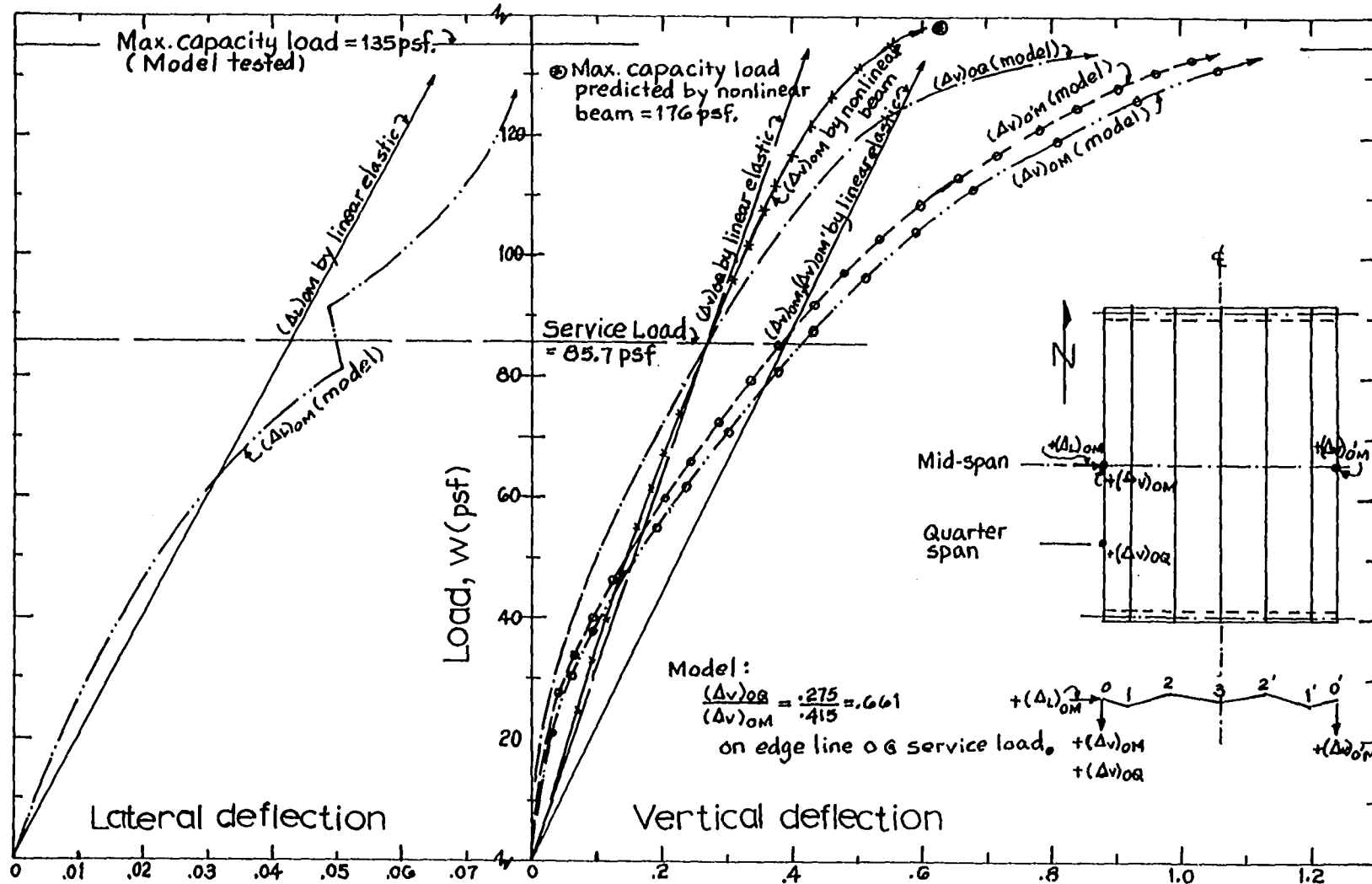


Figure 5.7d Deflections of ridge lines O and O' (in.).

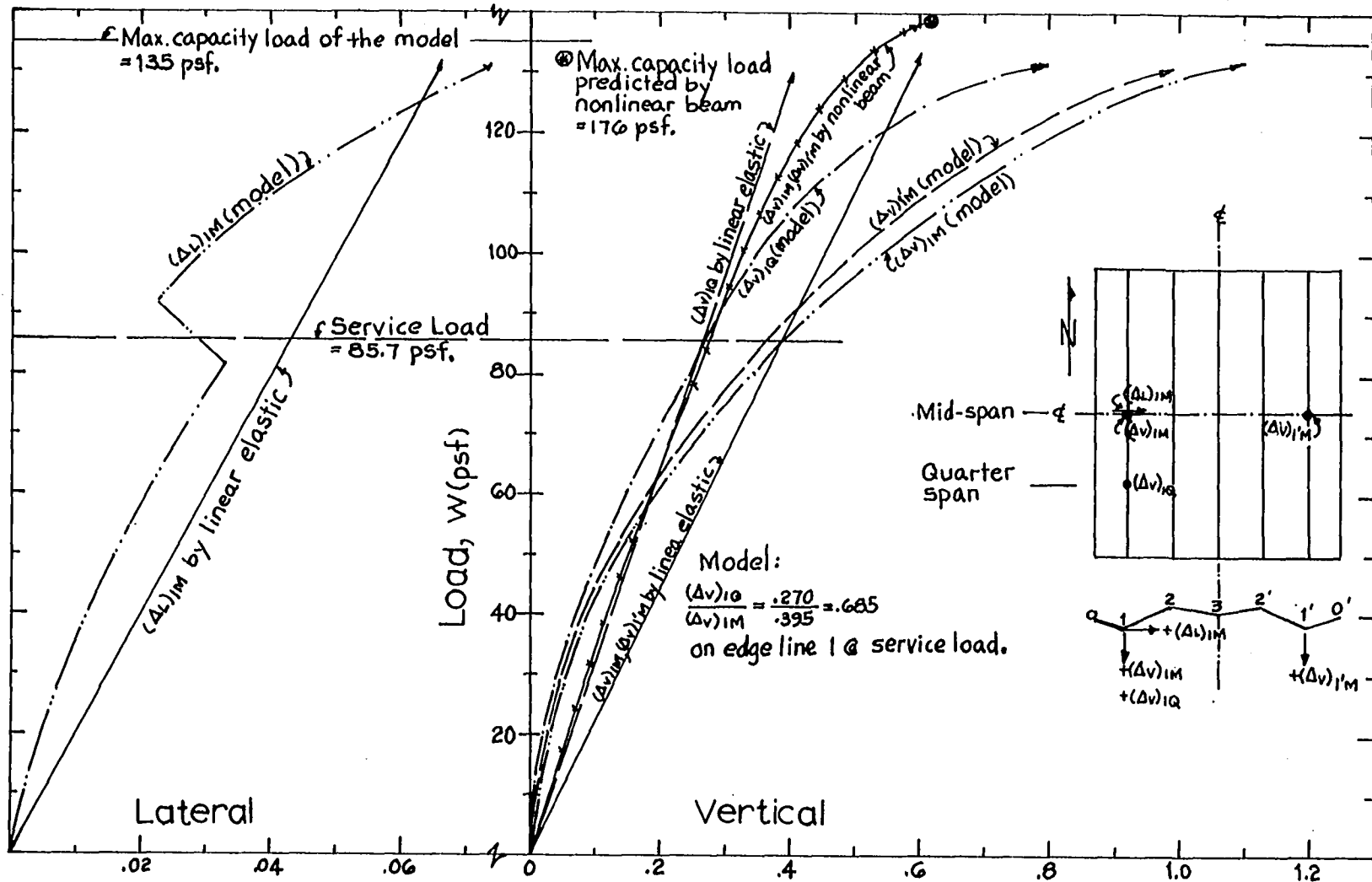


Figure 5.7e Deflections of ridge lines 1 and 1' (in.).

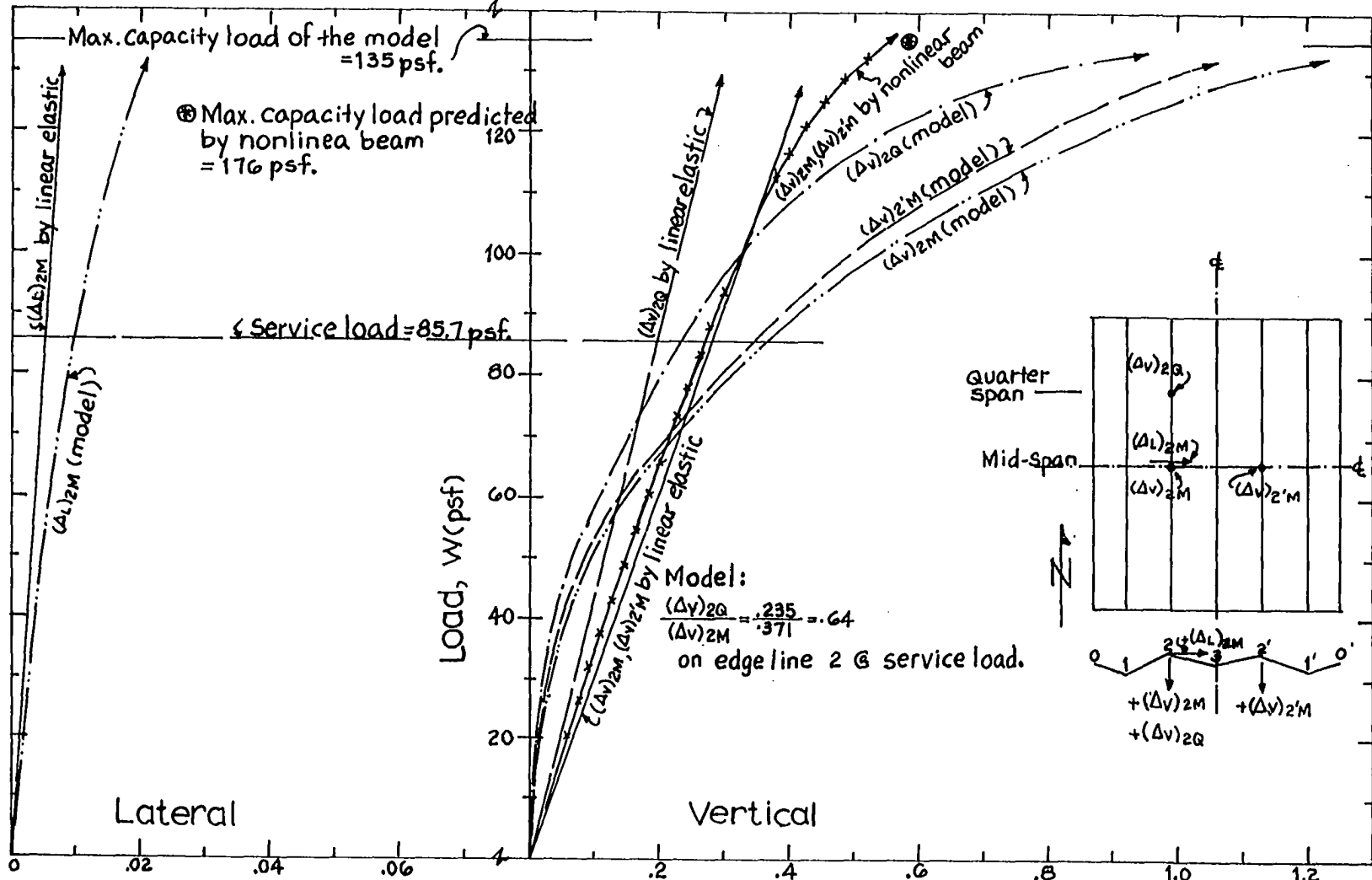


Figure 5.7f Deflections of ridge lines 2 and 2' (in.).

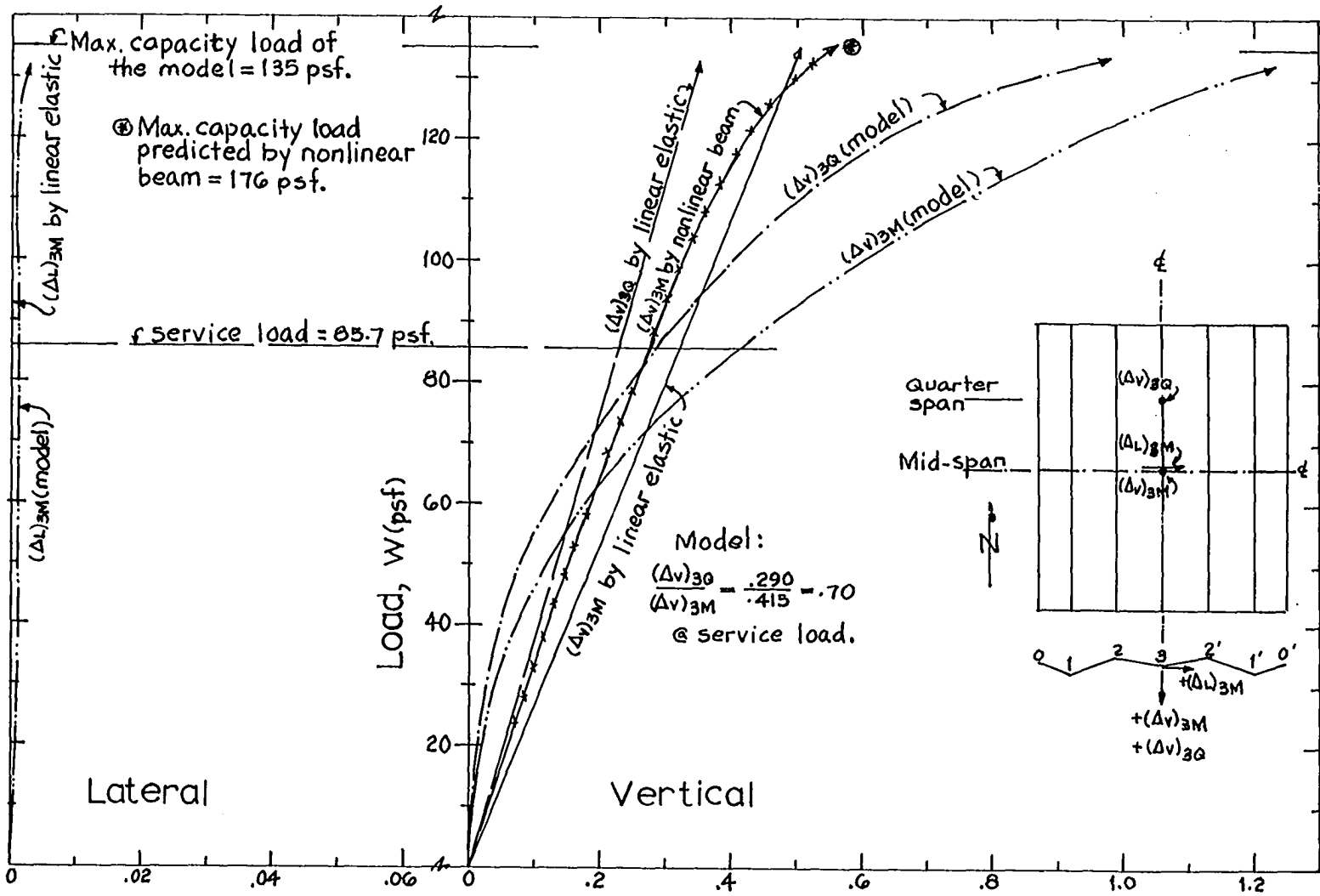


Figure 5.7g Deflections of ridge line 3 (in.).

	Ridge line	0'	1'	2'	3
Test	f @ 1/4L f @ 1/2L	2.5	.795	.710	.900
Design	f @ 1/4L f @ 1/2L	.812	.745	.790	1.590

Table 5.6 Comparison of the plate load variations along the ridge lines between the test results and that of the design calculated with the plate theory considering relative joint displacement

Method	Working load $P_w$ (psf)	Yielding load $P_y$ (psf)
Linear elastic theory	85.7	.....
Nonlinear inelastic beam theory	71.5	113.0
Load-strain response of the test model	83.5	108.0+

Table 5.7 Comparison of the load obtained from the load-strain response with that of the design and that of response obtained with nonlinear inelastic beam theory

did not agree exactly due to errors in construction. However, the variation of approximately 10% is not considered serious. The variation of the vertical deflections along the same joint line is shown in Table 5.8 as a ratio of deflection at  $l/4L$  with respect to that of  $l/2L$ . The ratio ranges from .64 to .70 and thus agrees closely with .707 which is used in the linear elastic theory with a half sine wave variation. The decreasing rates of slope at the various ridge lines in the load-deflection response were not equal and these rates were much higher at the ridge lines 2,3 and 2'. These variations are probably due to the disturbance of the edge plate, the influence of the parameter  $\alpha$ , as well as the support boundary conditions as described in the previous section. The model exhibited amazing "ductility", sustaining maximum deflections of nearly  $4\frac{1}{2}$  in. at the ridge line 3 before collapse.

The lateral deflections demonstrated the trends in the variation of the transverse stiffness of the cross section, and illustrated a definite loss in transverse stiffness after the yielding load level as shown in the abrupt change of slope in the curves (Figure 5.7). This may be also the principal reason for the higher rate of slope change in the load-vertical deflection response at the flatter edge lines.

#### (b) Comparison of the Load-deflection Responses

Several observations made on the comparisons of

Ridge Line	0 --	1	2	3
Vertical deflection @ 1/4L, $\Delta_Q$	.275	.270	.235	.290
Vertical deflection @ 1/2L, $\Delta_M$	.415	.395	.371	.415
$\frac{\Delta_Q}{\Delta_M}$	.661	.685	.640	.70

Table 5.8 Summary of vertical deflections at 1/4L and 1/2L along the same edge line at service load

the test load-deflections with the theoretical predictions based on the linear elastic folded plate and the nonlinear beam theories are:

1. The actual load-deflection responses are not single stage linear elastic and they do not follow exactly in a manner predicted by the linear elastic theory even though they are satisfactorily close at the working load level. Actually they are much closer to the nonlinear beam theory up to the load of 55 psf.

2. All of the observed deflections were smaller (as small as one-half) than the linear elastic predictions for load levels up to 85% of the yield load. These results are in direct contrast with those (intermediate L/R ratio structures) reported by Aldridge.<sup>(7)</sup> Thus the influence of the geometric parameters, L/R, h/t,  $\alpha$ , and  $\phi$  on the folded plate structures, as proven in Chapter III, is very significant. However, predictions using the linear elastic theory are conservative for loads up to 85% of working load and agree satisfactorily close at the working load level.

3. The nonlinear beam theory failed to accurately predict load-deflection responses except for low ranges of the load (up to 55 psf) and is on the unsafe side.

4. Both theories failed to predict the load-deflection responses after the yield load, and both predicted a much greater longitudinal stiffness than was indicated by the actual deflection.

(c) Suggested Method of Analysis and Prediction of Responses of Supported Reinforced Concrete Folded Plate Structures

The principal characteristics demonstrated by the actual load-deflection and load-strain responses were:

- (1) the actual load-deflection responses followed closely a half sine wave variation along the longitudinal direction,
- (2) the actual load-deflection responses illustrated a definite loss in longitudinal and transverse stiffness as reported by Aldridge,<sup>(7)</sup>
- (3) the linear elastic folded plate theory (considering the effects of the relative joint displacements) did predict with reasonable accuracy at the working level and was on the safe side for load-deflection responses up to 85% of prototype service load,
- (4) the nonlinear beam theory did predict quite accurately for loads up to 55 psf (64%) and at yield load,
- (5) the actual responses of load-deflection and load-strain are three different stage nonlinear and can be expressed by a general equation  $P = \frac{x}{a+bx}$ , where  $P =$  load in psf,  $x =$  strain ( $\mu$  in./in.) or deflection (in.) and  $a, b =$  constants.

For example, the load-deflection responses of the ridge lines 0,0', 1 and 1' at mid-span of the model tested can be expressed by three nonlinear equations, (1)  $P =$

$$\frac{\Delta}{.010\Delta + .0014} \text{ for load up to 60 psf, (2) } P = \frac{\Delta}{.00528\Delta + .00238}$$

for load from 60 psf to 108 psf, and (3)  $P = \frac{\Delta}{.00505\Delta + .00254}$

for load 108 psf to collapse ( $\Delta =$  deflection in inch).

(See Figure 5.8 for comparison of the load-deflection response with different methods)

The characteristics of the actual responses described above indicate that a reliable analysis and prediction of the load-deflection responses can be made by using a combination of the linear elastic theory and the nonlinear beam theory if there is a dependable load (or stress) - strain response for the structure which can be developed from a model test. The method described in Chapter III is suggested for analysis and prediction of the load-deflection of the reinforced concrete folded plate structure with the modification of the calculation of the individual plate deflections using the nonlinear beam theory with the actual stress-strain responses. The calculation of the deflection using the method suggested is a laborious work. However, it can be alleviated by using the rational equation  $P = \frac{X}{a+bx}$  or by application of high-speed digital computers.

(d) Predicted Prototype Responses

The load-deflection responses of the proposed prototype structures can be obtained by applying the principles of similitude described in Chapter IV to the load-deflection responses of the model structures and adding a correction for the dead load distortion by considering the appropriate part of the applied load to be dead load of the prototypes.

### 5.6.3 Collapse

Final collapse of the model was gradual and occurred at a load of 135 psf. The model failed by extensive flexural cracking combined with crushing of the concrete, diagonal cracking, and bond failure as described below:

1. Flexural cracks - (a) large transverse cracks extending through from top to bottom surfaces of plates #3 and #3', (b) transverse cracks on the top surfaces of the plates #2, #3, #3' and #2' along the end diaphragms, (c) longitudinal cracks on the top surfaces of the plates #3 and #3' near the ridge line 3, and (d) longitudinal cracks along the ridge line 1 and 1', on the top surface;
2. Crushing - (a) longitudinal crushing near the ridge line 3 on the top surface, (b) longitudinal crushing along the ridge line 1 on the bottom surface, (c) local crushing at end of the ridge lines 2 and 2' on the bottom surface;
3. Diagonal cracks - Diagonal tension crack across the ridge line 2 and 2' near end supports on the bottom surface;
4. Bond failure at the end of the model on the top surface along the end diaphragms -- in this area, the reinforcement did not fracture but bond failure permitted slipping of the wires, opening of the cracks, and a final deterioration of the surrounding concrete.

The stresses at the collapse of the model were obtained from Figure 5.7 coupled with Figure 4.4 and 4.6 and are shown in Table 5.9.

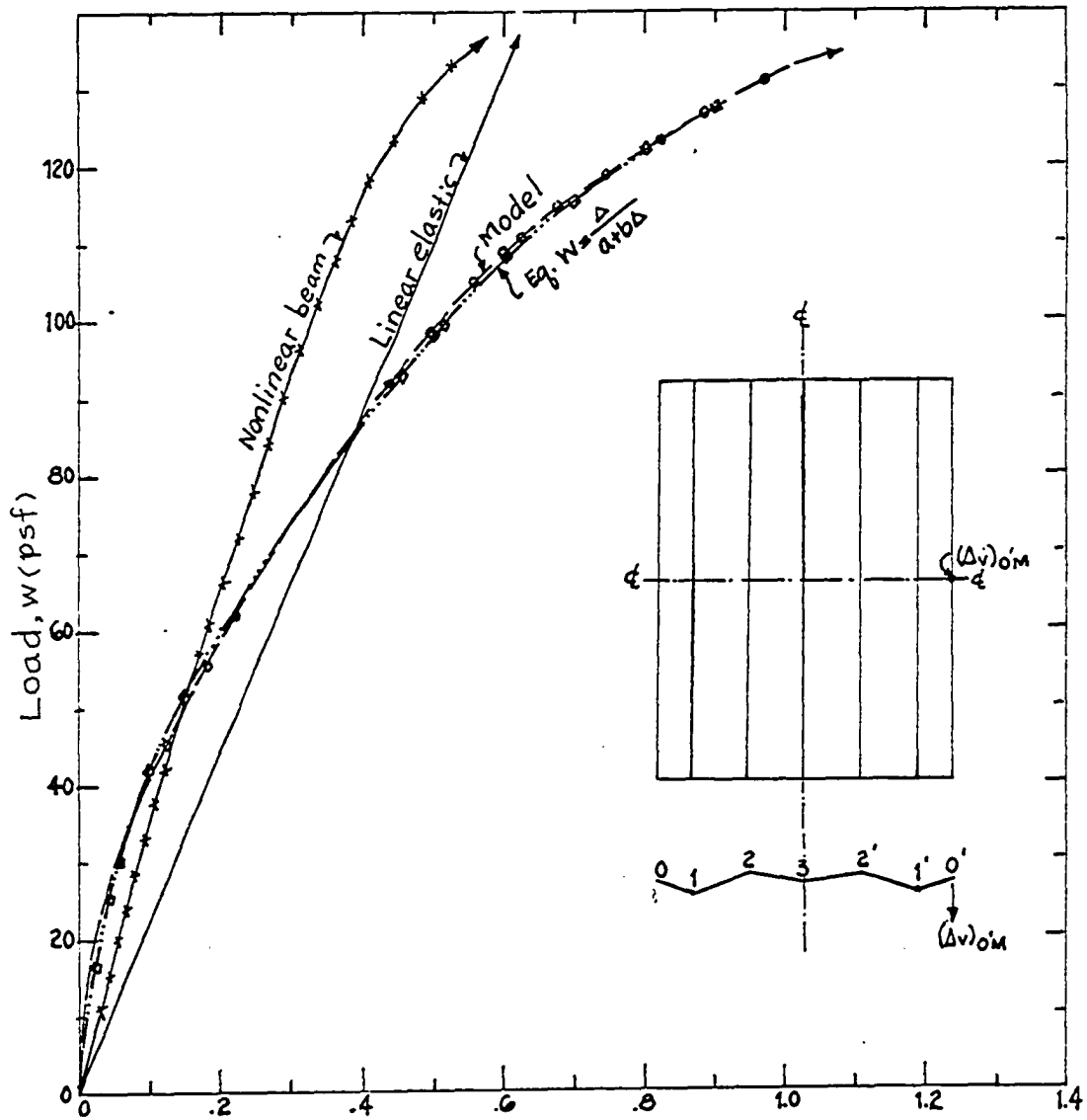


Figure 5.8 Comparison of deflection at mid-span of ridge line  $O'$ ,  $(\Delta v)_{0M}$ , predicted by different methods.

Ridge line	Longitudinal stresses (psi)												Transverse stresses (psi)		
	0'			1'			2'			3'			0'	1'	2'
Strain gage designation	S <sub>0E</sub>	S <sub>0Q</sub>	S <sub>0M</sub>	S <sub>1E</sub>	S <sub>1Q</sub>	S <sub>1M</sub>	S <sub>2E</sub>	S <sub>2Q</sub>	S <sub>2M</sub>	S <sub>3E</sub>	S <sub>3Q</sub>	S <sub>3M</sub>	C <sub>0E</sub>	C <sub>1E</sub>	C <sub>2E</sub>
f <sub>s</sub>	- 665	-12,300	-13,100	8,230	47,100	47,100	14,200	-15,800	-47,100	11,700	19,200	20,000	-	-	-
f <sub>c</sub>	- 50	- 1,550	- 1,675	150	0	0	0	- 1,950	- 3,910	0	0	0	- 375	- 2,750	0

Table 5.9 Final stresses of the plates at failure of the model.

Maximum capacity load of moment (psf)	Calculated maximum capacity load by nonlinear beam theory (psf)	Required ultimate load by ACI Code (psf)
135	176	138

Table 5.10 Comparison of the maximum capacity load of the model with the calculated maximum capacity load based on the nonlinear beam theory and with the required ultimate capacity load by the ACI Code.

From the final stresses and the cracking pattern in Figure 5.6 the following conclusions were made:

1. Positive reinforcement requirement by the working stress design method based on the cracked section is reasonable.

2. After yielding load the torsion bending effect was very significant and seriously affected the transverse stresses at the supports. The negative stresses measured on the edge plate and the ridge line 1' and 1, were in direct contrast with those predicted by the linear elastic theory.

3. After yielding load the influences of parameters,  $\alpha$  and  $\phi$  were very significant. The stresses along ridge 3 underwent a considerable redistribution and as a consequence failure occurred at ridge 3. (Note that 1 SWG 13 and 8 SWG 18 wires were provided along the ridge line 3 even though the reinforcement was not required in this region.)

4. Dowels inserted at the construction joint made the joint stiffer and produced a significant negative moment at ultimate load and caused transverse cracks of the end plates.

The maximum capacity load of the test model was compared with the calculated maximum capacity load based on the nonlinear beam theory and also with the design ultimate capacity required by the ACI (see Table 5.10). The ultimate capacity required by the ACI Code is  $U = 1.5D + 1.8L$  where  $U$  is required ultimate load capacity of structure,  $D$  is

dead load and  $L$  is specified live load. The results indicated that the maximum capacity load of the model analyzed by the folded plate theory considering relative joint displacements and designed by the working stress method was nearly the same as the ultimate capacity load required by the ACI Code; however, the ratio of the service load to the maximum capacity load was only 1.57 which was considered too low as a safe factor for the working stress design. The nonlinear beam theory failed to predict the maximum capacity load of the test model; however, this theory predicted very closely the load at yield level (Table 5.7) which was considered as the ultimate capacity load of the model.

## CHAPTER VI

### CONCLUSIONS AND RECOMMENDATIONS

#### 6.1 General

The principal objectives of this study were: 1) the investigation of the effects of geometric parameters on the ultimate strength behavior of model reinforced concrete folded plate structures which have unusual dimensional parameters but which are obviously realistically dimensional and 2) the critical evaluations of the currently recommended analysis <sup>(1,2)</sup> and design procedure <sup>(2,3)</sup> by using a computer solution and a direct model analysis. The conclusions and recommendations are restricted by the general range of variables outlined in detail in sections 1.3, 1.4.1.1, and 2.1 and Chapter IV. Effects of creep and relaxation, shrinkage, energy dissipation, repetitive loading, and temperature variations on the responses have not been considered.

Three theories dealing with the analysis and design of reinforced concrete folded plate structures investigated in this study are:

Linear Elastic Theories (section 1.4.1.1)

1. Folded Plate Theory Neglecting Relative Joint Displacements,

2. Folded Plate Theory Considering Relative Joint Displacements, and Nonlinear Theory (section 1.4.1.2),
3. Nonlinear Beam Theory.

"Folded Plate Theory Considering Relative Joint Displacements" was used in the computer solution study and it was found that the influences of the geometric parameters, the L/R (span-to-rise ratio), h/t (plate height-plate thickness),  $\alpha$  (the angle between adjoining plates), and  $\phi$  (the angle between plate and the horizontal) and the disturbances of the edge plates are very significant. The "Folded Plate Theory Neglecting Relative Joint Displacements" did not produce a feasible design; therefore, only two theories (2 and 3) were compared with the test data of the model. The "Folded Plate Theory Considering Relative Joint Displacements" predicted quite closely the cracking and load-deflection responses at the service load. The "Nonlinear Beam Theory" predicted the load at the yielding load level quite closely. But neither theory yielded reliable and comprehensive descriptions of the overall structural behavior of the test model except at the particular load levels as described above. The test data also indicated that the influences of the geometric parameters and the disturbances of the edge plates were very significant, as found in the computer solution study, particularly in the inelastic load level where the effect of the torsional bending caused by the warping of plate at the ends

was significant. The complexity of the reinforced concrete properties as described in Section 5.6.1 is the key characteristic which leads to deviation between actual and theoretical responses.

The strain gage system used in the model test in this study performed very well and it is probable that the accumulation of more load-strain data may materially assist in the development of an accurate theory such as Farmer's Non-linear Folded Plate Theory<sup>(29)</sup> which considers the warping of the cross section to provide an accurate prediction of the load-deflection responses.

The cracking and load-responses of the test model indicated that the tensile and diagonal tension reinforcements layout in accordance with the "Folded Plate Theory Considering Relative Joint Displacements Analysis" and "Working Stress Design Method" performed quite well even though the effect of the torsional bending was neglected in the analysis and design of the model. However, the compressive reinforcements provided were too conservative. The load-responses also indicated that the internal stresses underwent a redistribution with loadings especially in the first and third ranges. Clearly the warping of the cross section exists and its effects on the overall structural behavior was very significant in the inelastic range.

## 6.2 Conclusion

The following conclusions are justified by the test

results combined with that of the computer solution study:

1. The warping of the cross section is inevitable and must not be ignored in the inelastic load range.
2. The service load can be predicted quite closely by the linear elastic theory considering the effect of the relative joint displacements.
3. Nonlinear Beam Theory failed to predict either service load but was accurate in predicting yielding load.
4. The overall load-deflection responses cannot be predicted accurately by either method but the load-deflection response at the service load can be predicted satisfactorily by the linear elastic theory.
5. The internal stresses underwent a redistribution with loadings to ultimate.
6. The influence of the geometric parameters, the L/R ratio, h/t ratio,  $\alpha$ , and  $\phi$  and disturbances of the edge plates are significant, and further study of these problems are necessary.
7. The accurate prediction of the load-deflection response can be achieved only by developing the nonlinear folded plate theory considering the warping of the cross section such as Farmer's Method <sup>(29)</sup> coupled with the principles of redistribution of the internal stresses based on the cracked section of concrete and its inelastic behavior as well as the relatively higher ductility of the reinforcement. This could probably be accomplished if more

test data of the load-strain response were available.

8. The actual load-deflection and load-strain responses are three different stage nonlinear and can be expressed by a general equation  $P = \frac{K}{a+bx}$  where  $P$  = load in psf,  $x$  = strain ( $\mu$ in./in.) or deflection (in.), and  $a, b$  = constants.

### 6.3 Recommended Practice

#### 6.3.1 General

As described in detail in Chapter III, Folded Plate Structures can be classified into three categories and three different methods of analysis should be applied for three different categories of structures depending on the span-to-rise ratio ( $L/R$ ). A great deal of work has been done on the first range structure, in which the slab action prevails, and practice of the analysis and design have been recommended by Aldridge<sup>(7)</sup>. The third range structure (with the  $L/R > 50$ ), in which the beam action prevails, may be analyzed and designed by the ordinary beam method provided the transverse slab is designed by some other reliable method. However, the real form of this range structure rarely exists and even if it exists it can be analyzed and designed more accurately by the methods which are recommended for the second range structure as described below. This study is solely concerned with the second range structure, which is a combination of slab and beam actions and the recommended

practice of the analysis and design is described in detail in the following section.

### 6.3.2 Recommended Practice for the Second Range Structure

Since the "Folded Plate Theory Considering Relative Jt. Displacements" has shown satisfactory predictions of the load-deflection and cracking responses at the service load, and the load-deflection predicted by this theory is generally on the safe side up to 85% of the service load for the L/R ratio studied. Therefore, this theory is recommended for design purposes until a more reliable nonlinear folded plate theory can be developed. Particular care should be devoted to the construction joints to provide satisfactorily simple support boundary conditions, as well as bond or anchorage of the reinforcement to the concrete at the face of the support.

## 6.4 Suggestions for Future Research

As indicated in Section 6.2, more test data and rational studies are needed to establish definitely the effects of geometric parameters on the load-deflection responses of reinforced concrete folded plate structures. These data may be used as an aid in the development of a reliable analytical description of the behavior of these structures. A reliable nonlinear folded plate theory considering the warping of the cross section such as Farmer's Method <sup>(29)</sup> must be developed to include the effects of the variations: a) stress-strain response of the reinforced

concrete, b) influence of the geometric parameters (the L/R ratio, h/t ratio,  $\alpha$  and  $\phi$  ), c) disturbance of the edge plates, d) detailing of the compressive reinforcement, e) continuous spans, and f) loading arrangements and history.

## SYMBOLS AND NOTATIONS

Unless otherwise indicated the symbols and notations which follow are used throughout this dissertation.

- $A_n$  = cross-sectional area (ht) of plate n
- $A_s, A'_s$  = area of tensile and compressive reinforcement in flexural members respectively
- a = coefficient used in  $A_s = M/(ad)$ ; constant
- B = width of the folded plate structure
- C = cement; carryover factor
- $C_{n,n+1}$  = carryover factor from joint n to joint n+1
- c = constant; subscript referring to concrete
- D.F = distribution factor
- $D_{n,n+1}$  = stress distribution factor at joint n of plate n+1
- d = effective depth of flexural member
- $e_t, e_b$  = longitudinal strain in the plates at top, at bottom
- E = modulus of elasticity
- F, f = function
- FEM = fixed end moment
- $f_c$  = stress in concrete
- $f'_c$  = ultimate compressive strength of concrete by standard test
- $f_c''$  =  $0.85 f'_c$
- $f_n$  = balanced stress at joint n

SYMBOLS AND NOTATIONS - continued:

$f_s$	=stress in tensile reinforcement
$f'_s$	=stress in compressive reinforcement in flexural members
$f_t''$	=assumed flexural tensile stress of concrete
$f'_{sp}$	=split cylinder tensile ultimate strength of concrete by standard test
$f_y$	=yield strength of reinforcement
$f_u$	=ultimate strength of reinforcement
$h$	=plate height (slab span)
$h'$	=edge plate height
$I_n$	=moment of inertia of the cross-sectional area of plate n about the centroidal axis perpendicular to the plate height h
$i$	= $1/(1-jd/e)$
$j$	=ratio of distance between resultants of compressive and tensile stresses to effective depth
$K_l, K_t$	=longitudinal stiffness and transverse stiffness
$k$	=ratio of distance between extreme fiber and neutral axis to effective depth; constant
$L$	=structure span length
$M_n$	=longitudinal bending moment of plate n
$M_{n,n+1}$	=transverse end moment at joint n of plate n+1
$M_n$	=transverse moment at joint n
$N_n$	=longitudinal shearing force at joint n
$n$	=ratio of modulus of steel ( $E_s$ ) to that of concrete ( $E_c$ ) (modular ratio) or subscript referring to joint
$\sum o$	=sum of perimeters of bars
$p$	=steel percentage = $A_s/bd$

SYMBOLS AND NOTATIONS - continued:

pcf	=pounds per cubic foot
plf	=pounds per linear foot
psf,psi	=pounds per square foot; pounds per square inch
$P_{n,n+1}$	=plate load per linear foot on plate n+1 at joint n
$P_n$	=plate load per linear foot on plate n
R	=rise of a folded plate structure
$r_n$	=reaction at joint n
$S_n$	=sectional modulus of plate n
SWG	=Steel Wire Gage
S	=subscript referring to steel; scale factor
t	=plate thickness in a folded plate structure
U	=ultimate load capacity of a section
u	=bond unit stress; subscript referring to ultimate
V	=total shear force; coefficient of variation
$V_c$	=shear carried by concrete
v	=shearing stress
w	=unit weight in pcf; uniformly distributed load in plf
$\alpha_n$	=the angle between plates n and n+1 at joint n
$\Delta_n$	=relative joint displacement of plate n
$\delta_n$	=deflection of plate n
e	=unit strain in inches per inch
$e_u$	=ultimate strain
$e_{oc}$	$=2f'_c/E_c$
$e_{ot}$	$2f''_t/E_c$

SYMBOLS AND NOTATIONS - continued:

- $\mu$  =  $10^{-6}$
- $\nu$  = Poisson's Ratio
- $\sigma$  = standard deviation
- $\phi_n$  = the angle between plate n and the horizontal

## BIBLIOGRAPHY

1. "Phase I Report on Folded Plate Construction," Committee on Masonry and Reinforced Concrete. Journal of the Structural Division ASCE, St. 6, December, 1963.
2. "Concrete Shell Structures Practice and Commentary" ACI Journal, Proc. V61, September, 1964, pp. 1091-1108.
3. "Building Code Requirements for Reinforced Concrete," ACI 318-63, June, 1963.
4. Abels, P. W., "Introduction to Prestressed Concrete," Vol. 1, Concrete Publications Limited, London, 1964.
5. Whitney, C. S., B. G. Anderson and H. Birnbaum, "Reinforced Concrete Folded Plate Construction," Journal of the Structural Division ASCE, St. 8, 1959.
6. Posey, C. J., "Reinforced Concrete Folded Plate Construction," Journal of the Structural Division ASCE, Vol. 86, St. 4., April, 1960.
7. Aldridge, W. W., "Ultimate Strength Test of Model Reinforced Concrete Folded Plate Structures," a dissertation presented at the University of Texas, Austin, Texas., January, 1966, in partial fulfillment of the requirements for the Doctor of Philosophy degree.
8. Scordelis, A. C. and P. V. Gerasimenko, "Strength of Reinforced Concrete Folded Plate Models," Journal of the Structural Division, ASCE, Proc. Paper 4688, February, 1966.
9. Breen, J. E., and W. W. Aldridge, a discussion of the paper, "Strength of Reinforced Concrete Folded Plate Models," Journal of the Structural Division, ASCE, October, 1966., p. 375.

BIBLIOGRAPHY - continued:

10. Calvo, J., "Effects of Span-to-Rise Ratio on Behavior of Reinforced Concrete Folded Plate Structures," a thesis written for presentation at the University of Texas, Austin, Texas, in partial fulfillment of the requirements for the Master of Science degree, June, 1966.
11. Winter G. and M. Pei, "Hipped Plate Construction," Journal American Concrete Institute, Vol. 43, January, 1947, pp. 505-532.
12. Traum, Eliahu, "Design of Folded Plate," Journal of the Structural Division, ASCE, Vol. 85, No. St. 8, Proc. Paper 2229, October, 1959, pp. 103-123.
13. Vlassow, W. Z., "Structural Mechanics of Shells," (in Russian), Moskwa, 1936.
14. "Direct Solution of Folded Plate Concrete Roofs," Advanced Engineering Bulletin No. 3, Portland Cement Association, 1960.
15. Gaafar, I., "Hipped Plate Analysis Considering Joint Displacement," Transactions, ASCE, Vol. 119, 1954.
16. Yitzhaki, David, "Prismatic and Cylindrical Shell Roofs," Haifa Science Publishers, Haifa, Israel, 1958.
17. Yitzhaki, David and M. Reiss, "Analysis of Folded Plates," Journal of Structural Division, ASCE, St. 5, October, 1962.
18. Brielmaier, A. A., "Prismatic Folded Plates," Journal American Concrete Institute, March, 1962.
19. Rudiger, D., "Die Strenge Theorie Anisotropischer Prismatischer Faltwerke," Ingenieur Archiv, Berlin, West Germany, Vol. 23, 1955.
20. Goldberg, I. E. and H. L. Leve. "Theory of Prismatic Folded Plate Structures," International Association for Bridge and Structural Engineering. Zurich, Switzerland, Vol. 17, 1957.
21. Werfel, A., "Die Genaue Theorie der Prismatischen Faltwerke," International Association for Bridge and Structural Engineering. Zurich, Switzerland, Vol. 14, 1954.

BIBLIOGRAPHY - continued:

22. Mast, P. E., "New Method for Exact Analysis of Folded Plates," Journal of the Structural Division, ASCE, St. 2, April, 1967.
23. Aldridge, W. W. and J. E. Breen, "Literature Review of Reported Results in the Field of Ultimate Strength of Reinforced Concrete Folded Plate Structures," presented to the ASCE Task Committee on Folded Plate Construction at the Annual Meeting of the American Concrete Institute; Philadelphia, Pennsylvania, March, 1966.
24. Chacos, G. P. and J. B. Scalzi, "Ultimate Strength of a Folded Plate Structure," ACI Journal. February, 1961, pp. 965-971.
25. Edwards, H. H., "Precast and Prestressed Folded Plate Slabs," ACI Journal, Vol. 32, No. 10. April, 1961, pp. 1313-1322.
26. Glanville, J. I., "Full-Scale Pretensioned Folded Plates Test-Loaded to Failure," ACI Journal. March, 1963.
27. Schwaighofer, J. and N. Seethaler, "Experimental Study of Folded Plates," ACI Journal, Proc. V. 60. January, 1963, pp. 101-111.
28. "Test of a Reinforced Concrete Folded Plate Structure," Syracuse University Research Institute, Civil Engineering Department. Report No. CE-335-5910F.
29. Farmer, L., "A Numerical Solution for Reinforced Concrete Folded Plate Structures," a thesis presented at the University of Texas; Austin, Texas, in partial fulfillment of the requirements for the Master of Science degree, June, 1964.
30. Enami, A., "Fundamentals on Limit Analysis of Reinforced Concrete Prismatic Folded Plate Structures." A dissertation (in Japanese) presented at the University of Tokyo; Tokyo, Japan. In partial fulfillment of the requirements for the Doctor of Philosophy degree, December, 1960.
31. Dykes, A. R., "Folded Plate Construction: An Investigation of Collapse Conditions," The Structural Engineer, Vol. 38, No. 2. London, February, 1960, pp. 60-67.

BIBLIOGRAPHY - continued:

32. Johansen, K. W., Pladeformler, Polyteknish Forening. Copenhagen. 2nd ed., 1949
33. Johansen, K. W., Pladeformler, Formelsamling, Polyteknish Forening. Copenhagen. 2nd ed, 1954.
34. Hognestad, E., "Yield-Line Theory for the Ultimate Flexural Strength of Reinforced Concrete Slabs," Journal ACI, Vol. 24, No. 7. March, 1953. Proc. 49, p. 637.
35. Johansen, K. W., "Yield-Line Theory," (English translation) Cement and Concrete Association. London, 1962.
36. Ehlers, G., "Ein Neues Konstruktion Sprinzip," Bauingenieur, Vol. 9. 1930, p. 125.
37. Craemer, H., "Theorie der Kaltwerke," Beton und Eisen, Vol. 29, 1930. p. 276.
38. Craemer, H., "Die Heutige Stand der Theorie der Scheibentraeger und Faltwerken in Eisenbeton," Beton und Eisen, Vol. 36, 1937. pp. 264-297.
39. Gruber, E., "Berechnung Prismatischer Scheibenwerke," International Association of Bridge and Structural Engineering; Memoirs, Vol. 1, 1932. p. 225.
40. Gruening, G., "Die Nebenspannungen in Prismatischen Faltwerken," Ingenieur-Archiv., Vol. 3, No. 4, 1932.
41. Craemer, H., "Design of Prismatic Shells," ACI Journal, Vol. 49. February, 1953.
42. Bikhovsky, V. A., A. V. Hennerling, B. G. Korenev, A. R. Rzhantsin, and M. N. Rouchimsky, "Test on Reduced Modes of Structure," Bulletin No. 14 RILEM. March, 1962. pp. 109-119.
43. Washwanath, T., R. P. Mhatre, and K. Seethramulu, "Test of a Ferro-Cemento Precast Folded Plate," Journal of the Structural Division, ASCE, Vol. 91, St. 6. December, 1965.
44. Enami, A., "The Equilibrium of Reinforced Concrete Prismatic Folded Plate Structures at Collapse," Proc. of the 11th Japan National Congress for Applied Mechanics. 1961.

BIBLIOGRAPHY - continued:

45. Enami, A., "The General Theory on Collapse Mechanism of Reinforced Concrete Prismatic Folded Plate Structures," Proc. of the 10th Japan National Congress for Applied Mechanics. 1960.
46. Pozo, F., "A 20 Metre Free Span Folded Prestressed Thin Shell Roof," Proc. World Conference on Prestressed Concrete. World Conference on Prestressed Concrete, Ins., July, 1957. pp. 11-1; 11-5.
47. Senler, O. H., "Test, Design and Construction of Folded Plate Roof Models," a thesis presented at the State University of Iowa in partial fulfillment of the requirements for the Master of Science degree, June, 1958.
48. Posey, C., "Reinforced Concrete Folded Plate Construction," Journal of the Structural Division, ASCE, Vol. 86, No. St. 4. April, 1960.
49. Scordelis, A. C., "Matrix Formulation of Folded Plate Equations," Journal of the Structural Division, ASCE. Proceeding paper 2617, October, 1960.
50. Phanasomburana, S., "The Design and Behavior of a Folded Plate Reinforced Concrete Roof," a thesis presented to the SEATO Graduate School of Engineering, Bangkok, Thailand in partial fulfillment of the requirements for the degree of Master of Engineering, 1963.
51. Girkmann, K., "Flachentragwerke" 2 Aufl., Springer Verlag Wien, 1948.
52. Hognestad, E., "A Study of Combined Bending and Axial Load in Reinforced Concrete Members," reprint of a University of Illinois Engineering Experimental Station Bulletin Series No. 399. June, 1961.
53. Breen, J., "The Restrained Long Concrete Column as a Part of a Rectangular Frame," a dissertation presented at the University of Texas in partial fulfillment of the requirements for the Doctor of Philosophy degree, June, 1962.
54. Matlock, A., "Structural Model Testing - Theory and Applications," Journal of PCA. Research and Development Laboratories, Vol. 4, No. 3. September, 1962.

BIBLIOGRAPHY - continued:

55. Alami, Z., "Accuracy of Models Used in Research on Reinforced Concrete." A dissertation presented to the University of Texas; Austin, Texas, in partial fulfillment of the requirements for the Doctor of Philosophy degree, June, 1962.
56. Harris, H. G., G. M. Sabnis, and R. N. White, "Small Scale Direct Models of Reinforced and Prestressed Concrete Structures." Cornell University, Civil Engineering School, Ithaca, New York. Report No. 326. September, 1966.
57. Pahl, P. J., K. Soosaar, and R. J. Hansen, "Structural Models for Architectural and Engineering Education," Research Report R64-03. MIT, Civil Engineering Department. Cambridge, Massachusetts. February, 1964.
58. Guralnick, S. A. and R. W. LaFranch, "Laboratory Study of a 45-foot Square Flat Plate Structure," ACI Journal, Proc. Vol. 60, September, 1963.
59. Hatcher, D. S., M. A. Sozen, and C. P. Siess, "A Study of Tests on a Flat Plate and a Flat Slab," Structural Research Series 217; Civil Engineering Studies, University of Illinois; Urbana, Illinois, July, 1961.
60. White, R. N., "Small Scale Models of Concrete Structures," ASCE Structural Engineering Conference and Annual Meeting, October, 1954.
61. Brock, G., "Direct Models As An Aid to Reinforced Concrete Design," Engineering. (London) Vol. 187, No. 4857. April, 1959. pp. 468-470.
62. Biggs, J. M. and R. J. Hansen, "Model Techniques Used in Structural Engineering Research," Bulletin No. 10 RILEM. March, 1961. pp. 35-48.
63. Borges, J. F. and J. A. E. Lima, "Crack and Deformation Similitude in Reinforced Concrete," Bulletin No. 7 RILEM. June, 1960. pp. 79-90.
64. Beaujoint, N., "Similitude and Theory of Models," Bulletin No. 7 RILEM. June, 1960. pp. 14-39.
65. Fumagalli, E., "The Use of Models of Reinforced Concrete Structures," Magazine of Concrete Research, Vol. 12, No. 35. July, 1960. pp. 63-72.

BIBLIOGRAPHY - continued:

66. Concrete Manual. U. S. Department of Interior,  
Bureau of Reclamation, 6th ed., Denver, Colorado,  
1956. p. 462.
67. Harris, H., P. Schwindt, I. Tahr, and S. Werner,  
"Techniques and Materials in the Modeling of Rein-  
forced Concrete Structures Under Dynamic Loads,"  
R63-54, Department of Civil Engineering, MIT,  
Cambridge, Massachusetts, December, 1963.

APPENDIX A

PROGRAM LDDFN, NONLINEAR BEAM THEORY

```

DIMENSION ACUNC%176<,HST%176<
DIMENSION AST%176<,FCUNC%176<
DIMENSION FST%176<,BEND%300<
DIMENSION PHE%300<,ESTI%10<
DIMENSION TRIM%82<,RUT%82<
DIMENSION TY%82<,FSBI%10<
DIMENSION ESBI%10<,FSTI%10<
COMMON NSI,EP3,PHI,EPSIU,FPPC,FCUNC,FST,ACUNC,PCALC,AST,HST,FPC
COMMON EPSMAX,FSBI,FSTI,ESBI,ESTI

```

```

C PROGRAM LUDFN
999 FORMAT %1H1<
1 FORMAT % / 30H      TABLE 1. CONTROL DATA      //
1 40H                NUM SECTION INCS              #      I5, /
2 40H                MAX ALLOWABLE CUMP STRAIN      #      1E10.3, /
3 48H                DELTA PHI                      #      VARIES, /
5 40H                SPAN                          #      1E10.3, /
4 40H                DEPTH                         #      1E10.3, /
5 48H                WIDTH                         #      VARIES, /
4 40H                A                             #      1E10.3, /
4 40H                B                             #      1E10.3, /
5 22H                BEAM NUMBER ,I5,/ <
2 FORMAT%// 42H      TABLE 2. PROPERTIES OF THE MATERIALS //
1 35H                CONC CYLINDER STRENGTH        #      1E10.3, /
2 35H                K FOR FPPC # K * FPC          #      1E10.3, /
3 35H                STEEL YIELD POINT %BOT<      #      1E10.3, /
4 35H                STEEL YIELD POINT %TOP<      #      1E10.3, /
5 35H                STEEL MOD OF ELASTICITY      #      1E10.3, / <
1441 FORMAT%//17X,5H SPAN,7X,5H XINC,6X,5H      P ,10X,2HWU,9X,3H A ,9X,3H
1 B ,8X,4HM/MY/<
1443 FORMAT%/ 4X,8H RUT%41<,6X,4HTRH1,7X,5H TRHM,6X,9H TRIM%41<,4X,6H T
1Y%1<,6X,7H TY%27<,5X,7H TY%41<,5X,7H TY%54<,5X,7H TY%81< //<
9 FORMAT %2I5,6F10.0)
11 FORMAT %7F10.0<
12 FORMAT %1X,E9.3,6E10.3<
14 FORMAT %4E10.3<
4010 READ %1,9<NSTB,NSI,SH,SPAN,FPC,EPSMAX,      A,B
IF %NSTB<5,99,5
5 READ %1,14<%FSBI%1<,ESBI%1<,FSTI%1<,ESTI%1<,I#1,10<
READ %1,11<%AST%1<,I#1,NSI<
READ %1,11<%ACUNC%1<,I#1,NSI<
ZNSI#NSI
H#SH*ZNSI
ZK3#.85
DELPHI#.000025
ES#FSBI%2</ESBI%2<
WRITE %3,1<NSI,EPSMAX,SPAN,H,      A,B,NSTB
WRITE %3,2<FPC,ZK3,FSBI%4<,FSTI%4<,ES
WRITE %3,3<
31 FORMAT %//23H PLACEMENT OF CONCRETE//<
WRITE %3,12<%ACUNC%1<,I#1,NSI<
HST%1<#SH/2.
DO 4005 I#2,NSI
J#I-1
4005 HST%1<#HST%J<&SH

```

03/07/68

FORTMAIN

```
WRITE 3,999<
WRITE 3,32<
32 FORMAT ///20H PLACEMENT OF STEEL//<
WRITE 3,12<%AST%I<,I#1,NSI<
WRITE 3,19<
19 FORMAT ///27H STEEL STRESS-STRAIN CURVE//<
WRITE 3,14<%FSBI%I<,%SBI%I<,%FSTI%I<,%ESTI%I<,I#1,10<
FPPC#ZK3#FPC
EC#60000.0#ABS#FPC<#*0.5
EPSIU#2.0#FPPC/EC
EPSCUN#EPSMAX#.8
PHI#0.0
HCL#H/2.0
L#NSI/2
NN#0
HSTL#0.0
DO 301 I#L,NSI
IF %AST%I<< 302,301,302
302 HSTL#HSTL&HST%I<
NN#NN&I
301 CONTINUE
DIV#NN
STLHT#%H-HSTL/DIV</H
M#0
WRITE 3,999<
WRITE 3,33<
33 FORMAT 12X,5H ZMOM,15X,5H PHI,15X,5H EPST,15X,5H EPSB<
104 EP1#EPSMAX-DELPHI
K#0
EP2#0.00150
107 EP3#%EP1&EP2</2.0
K#K&I
CALL AXLD
IF %ABS#PCALC<-5.0<108,108,109
109 IF %K-99<110,110,111
110 IF %PCALC<113,108,112
112 EP2#EP3
GO TO 107
113 EP1#EP3
GO TO 107
111 WRITE 3,114<PCALC
114 FORMAT 5X,30HPCALC DID NOT CONVERGE ON P ,1E10.3<
108 EPST#EP3
EPSB#EP3&H#PHI
ZMOM#0.0
DO 115 J#1,NSI
115 ZMOM#ZMOM&%HST%J<-HCL<#%FCUNC%J<&%FST%J<<
WRITE 3,24<ZMOM,PHI,EPST,EPSB
24 FORMAT 1X,E20.5,E20.4,E20.5,E20.5<
M#M&I
122 BEND%M<#ZMOM
123 PHE%M<#PHI
EYLD#EPSB-%EPSB-EPST<#STLHT
IF%EYLD-ESBI%4<<170,170,169
170 YLDMOM#ZMOM
```

03/07/68

FORTMAIN

```
169 CONTINUE
  IF %M-299< 1002,1103,1103
1002 IF %EPST-EPSTMAX<1103,118,118
  118 IF %EYLD*1.1-ESBI%4<<8868,8878,8878
8868 PHI#PHI&DELPHI
  GO TO 104
8878 IF %EYLD-ESBI%4<<8858,8848,8848
8858 DELPHI#.000001
  PHI#PHI&DELPHI
  GO TO 104
8848 IF %EPST-EPSCUN<8828,8838,8838
8838 DELPHI#.0001
  PHI#PHI&DELPHI
  GO TO 104
8828 DELPHI#.00005
  PHI#PHI&DELPHI
  GO TO 104
1103 WRITE %3,1003<M
1003 FORMAT %1X,28H NUMBER OF POINTS ON CURVE #114/<
  BEND%1<#0.0
  BENDCK#0.0
  DO 444 I#2,M
  IF %BEND%I<-BENDCK<444,443,443
443 BENDCK#BEND%I<
  KKK#I
444 CONTINUE
  WRITE%3,445<BENDCK,KKK,YLDMUM
445 FORMAT %13X,23HMAX RESISTING MOMENT # ,E12.5,14H AT POINT NO.,I4,
  111H ON CURVE.//13X,15HYIELD MOMENT # ,E12.5<
  WRITE %3,999<
  WRITE%3,497<
497 FORMAT %12X,5H ZMOM,15X,5HRATIO,15X,4H PHI<
  DO 499 I#1,M
  RATIO#BEND%I</YLDMUM
  WRITE %3,24<BEND%I<,RATIO,PHE%I<
499 CONTINUE
  WRITE %3,999<
  MM#M&1
  DO 333 I#MM,300
41 PHE%I<#0.0
333 BEND%I<#0.0
  J#80
  M#J&1
  AM1#J
  XINC#SPAN/AM1
  P#%ZMOM/SPAN</2.0
  W#ZMOM/%SPAN*SPAN<
  IF %A< 500,501,500
501 P#0.0
  GO TO 502
500 W#0.0
502 W1#W/25.0
  W2#W/100.0
  ZMOM2#ZMOM*.85
  PC1#P/5.0
```

03/07/68

FURTMAN

```
PC2#P/50.0
WRITE %3,1441<
WRITE %3,1443<
550 CALL CMOM%P,SPAN,TRIM,XINC,A,B,W<
3064 DO 3080 K#1,M
IF %TRIM%K<<3065,3066,3067
3065 ZZ#-1.0
TRM#-1.0*TRIM%K<
GU TO 7067
3066 ROT%K<#0.0
GU TO 3080
3067 ZZ#1.0
TRM#TRIM%K<
7067 DO 3068 L#1,MM
IF %TRM-BEND%L<<3070,3069,3068
3068 CONTINUE
GU TO 6000
6000 WRITE %3,6001<J,K
6001 FORMAT %1X,11H FAILURE ,2I10//<
WRITE %3,999<
GU TO 4010
3069 ROT%K<#PHE%L<
IF %ZZ<7075,7076,3080
7075 ROT%K<#-1.0*ROT%K<
GU TO 3080
7076 GU TO 4010
3070 YA#TRM
YO#BEND%L-1<
Y1#BEND%L<
X0#PHE%L-1<
X1#PHE%L<
7 X#X1E%YA-Y1</%Y1-Y0<<#%X1-X0<
IF %ZZ<3075,3076,3077
3075 ROT%K<#-1.0*X
GU TO 3080
3076 GU TO 4010
3077 ROT%K<#X
3080 CONTINUE
3082 CALL SHAPE%ROT,XINC,TRH1,TRHM,TY,MC
RATUO#TRIM%41</YLDMMOM
WRITE %3,1442<SPAN,XINC,P,w,A,B,RATUO
1442 FORMAT %12X,8E12.4<
WRITE%3,1444<ROT%41<,TRH1,TRHM,TRIM%41<,TY%1<,TY%27<,TY%41<,TY%54<
L,TY%81<
1444 FORMAT %1X,9E12.4<
560 IF %TRIM%41<-ZMOM2<571,572,572
571 P#P&PC1
W#W&W1
GU TO 550
572 P#P&PC2
W#W&W2
GU TO 550
99 STOP
END
```

```

SUBROUTINE AXLD
DIMENSION ACONC%176<,HST%176<
DIMENSION AST%176<,FCONC%176<
DIMENSION FST%176<,FSBI%10<
-DIMENSION ESBI%10<,FSTI%10<
DIMENSION ESTI%10<
COMMON NSI,EP3,PHI,EPSIO,FPPC,FCONC,FST,ACONC,PCALC,AST,HST,FPC
COMMON EPSMAX,FSBI,FSTI,ESBI,ESTI
PCALC#0.0
DO 100 J#1,NSI
EPS#EP3&HST%J<#PHI
IF %EPS<10,10,20
10 IF %ABS%EPS<&EPSIO<11,12,12
11 FC#FPPC*%2.0*%EPS/EPSIO<-ABS%EPS/EPSIO<##2.0<
GO TO 50
12 IF %ABS%EPS<&EPSMAX<14,14,42
14 FC#FPPC-%EPSIO-EPS</%EPSIO-EPSMAX<<#%0.15*FPPC<
GO TO 50
20 FPPT#-0.08*FPC
EPT#&0.0001
IF %EPS-EPT<30,30,40
30 FC#2.0*FPPT*%EPS/EPT</%1.0&%EPS/EPT<##2.0<<
GO TO 50
40 IF %EPS-J.0004<41,41,42
41 FC#FPPT-%EPS-EPT</%0.0003<<#%-0.03*FPC<
GO TO 50
42 FC#0.0
50 FCONC%J<#ACONC%J<#FC
100 PCALC#PCALC&FCONC%J<
DO 99 J#1,NSI
300 EPS#EP3&HST%J<#PHI
IF %AST%J<#EPS<102,150,202
102 DO 110 I#1,10
IF %EPS-ESTI%I<<110,106,107
110 CONTINUE
106 FS#FSTI%I<
GO TO 150
107 FS#FSTI%I-1<&%EPS-ESTI%I-1<<#%FSTI%I<-FSTI%I-1<</%ESTI%I<-ESTI%I-1
1<<
GO TO 150
202 DO 210 I#1,10
IF %EPS-ESBI%I<<207,206,210
210 CONTINUE
206 FS#FSBI%I<
GO TO 150
207 FS#FSBI%I-1<&%EPS-ESBI%I-1<<#%FSBI%I<-FSBI%I-1<</%ESBI%I<-ESBI%I-1
1<<
150 FST%J<#FS*AST%J<
200 PCALC#PCALC&FST%J<
99 CONTINUE
RETURN
END

```

```

SUBROUTINE SHAPE DT, G, TH1, THM, YD, M<
DIMENSION YD%82<
DIMENSION R%82<, DT%82<
DIMENSION TA%82<, CONJ%82<
R%1<#%G/24.0<#%7.0*DT%1<&6.0*DT%2<-DT%3<<
MIN#M-1
DU 2 K#2, MIN
0002 R%K<#%G/12.0<#%DT%K-1<&10.0*DT%K<&DT%K&1<<
R%M<#%G/24.0<#%7.0*DT%M<&6.0*DT%M-1<-DT%M-2<<
TA%1<#0.0
MPI#M&1
DL 3 K#2, MPI
0003 TA%K<#TA%K-1<&R%K-1<
CONJ%1<#0.0
DL 4 K#2, M
0004 CONJ%K<#CONJ%K-1<&%G*TA%K<<
AMI#MIN
CORR#CONJ%M</AMI
DU 5 K#1, M
AK1#K-1
0005 YD%K<#AK1#CORR-CONJ%K<
TH1#CORR/G
THM#TH1-TA%M&1<
RETURN
END

```

```

SUBROUTINE CMUM%P,SPAN,TRIM,XINC,A,B,W<
DIMENSION TRIM%82<
I#1
X#0.0
IF %A<1,2,1
1 IF %B<7,8,7
8 RLEFT#P*%SPAN-A</SPAN
9 IF%X-A<10,10,11
10 TRIM%I<#RLEFT*X
X#X&XINC
I#I&1
GO TO 9
11 IF %X-SPAN< 13,13,14
13 TRIM%I<#RLEFT*X-P*%X-A<
X#X&XINC
I#I&1
GO TO 11
7 RLEFT#P*%SPAN-A&B</SPAN
20 IF%X-A<21,21,22
21 TRIM%I<#RLEFT*X
X#X&XINC
I#I&1
GO TO 20
22 IF %X-%SPAN-B<<23,23,24
23 TRIM%I<#RLEFT*X-P*%X-A<
X#X&XINC
I#I&1
GO TO 22
24 IF %X-SPAN< 25,25,14
25 TRIM%I<#RLEFT*X-P*%X-A<-P*%B&X-SPAN<
X#X&XINC
I#I&1
GO TO 24
2 RLEFT#W*SPAN/2.0
3 IF %X-SPAN<4,4,14
4 TRIM%I<#W*X*%SPAN-X</2.0
X#X&XINC
I#I&1
GO TO 3
14 RETURN
END

```

APPENDIX B

PROGRAM YIT 3, FOLDED PLATE THEORY CONSIDERING  
RELATIVE JOINT DISPLACEMENT

```

DIMENSION X%20<,Y%20<
DIMENSION Z%20<,T%20<
DIMENSION DL%20<,SK%20<
DIMENSION SM%20<,VC%20<
DIMENSION VG%20<,V%20<
DIMENSION P%20<,PL%20<
DIMENSION PF%20<,S%20<
DIMENSION F%20<,W%20<
DIMENSION VS%20<,CLD%20<
DIMENSION DIS%20<,I1%20<
DIMENSION J1%20<,ROT%20<
DIMENSION DEFM%20<,DV%20<
DIMENSION DP%20<,BM%20<
DIMENSION DPF%20<,DW%20<
DIMENSION DF%20<,DLS%20<
DIMENSION SS%20<,DLD%20<
DIMENSION DDS%20<,I2%20<
DIMENSION J2%20<,RDT%20<
DIMENSION RCT%20<,WT%20<
DIMENSION RO%20<,H%20<
DIMENSION C1P%20<,C2P%20<
DIMENSION P1F%20<,P2F%20<
DIMENSION F1%20<,F2%20<
DIMENSION V1S%20<,V2S%20<
DIMENSION C1LD%20<,C2LD%20<
DIMENSION D1IS%20<,D2IS%20<
DIMENSION R1OT%20<,R2OT%20<
DIMENSION D1EFM%20<,D2EFM%20<
DIMENSION D1V%20<,D2V%20<
DIMENSION EFB%20<,PARA%20<
DIMENSION PARB%20<,SIG%20<
DIMENSION FM%20<,AL%20<
DIMENSION FEM%20,2<,ZER%20,2<

```

```

C PROGRAM YIT 3
0001 FORMAT %28F JOHN E. BREEN PROGRAM YIT 3//<
WRITE %3,1<
0002 FORMAT %1X,19<
996 CCNTINUE
READ %1,2<ID
IF %ID<104,104,6556
998 FORMAT %27H DATA IDENTIFICATION NUMBER/<
6556 WRITE %3,998<
WRITE %3,2<ID
READ %1,2<N
WRITE %3,2<N
IF %N<3,3,4
0003 STOP 1
0004 CCNTINUE
0005 FORMAT %1X,F9.3,2F10.3<
READ %1,5<%X%I<,Y%I<,T%I<,I#1,N<
WRITE %3,5<%X%I<,Y%I<,T%I<,I#1,N<
CC 6 I#1,N
0006 Z%I<#SQRT%X%I< *X%I< &Y%I< *Y%I<<
WET#150.0

```

06/29/68

FORTMAIN

```
DC 7 I#1,N
0007 DL%I<#%T%I</12.0<#WET
0008 FCRMAT %1X,F9.3,7F10.3<
      READ %1,8<%AL%I<,I#1,N<
      WRITE %3,8<%AL%I<,I#1,N<
0022 FCRMAT %1X,F9.2<
      READ %1,22<SPAN
      WRITE %3,22<SPAN
DC 9 I#1,N
APL#AL%I<
APL#APL*%X%I</Z%I<<
WT%I<#DL%I<&APL
EM#%WT%I<#Z%I<#X%I<</12.0
FEM%I,1<#EM
0009 FEM%I,2<#%-1.0<#EM
0010 FEM%1,1<#0.0
      FEM%1,2<#6.0*FEM%1,2<
0013 EC#3000CUC.0EO*144.0
DC 14 I#1,N
      SK%I<#%EC*%T%I</12.0<##3.0</%Z%I<*12.0<
0014 RC%I<#0.0
      CALL SLCDEF%SK%1<,SK%2<,SK%3<,FEM%1,1<,FEM%1,2<,FEM%2,1<,FEM%2,2<,
      1FEM%3,1<,FEM%3,2<,RO%1<,RO%2<,RO%3<,SM%1<,SM%2<,SM%3<,SM%4<,SM%5<,
      1SM%6<<
0155 FORMAT %27H GRAVITY TRANSVERSE MUMENTS/<
      WRITE %3,155<
0015 FCRMAT %1X,6E12.3//<
      WRITE %3,15<%SM%I<,I#1,6<
0157 FCRMAT %24H CCNTINUITY SHEARS-BASIC/<
      WRITE %3,157<
      VC%1<#0.0
      VC%2<#0.0
DC 16 J#1,3
K#2*J
L#K-1
H%K<#X%J<
0016 H%L<#X%J<
DC 17 I#3,5,2
SLM#SM%I<&SM%I&1<
VC%I<#SUM/H%I<
0017 VC%I&1<#%SUM/H%I<<#%-1.0<
      WRITE %3,15<%VC%I<,I#1,6<
      VG%1<#0.0
      VG%2<#WT%1<*Z%1<
DC 18 J#2,3
K#2*J
L#K-1
VG%K<#WT%J<*Z%J</2.0
0018 VG%L<#VG%K<
DC 19 J#1,6
0019 V%J<#VC%J<&VG%J<
0252 FCRMAT %18H JOINT LOADS-BASIC/<
      WRITE %3,252<
      P%1<#V%2<&V%3<
      P%2<#V%4<&V%5<
```

06/29/68

FORTMAIN

```
P%3<#V%6<
WRITE %3,25<%P%I<,I#1,N<
DC 20 J#1,2
JP#J&1
K#2*J
L#K-1
0020 CALL PLCAD%P%J<,PF%L<,PF%K<,X%J<,Y%J<,Z%J<,X%JP<,Y%JP<,Z%JP<<
PF%5<#%Z%3</Y%3<<#P%3<#%-1.<
0150 FORMAT %27H FORCES IN PLANES OF PLATES/<
WRITE %3,150<
0115 FORMAT %1X,5E12.3//<
WRITE %3,115<%PF%I<,I#1,5<
DC 21 I#1,N
0021 S%I<#%T%I</72.0<#Z%I<#Z%I<
W%1<#PF%1<
W%2<#PF%2<&PF%3<
W%3<#PF%4<&PF%5<
DC 23 I#1,N
J#2*I
K#J-1
F%J<#%W%I<#SPAN*SPAN/8.0</S%I<
0023 F%K<#%-1.0<#F%J<
A1#%-2.0<#Z%1<</%3.0*S%1<<
A2#%2.0*Z%2<</%3.0*S%2<<
A3#Z%2</%3.0*S%2<<
A4#%-1.0<#A3
A5#%-1.0<#A2
A6#%2.0*Z%3<</%3.0*S%3<<
A7#Z%3</%3.0*S%3<<
A8#%-1.0<#A7
B1#A1-A2
B2#%-1.0<#A3
B3#F%3<-F%2<
B4#A4
B5#A5-A6
B7#F%5<-F%4<
C1#%B2*%B4<-%B5*%B1<
C3#%B3*%B4<-%B7*%B1<
0151 FORMAT %19H PLATE SHEARS-BASIC/<
WRITE %3,151<
TC#C3/C1
TB#%B3-%B2*TC<</B1
TD#C.0
WRITE %3,25<TB,TC,TD
0153 FORMAT %24H BALANCED STRESSES-BASIC/<
WRITE %3,153<
VS%1<#F%1<-%.50*A1*TB<
VS%2<#F%2<&%A1*TB<
VS%3<#F%3<&%A2*TB<&%A3*TC<
VS%4<#F%4<&%A4*TB<&%A5*TC<
VS%5<#F%5<&%A6*TC<
VS%6<#F%6<&.5*A6*%-TC<
WRITE %3,15<%VS%I<,I#1,6<
DC 24 J#1,N
L#2*J
```

06/29/68

FORTMAIN

```
      K#L-1
0024 CLD%J<#%SPAN*SPAN/%9.6*EC*Z%J<<<#%VS%L<-VS%K<<
0250 FORMAT %47H CEN LINE DEFLS OF PLATES DUE TO STRESSES-BASIC/<
      WRITE %3,250<
0025 FORMAT %1X,3E12.3//<
      WRITE %3,25<%CLD%J<,J#1,N<
      X%4<#X%3<
      Y%4<#-Y%3<
      Z%4<#Z%3<
      CLD%4<#-CLD%3<
      X%5<#X%4<
      Y%5<#%-1.0<#Y%4<
      Z%5<#Z%4<
      CLD%5<#%-1.0<#CLD%4<
      N#1#N&1
      DC 26 I#1,N
      L#2#I
      K#L&1
      M#I&1
      CALL WILLY%X%I<,Y%I<,X%M<,Y%M<,CLD%I<,CLD%M<,DIS%L<,DIS%K<,I1%L<,
      IJ1%L<,I1%K<,J1%K<<
0026 CONTINUE
0251 FORMAT %28H WILLIOT DISPLACEMENTS-BASIC/<
      WRITE %3,251<
      DIS%1<#0.0
      WRITE %3,15<%DIS%I<,I#1,6<
0352 FORMAT %26H DELTA BY L FOR SLOPE DEFL/<
      WRITE %3,352<
      RCT%1<#0.0
      DC 27 I#2,N
      J#2#I
      K#J-1
      CALL SIG1%X%I<,Y%I<,DIS%K<,I1%K<,J1%K<,R1<
      CALL SIG2%X%I<,Y%I<,DIS%J<,I1%J<,J1%J<,R2<
0027 ROT%I<#%R1&R2</Z%I<
      WRITE %3,25<%ROT%I<,I#1,N<
      DC 28 I#1,20
      ZER%I,1<#0.0
0028 ZER%I,2<#0.0
      CALL SLDEF%SK%1<,SK%2<,SK%3<,ZER%1,1<,ZER%1,2<,ZER%2,1<,ZER%2,2<,
      1ZER%3,1<,ZER%3,2<,ROT%1<,ROT%2<,ROT%3<,DEFM%1<,DEFM%2<,DEFM%3<,
      1DEFM%4<,DEFM%5<,DEFM%6<<
0029 FORMAT %13H DEFL MOMENTS/<
      WRITE %3,29<
0060 WRITE %3,15<%DEFM%I<,I#1,6<
0300 FORMAT %42H CONTINUITY SHEARS FROM DEFL MOMENTS-BASIC/<
      WRITE %3,300<
      DV%1<#0.0
      DV%2<#0.0
      DC 30 I#3,5,2
      SUM#DEFM%I<&DEFM%I&1<
      DV%I<#%1.0<#SUM/H%I<
0030 DV%I&1<#SUM/H%I<#%-1.0<
      WRITE %3,15<%DV%I<,I#1,6<
      DP%1<#DV%2<&DV%3<
```

06/29/68

FORTMAIN

DP%2<#DV%4<&DV%5<

DP%3<#DV%6<

0350 FCRRAT %19H UNIT PLATE LOADS A/<

WRITE %3,350<

C1P%1<#&1.0

C1P%2<#-1.0

C1P%3<#0.0

WRITE %3,25<%C1P%I<,I#1,N<

DO 31 J#1,2

JP#J&1

K#2\*J

L#K-1

0031 CALL PLOAD%2C1P%J<,P1F%L<,P1F%K<,X%J<,Y%J<,Z%J<,X%JP<,Y%JP<,Z%JP<<

P1F%5<#%Z%3</Y%3<<#C1P%3<#%-1.0<

WRITE %3,150<

WRITE %3,115<%P1F%I<,I#1,5<

W%1<#P1F%1<

W%2<#P1F%2<&P1F%3<

W%3<#P1F%4<&P1F%5<

DC 33 I#1,N

J#2\*I

K#J-1

PI#3.1417

F1%J<#%W%1<#SPAN\*SPAN/%PI\*PI<</S%I<

0033 F1%K<#%-1.0<#F1%J<

A1#%-2.0<#Z%1<</%3.0\*S%1<<

A2#%2.0\*Z%2<</%3.0\*S%2<<

A3#Z%2</%3.0\*S%2<<

A4#%-1.0<#A3

A5#%-1.0<#A2

A6#%2.0\*Z%3<</%3.0\*S%3<<

A7#Z%3</%3.0\*S%3<<

A8#%-1.0<#A7

B1#A1-A2

B2#%-1.0<#A3

B3#F1%3<-F1%2<

B4#A4

B5#A5-A6

B7#F1%5<-F1%4<

C1#%B2\*%B4<-%B5\*%B1<

C3#%B3\*%B4<-%B7\*%B1<

0152 FCRRAT %25H PLATE SHEARS-UNIT LOAD A/<

WRITE %3,152<

TC#C3/C1

TB#%B3-%B2\*TC<</B1

TD#0.0

WRITE %3,25<TB,TC,TD

V1S%1<#F1%1<-%0.50\*A1\*TB<

V1S%2<#F1%2<&%A1\*TB<

V1S%3<#F1%3<&%A2\*TB<&%A3\*TC<

V1S%4<#F1%4<&%A4\*TB<&%A5\*TC<

V1S%5<#F1%5<&%A6\*TC<

V1S%6<#F1%6<&0.5\*A6\*%-TC<

0154 FCRRAT %30H BALANCED STRESSES-UNIT LOAD A/<

WRITE %3,154<

06/29/68

FORTMAIN

```
WRITE %3,15<%VIS%I<,I#1,6<
DC 34 J#1,N
L#2#J
K#L-1
0034 CILD%J<#%SPAN*SPAN/%PI*PI*EC*Z%J<<<#%VIS%L<-VIS%K<<
0349 FORMAT %53H CEN LINE DEFLS OF PLATES DUE TO STRESSES-UNIT LOAD A/<
WRITE %3,349<
0035 FORMAT %1X,6E12.3//<
WRITE %3,25<%CILD%J<,J#1,N<
X%4<#X%3<
Y%4<#-Y%3<
Z%4<#Z%3<
CILD%4<#-CILD%3<
X%5<#X%4<
Y%5<#%-1.0<#Y%4<
Z%5<#Z%4<
CILD%5<#%-1.0<#CILD%4<
NPI#N&1
DC 36 I#1,N
L#2#I
K#L&1
M#I&1
CALL WILLY%X%I<,Y%I<,X%M<,Y%M<,CILD%I<,CILD%M<,DIIS%L<,DIIS%K<,I1%
I1<,J1%L<,I1%K<,J1%K<<
0036 CONTINUE
0351 FORMAT %34H WILLIOT DISPLACEMENTS-UNIT LOAD A/<
WRITE %3,351<
DIIS%1<#0.0
WRITE %3,35<%DIIS%I<,I#1,6<
WRITE %3,352<
RIOT%1<#0.0
DC 37 I#2,N
J#2#I
K#J-1
CALL SIG1%X%I<,Y%I<,DIIS%K<,I1%K<,J1%K<,R1<
CALL SIG2%X%I<,Y%I<,DIIS%J<,I1%J<,J1%J<,R2<
0037 RIOT%1<#%R1&R2</Z%I<
WRITE %3,25<%RIOT%I<,I#1,N<
DC 38 I#1,20
ZER%I,1<#0.0
0038 ZER%I,2<#0.0
CALL SLCDEF%SK%1<,SK%2<,SK%3<,ZER%1,1<,ZER%1,2<,ZER%2,1<,ZER%2,2<,
IZER%3,1<,ZER%3,2<,RIOT%1<,RIOT%2<,RIOT%3<,DIEFM%1<,DIEFM%2<,DIEFM%
13<,DIEFM%4<,DIEFM%5<,DIEFM%6<<
0039 FORMAT %25H DEFL MOMENTS-UNIT LOAD A/<
WRITE %3,39<
0040 WRITE %3,15<%DIEFM%I<,I#1,6<
0410 FORMAT %48H CONTINUITY SHEARS FROM DEFL MOMENTS-UNIT LOAD A/<
WRITE %3,410<
DIV%1<#0.0
DIV%2<#0.0
DO 41 I#3,5,2
SIUM#DIEFM%I<&DIEFM%I&1<
DIV%I<#%&1.0<#SIUM/H%I<
0041 DIV%I&1<#SIUM/H%I<#%-1.0<
```

06/29/68

FORTMAIN

```
WRITE %3,15<%D1V%I<,I#1,6<
0450 FORMAT %19H UNIT PLATE LOADS B/<
WRITE %3,450<
C2P%1<#0.0
C2P%2<#&1.0
C2P%3<#-1.0
WRITE %3,25<%C2P%I<,I#1,N<
DC 42 J#1,2
JP#J&1
K#2*J
L#K-1
0042 CALL PLGAD% C2P%J<,P2F%L<,P2F%K<,X%J<,Y%J<,Z%J<,X%JP<,Y%JP<,Z%JP<<
P2F%5<#%Z%3</Y%3<<#C2P%3<#%-1.0<
WRITE %3,150<
WRITE %3,115<%P2F%I<,I#1,5<
W%1<#P2F%1<
W%2<#P2F%2<&P2F%3<
W%3<#P2F%4<&P2F%5<
DC 43 I#1,N
J#2*I
K#J-1
F2%J<#%W%I<#SPAN*SPAN/%PI*PI<</S%I<
0043 F2%K<#%-1.0<#F2%J<
A1#%-2.0<#Z%1<</%3.0*S%1<<
A2#%2.0<#Z%2<</%3.0*S%2<<
A3#Z%2</%3.0*S%2<<
A4#%-1.0<#A3
A5#%-1.0<#A2
A6#%2.0*Z%3<</%3.0*S%3<<
A7#Z%3</%3.0*S%3<<
A8#%-1.0<#A7
B1#A1-A2
B2#%-1.0<#A3
B3#F2%3<-F2%2<
B4#A4
B5#A5-A6
B7#F2%5<-F2%4<
C1#%B2*%4<-#B5*B1<
C3#%B3*%4<-#B7*B1<
0156 FGRMAT %25H PLATE SHEARS-UNIT LOAD B/<
WRITE %3,156<
TC#C3/C1
TB#%B3-%B2*TC<</B1
TC#0.0
WRITE %3,25<TB,TC,TD
V2S%1<#F2%1<-#0.50*A1*TB<
V2S%2<#F2%2<&%A1*TB<
V2S%3<#F2%3<&%A2*TB<&%A3*TC<
V2S%4<#F2%4<&%A4*TB<&%A5*TC<
V2S%5<#F2%5<&%A6*TC<
V2S%6<#F2%6<&0.5*A6*%-TC<
0158 FGRMAT %30H BALANCED STRESSES-UNIT LOAD B/<
WRITE %3,158<
WRITE %3,15<%V2S%I<,I#1,6<
DC 44 J#1,N
```

06/29/68

FORTMAIN

```
L#2*J
K#L-1
0044 C2LD%J<#%SPAN*SPAN/%PI*PI*EC*Z%J<<<#%V2S%L<-V2S%K<<
0449 FORMAT %53H CEN LINE DEFLS OF PLATES DUE TO STRESSES-UNIT LOAD B/<
WRITE %3,449<
WRITE %3,25<%C2LD%J<,J#1,N<
X%4<#X%3<
Y%4<#-Y%3<
Z%4<#Z%3<
C2LD%4<#-C2LD%3<
X%5<#X%4<
Y%5<#%-1.0<#Y%4<
Z%5<#Z%4<
C2LD%5<#%-1.0<#C2LD%4<
NPI#N&1
DC 46 I#1,N
L#2*I
K#L&1
M#I&1
CALL WILLY%*X%I<,Y%I<,X%M<,Y%M<,C2LD%I<,C2LD%M<,D2IS%L<,D2IS%K<,I1%
IL<,J1%L<,I1%K<,J1%K<<
0046 CONTINUE
0451 FORMAT %34H WILLIOT DISPLACEMENTS-UNIT LOAD B/<
WRITE %3,451<
D2IS%1<#0.0
WRITE %3,35<%D2IS%I<,I#1,6<
WRITE %3,352<
R2OT%1<#0.0
DC 47 I#2,N
J#2*I
K#J-1
CALL SIG1%*X%I<,Y%I<,D2IS%K<,I1%K<,J1%K<,R1<
CALL SIG2%*X%I<,Y%I<,D2IS%J<,I1%J<,J1%J<,R2<
0047 R2OT%I<#%R1&R2</Z%I<
WRITE %3,25<%R2OT%I<,I#1,N<
DC 48 I#1,20
ZER%I,1<#0.0
0048 ZER%1,2<#0.0
CALL SLCDEF%*SK%1<,SK%2<,SK%3<,ZER%1,1<,ZER%1,2<,ZER%2,1<,ZER%2,2<,
1ZER%3,1<,ZER%3,2<,R2OT%1<,R2OT%2<,R2OT%3<,D2EFM%1<,D2EFM%2<,D2EFM%
13<,D2EFM%4<,D2EFM%5<,D2EFM%6<<
0049 FORMAT %25H DEFL MOMENTS-UNIT LOAD B/<
WRITE %3,49<
0050 WRITE %3,15<%D2EFM%I<,I#1,6<
0510 FORMAT %48H CONTINUITY SHEARS FROM DEFL MOMENTS-UNIT LOAD B/<
WRITE %3,510<
D2V%1<#0.0
D2V%2<#0.0
DC 51 I#3,5,2
S2UM#D2EFM%I<&D2EFM%I&1<
D2V%I<#%1.0<#S2UM/H%I<
0051 D2V%I&1<#S2UM/H%I<#%-1.0<
WRITE %3,15<%D2V%I<,I#1,6<
C EXTRANEUS FORCES BASIC CASE
EFB%I<#%DV%2<&DV%3<<
```

06/29/68

FORIMAIN

```
EFB%2<#%DV%4<&DV%5<<
C PARTICULAR LOAD CASE A
  PARA%1<#%D1V%2<&D1V%3<&%-1.0<#C1P%1<<
  PARA%2<#%D1V%4<&D1V%5<&%-1.0<#C1P%2<<
C PARTICULAR LOAD CASE B
  PARB%1<#%D2V%2<&D2V%3<&%-1.0<#C2P%1<<
  PARB%2<#%D2V%4<&D2V%5<&%-1.0<#C2P%2<<
C COEFFICIENTS FOR BASIC PLUS A PLUS B
  CCA#%%-1.0<#EFB%1<#PARB%2<&PARB%1<#EFB%2<</%PARA%1<#PARB%2<&%-1.0<
  1*PARB%1<#PARA%2<<
  COB#%%-1.0<#PARA%1<#EFB%2<&EFB%1<#PARA%2<</%PARA%1<#PARB%2<&%-1.0<
  1*PARB%1<#PARA%2<<
0098 FORMAT %37H COEFFICIENTS FOR BASIC PLUS A PLUS B/<
  WRITE %3,98<
0099 FORMAT %1X,2E12.4//<
  WRITE %3,99<CCA,COB
C FINAL PLATE STRESSES
  DC 100 I#1,6,1
0100 SIG%I<#VS%I<&COA#V1S%I<&COB#V2S%I<
0101 FORMAT %21H FINAL PLATE STRESSES/<
  WRITE %3,101<
  WRITE %3,15<%SIG%I<,I#1,6<
C FINAL TRANSVERSE MOMENTS
  DC 102 I#1,6,1
0102 FM%I<#SM%I<&DEFM%I<&COA#D1EFM%I<&COB#D2EFM%I<
0103 FORMAT %25H FINAL TRANSVERSE MOMENTS/<
  WRITE %3,103<
  WRITE %3,15<%FM%I<,I#1,6<
  GO TO 996
0104 CONTINUE
  END
```

```

SUBROUTINE WILLY%A,B,D,E,Z1,Z2,
  1ZZ1,ZZ2,I1,J1,I2,J2<
C  WILLIOT GEOMETRY
  AF#ABS%A<
  BF#ABS%B<
  DF#ABS%D<
  EF#ABS%E<
  C#SQRT%AF*AF&BF*BF<
  F#SQRT%DF*DF&EF*EF<
  T1#B*C-A*E
  T2#A*D&B*E
  ZZ1#%C/T1<*%Z1*T2/C<-%Z2*F<<
  ZZ2#%F/T1<*%C*Z1<-%T2*Z2/F<<
  IF %A<1,2,3
0001 IF %ZZ1<11,12,13
0011 J1#1
      GO TO 25
0012 J1#0
      GO TO 25
0013 J1#-1
      GO TO 25
0003 IF %ZZ1<31,32,33
0031 J1#-1
      GO TO 25
0032 J1#0
      GO TO 25
0033 J1#1
      GO TO 25
0002 J1#0
      GO TO 25
0025 IF %B<4,5,6
0004 IF %ZZ1<41,42,43
0041 I1#-1
      GO TO 50
0042 I1#0
      GO TO 50
0043 I1#1
      GO TO 50
0005 I1#0
      GO TO 50
0006 IF %ZZ1<61,62,63
0061 I1#1
      GO TO 50
0062 I1#0
      GO TO 50
0063 I1#-1
      GO TO 50
0050 IF %D<101,102,103
0101 IF %ZZ2<111,112,113
0111 J2#1
      GO TO 125
0112 J2#0
      GO TO 125
0113 J2#-1

```

06/29/68 WILLY

GC TO 125  
0102 J2#0  
GC TO 125  
0103 IF %ZZ2<131,132,133  
0131 J2#-1  
GC TO 125  
0132 J2#0  
GC TO 125  
0133 J2#1  
GC TO 125  
0125 IF %E<104,105,106  
0104 IF %ZZ2<141,142,143  
0141 I2#-1  
GC TO 150  
0142 I2#0  
GC TO 150  
0143 I2#1  
GC TO 150  
0105 I2#0  
GC TO 150  
0106 IF %ZZ2<161,162,163  
0161 I2#1  
GC TO 150  
0162 I2#0  
GC TO 150  
0163 I2#-1  
GC TO 150  
0150 ZZ1#ABS%ZZ1<  
ZZ2#ABS%ZZ2<  
RETURN  
END

SUBROUTINE SLODEF%SK1,SK2,SK3,F12,F21,F23,  
1F32,F34,F43,RS1,RS2,RS3,BM12,BM21,BM23,  
1BM32,BM34,BM43<

C SLOPE DEFLECTION 3 PLATES

R01#%-1.0<\*RS1  
R02#%-1.0<\*RS2  
R03#%-1.0<\*RS3  
A#%3.0\*SK2&4.0\*SK3<  
B#%2.0\*SK3<  
C#%3.0\*SK2\*R02-F32&0.5\*F23&0.5\*F21&6.0\*SK3\*R03-F34<  
D#B  
E#%4.0\*SK3<  
F#%6.0\*R03\*SK3-F43<  
TH4#0.0  
TH3#%C-%B\*TH4<</A  
BM12#0.0  
BM21#F21  
BM23#%-1.0<\*BM21  
BM32#%3.0\*SK2\*%TH3-R02<<&F32-%0.5\*%F23&BM21<<  
BM34#%-1.0<\*BM32  
BM43#%2.0\*SK3\*%TH3&2.0\*TH4-3.0\*R03<<&F43  
RETURN  
END

```

SUBROUTINE PLGAD%P3,P1,P2,H1,V1,Z1,
1H2,V2,Z2<
C PLATE LOADS TO VALLEY LOADS
  A#H1/Z1
  B#H2/Z2
  C#V1/Z1
  D#V2/Z2
  P2#%A/%A#D-B#C<<#P3*%-1.0<
  IF %A<2,1,2
0001 P1#%-P3-D#P2</C
      GO TO 3
0002 P1#%-1.0<#B#P2/A
0003 CCNTINUE
      RETURN
      END

```

```

SUBROUTINE SIG1%A,B,Z,II,JJ,ROD<
C WILLIOT SIGNS
  IF %A<1,2,3
0001 IF %JJ<11,12,13
0011 ROD#Z
      GO TO 100
0013 ROD#%-1.0<#Z
      GO TO 100
0002 IF %B<21,12,23
0021 IF %II<211,12,213
0211 ROD#%-1.0<#Z
      GO TO 100
0213 ROD#Z
      GO TO 100
0023 IF %II<231,12,233
0231 ROD#Z
      GO TO 100
0233 ROD#%-1.0<#Z
      GO TO 100
0003 IF %JJ<31,12,33
0031 ROD#%-1.0<#Z
      GO TO 100
0033 ROD#Z
      GO TO 100
0012 CCNTINUE
0100 CCNTINUE
      RETURN
      END

```

```
      SUBROUTINE SIG2%A,B,Z,II,JJ,RDD<  
      IF %A<1,2,3  
0001 IF %JJ<11,12,13  
0011 RDD#%-1.0<#Z  
      GO TO 100  
0013 RDD#Z  
      GO TO 100  
0002 IF %B<21,12,23  
0021 IF %I1<211,12,213  
0211 RDD#Z  
      GO TO 100  
0213 RDD#%-1.0<#Z  
      GO TO 100  
0023 IF %I1<231,12,233  
0231 RDD#%-1.0<#Z  
      GO TO 100  
0233 RDD#Z  
      GO TO 100  
0003 IF %JJ<31,12,33  
0031 RDD#Z  
      GO TO 100  
0033 RDD#%-1.0<#Z  
      GO TO 100  
0012 CCNTINUE  
0100 CCNTINUE  
      RETURN  
      END
```

## BIOGRAPHY

(Tony) Tien-Sheng Yang was born in Tainan, Formosa, on May 26, 1928. After completing his work at Tainan High School, Tainan, Formosa, in 1949, he entered National Taiwan University, Taipei, Formosa, and was awarded the degree of Bachelor of Science in July of 1953. He worked as a teaching assistant in National Taiwan University from 1953 to 1957. In July of 1957 he entered the graduate school of the University of Oklahoma; Norman, Oklahoma and was awarded the Master of Science in January of 1959. He worked as a bridge designer in the Bridge Division, Oklahoma State Highway Department, Oklahoma City, Oklahoma from 1958 to 1966. In September of 1966 he returned to the graduate school of the University of Oklahoma. He is a registered Professional Engineer in the state of Oklahoma and is a member of ASCE and ACI.